

Appendix B
Groundwater Flow Model Development

B.1 Introduction

B.1.1 Background

Hydrogeologic investigations have been conducted at the Dundalk Marine Terminal (DMT) starting with the work performed by EA Engineering Science and Technology, Inc. in 1987 (EA, 1987). The initial investigation included development of a groundwater flow model, which was used to assist in estimating the volumes of groundwater flow in the shallow fill aquifer toward the Patapsco River and the onsite storm drains. In a subsequent feasibility study (EA, 1992), the initial model was somewhat expanded and refined for use in simulating the potential effects of proposed remedial actions. In 2005, CH2M HILL, Inc. started a series of groundwater investigations conducted in three phases that have substantially increased the level of detail in the hydrogeologic understanding of the site. Because of the hydrogeologic complexity of the site, a new groundwater flow model was developed to incorporate the new information obtained in these more recent investigations. This appendix documents the model that has been developed in support of the Chromium Transport Study.

B.1.2 Purpose and Objectives

Specific objectives of the groundwater flow model are the following:

- To provide a computational framework that combines the diverse forms of hydrogeologic information collected at the DMT into a predictive tool governed by the equations of groundwater flow,
- To support estimates of the current potential for offsite migration of chromium dissolved in groundwater, both through groundwater discharge to the storm drains or through direct interactions between the aquifers and the Patapsco River, as required in the Chromium Transport Study,
- To provide a quantitative mechanism for future predictive simulations of potential remedial actions that could be taken to mitigate dissolved chromium migration.

B.1.3 General Model Characteristics

Figure B1-1 shows the layout of the DMT and the coverage of the groundwater model. The model is intended to realistically represent groundwater flow in the saturated portion of the shallow fill of the DMT port area, the alluvial sediments underlying the fill, the Patapsco Aquifer directly under the port, and the upland areas southwest of Broening Highway that are hydraulically connected to these groundwater flow zones. The model is implemented using the finite-difference computer code known as MODFLOW-2000 (Harbough, et. al., 2000), which simulates three-dimensional groundwater flow in terms of potentiometric head and volumetric flux. It is not a solute transport model, but its output can be used to quantify mass flux of mobile dissolved species by combining the predicted volumetric flux of groundwater with measured solute concentrations, should such be desired.

With the exception of verification runs to simulate aquifer testing, this model is designed to be run in the steady-state mode. Because the aquifers are relatively thin and the water table

is near the surface, changes in the flow regime caused by variations in aquifer stress occur quickly, and transient simulations are unlikely to be required.

This model is suitable for simulating a variety of future measures that may be considered to alter and control groundwater flow at the site, such as pumping of wells or trenches, installation of barriers, and modification of surface recharge or storm drain interactions with the groundwater. However, this report only documents the model, and does not include such simulations.

B.2 Hydrogeologic Conceptual Model

B.2.1 Regional Geologic Setting

The DMT lies within the western portion of the coastal plain physiographic province approximately 4 miles southeast of the Fall Line. The Coastal Plain is the relatively low part of the Atlantic Slope and is bounded on the east by the edge of the Continental Shelf in the Atlantic Ocean and on the west by the Piedmont Plateau. The boundary between the Coastal Plain and the Piedmont Plateau is known as the Fall Line and is characterized by a zone of rapids and/or waterfalls in the streams flowing from the relatively steeper Piedmont Plateau onto the Coastal Plain (Bennett and Meyers, 1952).

The topographic development of the Atlantic Slope region is directly related to the regional geology. Topographic elevations in the Coastal Plain are generally less than 300 feet above mean sea level (msl) whereas elevations in the Piedmont Plateau can exceed 500 feet msl. The Piedmont Plateau is underlain by relatively hard, structurally complex, crystalline Pre-Cambrian and early Paleozoic rocks. The Coastal Plain is underlain by relatively soft, generally unindurated, easily eroded sediments of the Cretaceous, Tertiary, and Quaternary Systems. These Coastal Plain sediments are underlain by the crystalline Pre-Cambrian and early Paleozoic rocks which extend from the Piedmont Plateau and are generally referred to as “basement” rocks (Bennett and Meyers, 1952).

The crystalline Pre-Cambrian and early Paleozoic basement rocks are unconformably overlain by the Patuxent Formation which is conformably overlain by the Arundel Formation. The Arundel Formation is unconformably overlain by the Patapsco Formation which represents the uppermost Cretaceous sediments. Pleistocene sediments unconformably overlie the Cretaceous sediments (Chapelle, 1985). In places, recent deposits of natural and anthropogenic origin overlie the Pleistocene sediments.

B.2.2 Site-Specific Hydrostratigraphy

The groundwater flow model deals with the recent geologic strata from the ground surface down to and including the Patapsco Formation. Figure B2-1 schematically illustrates the hydrogeologic concept that forms the basis of the numerical model, including the hydrostratigraphy and the major components of the hydrologic balance.

Shallow Fill Unit

The shallow fill unit is mainly comprised of materials that have been placed in the Patapsco River channel since 1928 to reclaim land from the river. These materials include dredge spoil, select (sandy) fill, and chromium ore processing residue (COPR). In Areas 1501 and

1602 there are also layers of clay fill and sand fill that were placed under and around the COPR placement cell and in the former drainage channel roughly paralleling the downgradient end of the 15th Street Storm Drain. More detail about the nature of these materials and the history of their placement are given in the COPR Report (CH2M HILL, 2008) and the main body of this Chromium Transport Study (CTS).

The fill area occupies approximately the western two thirds of the model area. The eastern third corresponds to land that was above the level of the Patapsco River before the start of land reclamation. In this area, the near surface soils include various kinds of fill that have been placed on the natural ground surface. Beneath these are natural alluvial soils comprised of silty sands with discontinuous silt and clayey silt lenses. These alluvial sand and silt beds are hydraulically connected to the shallow fill aquifer to the west, and they are simulated together with the shallow fill as the upper unconfined layer of the groundwater model.

Upper Semiconfining Unit

Beneath the fill materials in the area of land reclamation is a discontinuous layer of organic silt that previously was the bed of the Patapsco River. This is the material referred to as the "Upper Silt" in the CTS and the COPR report. It has relatively low hydraulic conductivity compared with the fill materials and acts hydraulically as a semiconfining unit between the shallow fill aquifer and the underlying alluvial sands. The semiconfining unit is discontinuous either because it was dredged out in some areas before the fill was placed, it was physically displaced in some areas by the weight of the fill, or because there were areas where the river bed was naturally sandy. This is particularly evident in the central portion of Area 1500, east of the 14th Street drain, in the vicinity of a former bulkhead, and in the west-central portion of Area 1300. In the eastern third of the model area, the semiconfining unit is not a distinct stratum. Rather, it is a conceptual layer that represents the hydraulic restriction to vertical flow caused by the silt lenses of the upper Patapsco Formation.

Alluvial Sands

The hydrostratigraphic unit referred to, in the conceptual model (Figure B2-1) as the alluvial sands, is a collection of fine sand and silty sand lenses lying just below the upper semiconfining unit. In the western two thirds of the site, these sand deposits contain relatively fewer fines and are laterally more continuous than in the east. The model represents these sands as a flow zone that is transmissive laterally and is hydraulically connected to the shallow fill aquifer by leakage through the discontinuous upper semiconfining unit.

Lower Semiconfining Unit

Beneath the Alluvial Sands is the Patapsco Formation, which is composed primarily of silts and clays. These form a relatively tight semiconfining unit between the alluvial sands and the Patapsco Aquifer. This unit is also referred to in the CTS and the COPR report as the "Lower Silt." The lower semiconfining unit is 40 to 50 feet thick under most of the fill area of the DMT. The contiguous silt and clay beds become thinner in the east. Aquifer testing in the central portion of the DMT (well DMT-01M) showed that the vertical component of hydraulic conductivity in the lower semiconfining unit there is low enough to practically eliminate hydraulic communication between the Patapsco Aquifer and the shallow aquifer.

In that area, the lower semiconfining unit may more properly be called a confining unit, although for modeling purposes, it is all represented as a semiconfining unit.

Patapsco Aquifer

Patapsco Aquifer occupies the lower 10 to 15 feet of the Patapsco Formation under the DMT. This transmissive zone is composed of sand and gravel, and is part of a regionally extensive aquifer. It is monitored at the DMT by the 25 M-series wells. The potentiometric surface in the Patapsco Aquifer appears to be essentially independent of flow in the shallow fill aquifer and the alluvial sands. This is due to the effective confinement provided by the lower semiconfining unit. However, the Patapsco Aquifer is included in the groundwater model because it represents a potential receptor of groundwater migrating downward from the DMT, albeit at a very low rate.

Arundel Formation

The Patapsco Aquifer is underlain by the Arundel Clay. This is a regionally extensive confining unit approximately 100 feet thick, which is characterized as a red-brown fat clay. It is simulated as the impermeable bottom of the groundwater flow model.

B.2.3 Site Hydrologic Boundaries and Stresses

There are several major physical features at the DMT that are characterized as either hydrologic boundaries or hydrologic stresses to the groundwater flow system. These are features external to the aquifers that influence groundwater flow in ways that are completely, or almost completely, independent of hydraulic conditions in the aquifer.

The Patapsco River is a hydrologic feature that serves as an outflow boundary for groundwater flow in the shallow fill aquifer and the alluvial sands. The river borders the site on the south and southwest sides. It is a tidal water body with a mean tidal range approximately 1.14 feet. The average water level in the river at the DMT is approximately mean sea level, which corresponds to an elevation of 1.67 ft. above the site datum, which is the Baltimore City Datum (BCD). Along the southwest and southern periphery of the DMT, the docks are bordered at the river by a steel sheet-pile wall, or bulkhead. The bulkhead is constructed of interlocking steel panels driven to depths of between 22 and 46 feet below sea level. This is deep enough to key the bulkhead into the lower semiconfining unit. As shown schematically in Figure B2-1, this bulkhead encompasses the southwestern part of the site, and extends along the river bank eastward past 13.5th Street. East of this point, the river bank has no sheet-pile bulkhead, but is lined with rip-rap for storm protection.

The land comprising the fill area of the DMT was reclaimed from the river in stages. The first areas to be filled were north of the East Service Road. This is an area that, prior to 1961, was the site of Baltimore Municipal Airport. The airport area was constructed in the early 20th century by filling the river in an area enclosed by an earthen dike and a construction bulkhead built of wood. This dike and bulkhead were buried by fill when the marine terminal was constructed, starting after 1961. However, they are still present in the subsurface and function as a partial hydraulic barrier to flow on the north side of the East Service Road and the consolidation sheds. Available water level data confirm the bulkhead's presence in the shallow fill unit by showing a substantial potentiometric head difference on opposite sides of the structure. This barrier does not extend into the alluvial sands.

South of the airport construction bulkhead, in the area from 13th Street to 15th Street, historical documents show additional bulkheads associated with later stages of land reclamation. Recent hydrogeologic investigations included installation and monitoring of piezometers to characterize the influences of these historical bulkheads on groundwater flow in the shallow aquifer. Except for the case of one short segment located at the north end of 14th Street, these investigations have detected no hydraulic influences that can be attributed to the historical bulkheads, which are shown as dashed bulkhead lines in Figure D2-1 and subsequent figures. The exception is the segment that extends from the airport construction bulkhead approximately 400 feet south southeast to the west side of 14th Street. This segment, shown as a solid bulkhead line in the figures, appears to accentuate the differences in water levels measured in wells located on either side of it. Therefore, it is believed to remain as a partial impediment to horizontal flow in the shallow aquifer.

Another kind of hydrologic boundary in the interior of the model area is the storm drains. These drains are buried at depths that put parts of their length at and below the water table in the shallow fill aquifer. In some areas, the drain pipes are damaged, and where this occurs below the water table they serve as an outflow boundary for groundwater flow. The major drains are constructed along the streets (see Figure B1-1), and they are designated by the street name (i.e., 10th Street Drain). Between the streets are the “half street” drains. These are generally shallower than the “whole street” drains, and in many cases they are not below the water table. Both half and whole street drains discharge to the river, either through the bulkhead in the western site area, or through controlled outlet structures at the 14th Street and 15th Street drains. The 14th Street and 15th Street outlet structures are equipped with sumps, pumps, and overflows so that the dry-weather flow in the drains can be contained and pumped to a groundwater treatment plant. These structures are designed to prevent the entrance of river water into the drains at high tide as well as to contain the dry-weather flow. These structures are designed to overtop under high flow conditions.

Average annual precipitation in the Baltimore area is approximately 42 inches per year. Direct recharge of precipitation to the shallow aquifer is restricted, but not completely prevented, by the asphalt pavement that covers nearly the entire site. This pavement exhibits some cracking and some locally low areas where shallow ponding is observed during wet weather. Therefore, direct recharge is a significant hydrologic stress to the groundwater system.

On the eastern side of the site, all groundwater flow zones are hydraulically connected to upgradient aquifers. Because the regional groundwater flow is westward toward the river in all of these aquifer zones, the eastern border of the site is an area of groundwater inflow from upgradient.

B.2.4 Aquifer and Aquitard Properties

Information on the flow properties of the aquifer materials has been generated from several sources. In-situ aquifer testing has been performed at four locations in the shallow fill aquifer and at one location in the Patapsco Aquifer. Estimates of hydraulic conductivity have also been made for the coarser granular materials on the basis of grain-size analysis. The flow properties of the fine sediments of the semiconfining units have also been estimated by running laboratory permeability tests on cored soil samples.

Aquifer Testing Results

Four multiwell aquifer tests were run in the shallow fill aquifer and the alluvial sands. The locations tests sites are shown in Figure B1-1.

Well DMT-21S was tested by pumping for approximately 8 hours at rates of between 0.6 and 1 gallon per minute (gpm). Two transmissivity estimates were obtained; one from each of two observation wells located approximately 20 feet from the test well. The estimates were 64.7 square feet per day (ft²/d) for observation well DMT-20S, and 107 ft²/day for observation well TPZ-24. These wells are all screened at elevations which put them in the alluvial sands. The thickness of this unit is approximately 14 feet in this location, indicating hydraulic conductivity values of 4.6 to 7.7 feet per day (ft/d).

The test at well DMT-23S was run for 53 hours at pumping rates between 3.5 and 4.3 gpm. Drawdown data from observation well DMT-02S, located approximately 25 feet away, yielded a transmissivity estimate of 1052.5 ft²/day. These wells were screened in a portion of the shallow fill aquifer occupied by sandy, non-COPR fill. The aquifer thickness was approximately 16 feet, and the hydraulic conductivity estimate is approximately 66 ft/d.

Several abbreviated aquifer tests were run at well DMT-24S. The tests ranged in length from 2.3 to 24 hours, with each test terminating in pump failure due to calcium carbonate encrustation. Pumping rates ranged from 5 to 20 gpm. These tests resulted in transmissivity estimates ranging from 296 to 546 ft²/d based on drawdown observed in well DMT-08S, located approximately 19 feet from the test well. The screens of these test wells are 30 feet long, and are completed in both the shallow fill aquifer, where the fill material was COPR, and in the alluvial sands. Based on a combined aquifer thickness of 34 feet, estimates of the joint hydraulic conductivity of the two aquifers would be from 8.7 to 16 ft/d. However, the flow properties of the separate material types, COPR and alluvial sand, cannot be determined from this information.

Two aquifer tests were attempted at well DMT-25S, but neither was successful. The first test lasted 57 hours with pumping rates believed to have varied between 0.25 and 0.5 gpm. The second test was run for 24 hours, and great care was taken to record the pumping rates, which varied between 0.375 and 0.5 gpm. However, neither of these tests produced a response that was clear enough to be analyzed at observation well DMT-10S, 19 feet away. On the basis of the low productivity of the test well, the transmissivity was estimated to be less than 5 ft²/d. However, it was not clear that these test results were actually indicative of the aquifer properties.

Two aquifer tests were run in the Patapsco Aquifer at well DMT-01M. Both tests were run for 48 hours with a pumping rate of 28 gpm. Drawdown results from 5 observation wells were analyzed, producing transmissivity estimates ranging from 1541 ft²/d to 3788 ft²/d. With an aquifer thickness of approximately 21 feet at the test location, the corresponding hydraulic conductivity estimates are 73 to 180 ft/d.

The two Patapsco aquifer tests at DMT-01M were designed to provide flow property estimates for both the Patapsco Aquifer and for the lower semiconfining unit, using the test procedure of Neuman and Witherspoon (1972). Small-diameter piezometers were installed at three depths within the semiconfining unit above the test well for the purpose of observing the vertical propagation of drawdown upward from the pumping well. Even

though drawdowns of several feet were produced by the test in the aquifer, no hydraulic response was detected at the semiconfining unit, even in the deepest piezometer approximately 5 feet above the top of the aquifer. It was concluded that the vertical component of hydraulic conductivity in the confining unit must be less than 6×10^{-4} ft/d (2.1×10^{-7} cm/s).

Grain-Size Analysis

Numerous soil samples taken from the shallow fill, alluvial sands and the Patapsco aquifer were taken for grain-size analysis during the groundwater investigations. Detailed results of the tests were presented in the COPR Investigation Report (CH2M HILL, 2008). For the purposes of the groundwater model, grain size distribution results were collected for samples having less than 10 percent fines. The empirical equation of Fair and Hatch (1933) was applied to these distributions to estimate the hydraulic conductivity of the samples. Table B2-1 lists the results of these estimates. The samples presented in the table are arranged according to soil types identified in the COPR Investigation Report. The materials of importance for the groundwater model are the following:

- Non-COPR fill (NCF) – This is a predominantly sandy material that was used as select fill in the reclamation of land to construct the DMT. As shown in Table B2-1, the geometric mean hydraulic conductivity for 13 soil samples identified as NCF was 77.43 ft/d.
- Gray-Black COPR (GBC) – This is COPR that has been used as fill material and has not been significantly transformed by geochemical processes after placement. Its physical characteristics are essentially those of a fine to medium poorly-graded sand. The geometric mean hydraulic conductivity estimate for 11 samples of this material is shown in Table B2-1 as 43.5 ft/d.
- Alluvial Sand (C2) – This is sand from the upper sand zone of the alluvial sands. Although it was placed by natural geologic processes rather than as fill, its hydraulic properties appear to be very similar to those of the fill material identified as NCF.
- Alluvial Sand (S1) – This is sand from the lower sand zone of the alluvial sands. As indicated in the table, its geometric mean hydraulic conductivity is slightly lower than that of the C2 sand (41 ft/day vs. 69 ft/d).
- Patapsco Sand – It is noteworthy that six samples of soil identified as sand from the Patapsco Aquifer had a geometric mean hydraulic conductivity of 182 ft/d, which is very close to the upper bound identified for the Patapsco Aquifer in the aquifer tests discussed above (180 ft/d).

Laboratory Permeability Tests

As reported in the COPR Investigation Report (CH2M HILL, 2008) laboratory permeability tests were run on numerous silt and clay samples collected from Shelby tube samples from the semiconfining layers. The average hydraulic conductivity values from these tests were 4.6×10^{-4} ft/day for samples from the upper semiconfining unit and 2.6×10^{-4} ft/day for the lower semiconfining unit.

B.3 Numerical Model Implementation

B.3.1 Code Selection

The hydrogeologic conceptual model discussed above has been implemented numerically using the modular, three-dimensional, finite-difference flow model code MODFLOW-2000. This is an updated version of the MODFLOW code that was originally developed by the U.S. Geological Survey (USGS) in 1984. The updates have included modernized programming, new numerical routines for solving the large system of simultaneous equations, new boundary-condition modules such as the Horizontal Flow Barrier package, and the option to use parameterized assignment of model input values.

The MODFLOW series of modeling codes have been in widespread use since the first introduction in 1984. They are capable of simulating steady-state or transient flow in combinations of confined, unconfined, and semiconfined aquifers with a variety of boundary conditions and hydrologic stresses. They have been thoroughly peer-reviewed and are considered highly reliable for numerical solution of the equations of flow in saturated porous media.

B.3.2 Code Characteristics and Limitations

MODFLOW-2000 uses the finite-difference method to approximate the mathematical equation describing three-dimensional flow of constant-density groundwater in a porous medium. The basic principles underlying the equation are Darcy's law and the conservation of fluid volume. Combination of the mathematical expressions of these principles results in the following governing equation:

$$\frac{\partial}{\partial x} \left(K_{xx} \frac{\partial h}{\partial x} \right) + \frac{\partial}{\partial y} \left(K_{yy} \frac{\partial h}{\partial y} \right) + \frac{\partial}{\partial z} \left(K_{zz} \frac{\partial h}{\partial z} \right) - W = S_s \frac{\partial h}{\partial t}$$

where

- K_{xx} , K_{yy} , and K_{zz} are the values of hydraulic conductivity components along the x , y , and z coordinate axes, which are assumed to be parallel to the principle axes of hydraulic conductivity;
- h is the piezometric head;
- W is a volumetric water influx per unit of aquifer volume representing groundwater sources and sinks;
- S_s is the specific storage of the porous medium; and
- t is time.

MODFLOW-2000 approximates the spatial derivatives in the equation as finite differences calculated between the centers of adjacent rectangular cells in a finite-difference grid. This is characteristic of a cell-centered code. The time-derivative is calculated as a finite difference between consecutive time steps. The DMT model will normally be used in the steady state mode, in which case the time derivative is not used.

MODFLOW-2000 assumes that the hydraulic conductivity and specific storage of the porous medium are uniform within each grid cell. The values can be different from one cell to the next. In approximating the spatial derivative terms, MODFLOW-2000 uses the harmonic mean of the hydraulic conductivity values in the two adjacent cells involved. When calculating the time derivative in transient simulations, MODFLOW-2000 assumes that the head value, h , and the specific storage value, S_s , are uniform over the whole cell. These assumptions limit the ability of the code to accurately represent flow situations in which the piezometric head gradient changes significantly within the distance covered by a single cell.

The source-sink term, W , appearing in the governing equation accounts for water flowing into or out of a computational cell from features external to the aquifer, such as drains, wells, rivers, or areal recharge from the ground surface. Not all cells necessarily have a source-sink term. MODFLOW-2000 has several different options for specifying source-sink terms. Those that are used in the DMT model are described below.

Areal Recharge

Areal recharge is used as a source term (water recharging the modeled aquifer) that is active in all of the cells representing the shallow fill aquifer. The areal recharge rate is specified as input to the model in the form of a two-dimensional array of infiltration rates, one for each model cell. The infiltration rate for each cell (with units of length-per-unit-time) is automatically multiplied by the cell's horizontal area and added to the W term for the cell. The W term is cumulative and accounts for the sum of all of the sources and sinks that may be applied to the cell. The aerial recharge rates are completely determined by the input values and are not affected by simulated piezometric head conditions in the aquifer. Hence, they function as a form of specified-flux boundary condition.

Constant-Head Cells

Constant-head cells are a type of source-sink option that is generally used to represent hydrologic boundaries at the edges of the actively modeled area. They can also be used in the interior of the model for hydrologic features that completely control the piezometric head in the model cells that contact them. Constant-head cells are not fully active parts of the model in the sense that the code does not calculate piezometric heads for them. Instead, the piezometric head values in those cells must be specified as input by the modeler. The code then uses the specified head value to calculate finite-difference approximations of the spatial derivatives linking the constant-head cells to all adjacent active cells in the grid. The hydraulic conductivity components specified for the constant-head cells are also used in the calculation. However, no equation is solved for the head in the constant-head cell. This arrangement results in groundwater fluxes being calculated to and from the constant-head cells as controlled by the simulated heads in the adjacent cells and by the cell dimensions and hydraulic conductivity values. The constant-head cell is therefore, a special kind of head-dependent-flux boundary that is appropriate for locations where the potentiometric head is known.

Two-Way Head-Dependent Flux (RIV)

Another kind of source-sink term supported by MODFLOW-2000 is the head-dependent flux boundary condition called the river cell option. It is most commonly used to represent

the interactions of rivers and streams with the simulated aquifer, but it can be used for any kind of boundary feature that interacts with the aquifer according to the following equation:

$$Q_{riv} = C_{riv} (H_{riv} - h)$$

where

- Q_{riv} is a volume-per-unit-time added to the W term for the cell,
- C_{riv} is a user-specified conductance term with units of area-per-unit-time, and
- H_{riv} is a user-specified reference elevation.

A cell of this type permits flow into or out of the model to occur at a rate determined by the calculated piezometric head at the cell, h , in relation to reference elevation, H_{riv} . The river boundary cell has the additional characteristic involving a specified river bed elevation, H_{bed} . If the calculated aquifer head, h , at the river cell falls below the H_{bed} elevation, then H_{bed} is used instead of H_{riv} in the boundary equation.

Two-Way Head-Dependent Flux (GHB)

A variation of the two-way head-dependent boundary condition is the general head boundary (GHB). This type of cell functions in the same way as the river type boundary described above, except that no bed elevation, H_{bed} is used to modify the flux calculation then the aquifer head falls below a specified elevation. Therefore, the flux into or out of the aquifer at such a cell is calculated in the same way regardless of the potentiometric head value at the cell.

A boundary condition of the GHB type is commonly used at the periphery of the model grid instead of a constant-head cell, if the intention is to allow both the boundary head and the boundary flux to vary in response to the calculated heads in the interior of the model. However, the GHB cell can also be used in the interior of the model to simulate aquifer interactions with a hydrologic feature having a fixed head that is not part of the aquifer itself.

One-Way Head-Dependent Flux (DRN)

The MODFLOW-2000 code provides another kind of head-dependent-flux boundary condition known as the drain cell. It is very similar to the GHB cell except that it only permits outflow from the aquifer. The modeler must specify the drain elevation and the drain conductance. If the simulated piezometric head in the cell is higher than the drain elevation, MODFLOW-2000 calculates an outflow rate using an equation analogous to the river cell equation above. However, if the piezometric head is below the drain elevation, the drain flow is zero.

Specified Flux Cells (WEL)

Specified flux cells are point sources and sinks where water is added to or removed from the model at a user-specified rate. This is most commonly done to represent pumping or injection wells. However, the specified flux could also represent leaking utility lines or any other features that add or remove water at a fixed rate.

Horizontal Flow Boundaries

The horizontal flow barrier (HFB) is a feature of MODFLOW-2000 that is not a boundary condition in the mathematical sense. That is, it does not represent an external control on flow in the aquifer. Rather, it is a way of modifying the numerical representation of the governing equation at specific locations between the finite-difference cells. Normally, the calculated volumetric flux of groundwater between any two cells is determined by the dimensions of the cells, the harmonic mean of the hydraulic conductivity values assigned to the two cells, and the calculated head values at the cell centers. However, when a horizontal flow barrier is placed between two cells, the flux is calculated from the difference in heads at the cell centers and the specified HFB leakage coefficient at the cell boundary between them. This feature is used to simulate the effects of a linear barrier that is thin relative to the dimensions of the model cells, such as a slurry wall or a sheet-pile wall. Realistically representing such a feature without the HFB option would be inefficient because the grid spacing would have to be very small. The HFB option of MODFLOW-2000 greatly facilitates simulation of features such as the subsurface bulkheads at the DMT.

B.3.3 Model Grid Design and Boundary Conditions

The groundwater flow model for the DMT was constructed with a finite-difference grid consisting of three layers, 107 rows, and 233 columns of rectangular cells. The horizontal grid spacing is 20 feet in the western two thirds of the DMT area, expanding to a maximum of 50 feet to the east and north. The grid is rotated 23.5 degrees counter-clockwise from the Maryland state-plane coordinate system to facilitate accurate placement of linear boundary condition features, such as the storm drains and the bulkheads.

Layer-1 Boundary Conditions

Figure B3-1 shows the configuration of the model grid for layer 1, which represents the shallow fill aquifer. The following six kinds of boundary conditions are used in layer 1:

- **Constant-Head Cells**—These boundary cells are used along the eastern and northern edges of the grid to represent the interaction of the simulated shallow fill aquifer with the upgradient groundwater flow system. They implement the upgradient inflow component of the site water balance (Figure B2-1). The specified head values supplied as model inputs at these cells were gridded from the observed water levels contoured in the June 2, 2009 potentiometric surface maps. Constant-head boundary cells are also applied for the Patapsco River in a line just outside the bulkheads along the southern and southwestern edges of the active grid. The head specified for those cells is 1.67 ft BCD, which is the mean river level. Lines of constant-heads were also placed along the mapped storm drains in the former airport area of layer 1 north of the northern bulkhead. Although this area has not been investigated in detail, water levels measured at the few monitoring wells in that area suggest that the water table is influenced by the presence of these subsurface drains. The airport area is essentially isolated from the DMT in layer 1 by the northern wooden bulkhead. However, the shallow aquifer in the airport area does have hydraulic interactions with the underlying alluvial sands. Therefore, active model cells were used in layer 1 with specified heads along the drains based on extrapolated water levels measured at the few monitoring points.

- **Head-Dependent Flux Cells (RIV)**— These cells were used to simulate the effects of the Patapsco River on groundwater flow in the shallow aquifer where that aquifer is simulated underneath the river bed. An alternative would have been to use constant-head cells at the river bank, as was done outside the bulkhead. However, that would be a tacit assumption that no groundwater flow occurs under the river. The use of RIV cells for a distance of 350 feet away from the river bank permits the model to simulate groundwater movement from the DMT under the river.
- **Head-Dependent Outflow (DRN) Cells**— These boundary condition cells were used to simulate the potential for groundwater leakage into the storm drains. The drain reference elevations for these boundary cells were assigned corresponding to the drain invert elevations, as measured at the manholes and interpolated linearly between the manholes. The drain leakage coefficients were adjusted during model calibration to obtain simulated leakage rates that closely approximated the measured or estimated rates.
- **Head-Dependent Flux Cells (GHB)**— Boundary cells of this type were used to represent the downgradient part of the 14th Street storm drain. GHB cell were used there instead of drain cells because the operation of that drain typically results in standing water within the pipe. This water is backed up by the outlet structure, and is periodically pumped out to the groundwater treatment plant. Most of the potentiometric monitoring rounds have indicated equalization of water levels along this segment of the 14th Street drain, suggesting that water can flow both into and out of the pipe through its damaged joints and walls.
- **No-Flow Boundaries**— No-flow boundary conditions were used along the straight southeastern edge of the model grid. This is an area that is slightly beyond the limits of the DMT where groundwater flow is assumed to be approximately perpendicular to the river. No flow boundaries were also used under the Patapsco River around the outer edges of the river boundary cells. This corresponds to an assumption that groundwater levels beyond 350 feet from the shoreline are completely controlled by the river, and under steady-state conditions are equal to mean sea level.
- **Specified-Flux Boundaries**— A specified-flux cell was used near the southeastern corner of the model to simulate a water source in the shallow aquifer coincident with a local groundwater mound at well DMT-62S. This shallow aquifer well consistently has higher water levels than any of the surrounding wells, indicating a local inflow to the aquifer. The source of the water is unknown but may be either leaking utility lines or concentrated recharge of water from nearby roofs or paved areas.
- **Horizontal Flow Barriers**— HFB segments were used to represent the sheet-pile bulkheads lining the southwest and south edges of the docks, the construction bulkhead north of Service Road that separates the DMT from the former airport area, and the 400-foot segment of historical bulkhead just west of 14th Street. The HFB leakage coefficients were adjusted during model calibration.

Layer-2 Boundary Conditions

Figure B3-2 shows the grid configuration and boundary conditions used in layer 2. The following three kinds of boundary conditions were used:

Constant-Head Cells—Constant-head cells were used along the eastern and northern edges of the active grid area to control simulated flow between the alluvial sands within the model area and the offsite aquifers. The head values assigned to these cells were based on the limited number of alluvial sand monitoring wells near the eastern site boundary and on the more well understood shallow water levels.

No-Flow Boundaries—No-flow boundary conditions were applied in layer 2 at the same locations where they were used in layer 1, and for the same reasons.

Horizontal Flow Barriers—HFB segments were specified along the south and southwest edges of the DMT to represent the extension of the bulkheads through the alluvial sands. This is based on evidence from the construction drawings that the sheet-pile bulkheads were driven into the lower semi confining unit below the alluvial sands.

Layer-3 Boundary Conditions

The grid and boundary conditions for layer 3 are shown in Figure B3-3. Constant-head boundaries were assigned around the periphery of this layer. The assigned head values were taken from the Patapsco Aquifer potentiometric surface map for June 2, 2009. This use of circumferential constant-head boundaries essentially fixes the direction of groundwater flow in layer 3. This model layer serves primarily as a lower boundary for vertical flow from the upper two model layers. By allowing the model to calculate layer-3 heads in the interior, the sensitivity of the layer-3 simulation to vertical flux through the lower semiconfining unit can be investigated.

B.3.4 Vertical Layering

Vertical discretization of the three-dimensional model consists of specifying the spatially variable top and bottom elevations of the simulated flow zones and semiconfining units. The DMT flow model is quasi-three-dimensional in the sense that implicit confining beds are used between the layers. Two-dimensional horizontal flow is calculated in the aquifers represented by the model layers, and spatially varying one-dimensional vertical flow is simulated through the confining beds between the layers.

Figure B3-4 shows the simulated bottom elevation of the Shallow Fill Aquifer, which is model layer 1. The bottom of the layer is generally deepest under the Patapsco River and on the west end of the DMT, where elevations of less than -20 ft BCD are present. Under the central part of the DMT there is considerable irregularity in the bottom elevation. This may be partly due to historical dredging, but it was also caused by movements of the loose mucky river bottom sediments (mud waves) as fill was placed to construct the DMT. In the eastern part of the model area, the bottom slopes upward to the east, and in the northeast corner there are elevations above 10 ft BCD. This spatial distribution of bottom elevations is based on the interpretation of more than 300 borings and cone penetrometer tests in the model area.

Figure B3-5 shows the simulated thickness of the upper semiconfining unit. This is an implicit model layer that regulates the simulation of vertical groundwater flow between the Shallow Fill Aquifer of model layer 1 and the alluvial sands of layer 2. The thickness ranges from zero to more than 10 feet, and the distribution is irregular. At locations where the

thickness is zero, the potentiometric head values simulated in the model will be practically the same in layers 1 and 2, because there is little hydraulic resistance to vertical flow.

Figure B3-6 shows the simulated thickness of the alluvial sands (model layer 2). The thickness ranges from a minimum of less than 4 feet to more than 26 feet. As for all the other model layers, this irregular thickness distribution was interpreted from the large number of borings and cone penetrometer tests performed on the site.

Figure B3-7 shows the simulated thickness of the lower semiconfining unit. It ranges from less than 18 feet in the northeast and northwest corners of the model to more than 50 feet in parts of the central DMT.

Figure B3-8 shows the simulated thickness of model layer 3, which represents the transmissive lower portion of the Patapsco Formation. The thickness generally increases to the east and ranged from less than 12 feet to more than 46 feet.

B.3.5 Assignment of Aquifer Properties

Hydraulic Conductivity of Layer 1

Prior to calibration of the model, the initial setup of the model was performed based on the spatial distribution of soil types that was recorded in the logs of more than 300 borings and cone penetrometer tests. The major material types identified in model layer 1 were COPR, non-COPR fill, sand fill, silt, and clay. At most locations, several of these soil types were present in varying percentages. However, in the central part of the fill area, the saturated thickness of the aquifer was nearly 100 percent COPR, and in the southwestern portion it was 100 percent non-COPR fill. In the eastern third of the site, a large portion of the aquifer thickness was alluvial sand and silt, with varying thicknesses of COPR and non-COPR fill on top. Therefore, the initial assignment of hydraulic conductivity was done according to the percentage of the aquifer thickness occupied by the different soil types.

During calibration, it was found that good agreement between simulated and measured water levels could not be obtained by assigning a hydraulic conductivity value to each soil type and calculating the aquifer hydraulic conductivity from the percentages of each type present. To improve the calibration, the layer was subdivided into 38 hydraulic conductivity zones (Figure B3-9). The geometry of these zones was based on the percentages of the various soil types present, the history of filling activities at the DMT, and spatial trends in horizontal hydraulic gradients observed in the potentiometric head maps.

As shown in Figure B3-9, a central band of hydraulic conductivity zones is shaded dark gray. This shading indicates the area where the saturated thickness of layer 1 contains more than 60 percent COPR. A light gray band of hydraulic conductivity zones is shown around the northern, western, and southern edges of this central area, indicating a transition zone in which the aquifer is composed of 40 percent to 60 percent COPR. Outside of the shaded areas on Figure B3-9, the aquifer was divided into zones based on fill history and observed gradient trends. The hydraulic conductivity values assigned to the 38 zones were chosen by a combination of trial-and-error and automated parameter estimation. The calibration procedure will be discussed further in Section B4.

Model calibration revealed the need to assign a band of relatively low hydraulic conductivity (0.1 ft/d) along the bank of the Patapsco River between 13 ½ Street and the outfall of the 15th Street Drain. This low permeability band serves hydraulically as an extension of the flow barrier represented by the sheet-pile bulkhead, which ends at approximately 13 ½ Street. Without this band of low hydraulic conductivity, the model was not able to maintain the groundwater levels approximately 2 feet higher than the mean river level, as has consistently been observed in groundwater monitoring. The history of staged construction of the DMT suggests that this zone may be associated with the placement of low permeability materials during construction of COPR containment cells north of Area 1501 and during the filling of a surface drainage channel that formerly conducted flow from the 15th Street storm drain to the river.

Hydraulic Conductivity of the Upper Semiconfining Unit

Figure B3-10 shows the spatial distribution of hydraulic conductivity assigned to the upper semiconfining unit. Three values were assigned on a zonal basis. The highest hydraulic conductivity value (9.6×10^{-3} ft/d) was assigned to areas where the semiconfining unit is thin or absent. Lower values of 2.3×10^{-3} and 2.1×10^{-3} ft/d were assigned where the unit was identified as more than 1 foot thick in the fill area and the upland area, respectively. The outlines of the zones used were determined on the basis of observed stratigraphy but the numerical values were determined during calibration.

Hydraulic Conductivity of Layer 2

The alluvial sand zone represented as model layer 2 is typically composed of an upper and lower sand layer (or lens) separated by a silt layer. The spatially varying assignment of simulated hydraulic conductivity for this layer was done as a continuous (rather than zonal) distribution based on the percentage of sand vs. silt present in the boring logs. Sand content percentages at the many boring locations were gridded to form a two-dimensional array covering the model layer. The hydraulic conductivity was then apportioned to each grid cell in the layer by multiplying the sand thickness fraction by a characteristic value for alluvial sand, and the silt thickness fraction (11 minus the fraction of sand) by a characteristic hydraulic conductivity value for each soil type. The characteristic hydraulic conductivity values were adjusted during calibration, resulting in calibrated values of 41.2 ft/d for alluvial sand and 6.1 ft/d for alluvial silt. Figure B3-11 shows the hydraulic conductivity distribution for layer 2 that resulted from this procedure.

During calibration, it was found necessary to extend the zone of low hydraulic conductivity assigned in layer 1 along the river bank between 13 ½ Street and the outfall of the 15th Street drain downward into layer 2. This was required to properly simulate the observed groundwater levels in this area, which are high relative to the river.

Hydraulic Conductivity of the Lower Semiconfining Unit

The lower semiconfining unit is a relatively thick (18 to 56 feet) layer of fine silty sands, silts and clays that hydraulically separates the top two model layers from the bottom layer representing the Patapsco Aquifer. As discussed in Section B2, the vertical component of hydraulic conductivity in this layer has been estimated to be less than 10^{-3} ft/d. Sensitivity analysis (see Section B5) has shown that the model is relatively insensitive to the lower semiconfining unit hydraulic conductivity as long as it is less than this value. Based on the

average of laboratory permeability test results for multiple samples taken from this unit, the simulated hydraulic conductivity was assigned as 2.8×10^{-4} ft/d.

Hydraulic Conductivity of the Layer 3

Hydraulic conductivity was assigned to model layer 3 in three zones, as shown in Figure B3-12. The delineation of these zones was based on trends in the horizontal hydraulic gradient as observed in multiple rounds of groundwater monitoring. The value of 112 ft/d assigned to the central zone is based on the results of aquifer testing at well DMT-01M. The other values are estimates based on the variations in hydraulic gradients observed from groundwater monitoring.

B.3.6 Simulation of Storm Drains

The hydraulic effects of groundwater leakage into submerged storm drains were simulated using head-dependent-flux boundary conditions, as discussed in Section B3.3.1 and illustrated in Figure B3-1. The invert elevations of the storm drains were taken from field measurements at the manholes, and were interpolated linearly for model cells located between manholes. The drain leakage coefficients were adjusted during model calibration, along with hydraulic conductivity values for layer 1, to obtain both realistic groundwater levels near the drains and the estimated rate of groundwater leakage into the drains. Drain coefficient values ranged from 0.2 to 200 ft²/d and were assigned on a cell-by-cell basis as needed for good model calibration.

B.3.7 Simulation of Bulkheads

The northern construction bulkhead that hydraulically separates the DMT fill area from the former airport area in layer 1 was simulated using the horizontal flow barrier, with a leakage coefficient of 5.036×10^{-3} ft²/d.

The sheet-pile bulkheads lining the river along the southern and southwestern edges of the port facility were simulated in both layers 1 and 2 using adjoining segments of horizontal flow barriers with different leakage coefficients. The nine flow barrier segments in layer 1 had leakage coefficients ranging from 3.91×10^{-5} ft²/d to 3.09×10^{-2} ft²/day, with an average of 1.12×10^{-2} ft²/d. Leakage coefficients of the nine segments in layer 2 ranged from 9.46×10^{-6} ft²/d to 1.56×10^{-1} ft²/d, with an average of 5×10^{-2} ft²/d. These leakage coefficient values were obtained by model adjustment during calibration.

B.3.8 Recharge

Spatially distributed recharge to the top layer of the model was assigned in six zones, as shown in Figure B3-13. The calibrated recharge rate applied over most of this area was 6.1 inches per year (in/yr).

In the southeastern quadrant of the model area, Areas 1501 and 1602 were constructed with a clay liner below the asphalt to minimize recharge to the COPR that is contained in these areas. The recharge rate used over most of this area was 0.01 in/yr.

Elevated recharge rates of 30.6 in/yr were assigned along the railroad tracks north of the East Service Road. The area along the tracks is not paved, and is believed to receive some runoff from the adjacent paved areas. Hence, the higher recharge rate.

The highest recharge rate, 117.4 in/yr, was assigned in a thin band just north of the consolidation sheds. This is an area that is consistently shown to have groundwater mounding in the period groundwater monitoring events. The potentiometric surface map shows a groundwater mound in this area, suggesting the presence of a hydraulic source. The source of the water is believed to be mainly roof drainage from the consolidation sheds, which is piped below the pavement into drain lines which may be leaking. However, leaking buried water lines have been discovered and repaired several times in this area, and some residual leakage may also contribute to the observed mounding.

In the southeastern corner of the model, the unpaved area south of the DMT property was simulated with a recharge rate of 14 inches per year. This is approximately one third of the average annual precipitation.

B.4 Calibration

B.4.1 Calibration Target Data

The model was calibrated by adjusting the input variables with the objective of obtaining a steady-state simulation that closely matched measured groundwater water levels and groundwater flow rates into the leaking storm drains.

Measured Groundwater Levels

Nine rounds of synoptic water level monitoring have been performed at the DMT since 2005. As the multi-phase groundwater investigation progressed, more wells and piezometers were included in the monitoring rounds. The most comprehensive monitoring round was conducted on June 2, 2009. It included measurements from 161 wells and piezometers, which were collected over a time span of approximately seven hours. Measurements made at wells that are tidally influenced were corrected, using each well's measured tidal efficiency and phase lag, so the potentiometric surfaces derived from the measurements would be representative of tidal mean water levels and hydraulic gradients.

Figures D4-1 shows the measured groundwater levels and contoured potentiometric surface in the Shallow Fill Aquifer for June 2, 2009. The groundwater levels and patterns of flow for June 2, 2009 were not significantly different than those found on previous monitoring dates. The June 2009 water levels were generally higher than those measured in the fall of 2008 by a few tenths of a foot. This is consistent with the relatively wet spring experienced in 2009.

The most prominent features of the potentiometric surface in the Shallow Fill Aquifer are:

- A relatively strong southward hydraulic gradient indicating flow into the site from the northern corner at well DMT-47S. This area of high horizontal gradient diminishes to the south and west of the early shoreline and bulkhead. The gradient lessens to the south and west of the former bulkhead in the area where shallow fill and COPR deposits and alluvial sands thicken significantly west of 14th Street.
- A mild groundwater mound suggesting increased recharge at the consolidation sheds, with the highest groundwater level measured at piezometer TPZ-34 just north of the eastern shed.

- A distinct difference in groundwater levels across the construction bulkhead that separates the DMT port area from the former airport area. The data confirm the hydraulic effectiveness of this subsurface barrier. The potentiometric surface is contoured separately on each side of the bulkhead.
- Groundwater levels along the inside of the present bulkhead surrounding the port area on the south and southwest sides of the DMT are generally 1.3 to 2.3 feet higher than the mean river level (1.67 ft BCD), indicating the hydraulic effectiveness of the sheet-pile bulkhead as a flow barrier. The relatively high groundwater levels are also present adjacent to the river near the 14th Street Drain outfall (wells DMT-12S and EA017S) indicating a flow barrier is present at the river bank even though the sheet piles do not extend that far east.
- Relatively low groundwater levels that wells P-09, EAS-01A, and EAS-01b, completed in an area near the 14th Street drain where the Upper Semiconfining Unit is thin or absent. These water levels are lower than the levels measured closer to the Patapsco River at DMT-12S and EA-017S, indicating groundwater flow northward from the area adjacent to the river bank toward the storm drain.
- Relatively low water levels near the south end of the 13th Street storm drain at piezometers TPZ-08, and TPZ-09. This is believed to be caused by flow into the drain line that was being pumped out during construction of an interim remedial measure for the drain on June 2, 2009.

The 88 groundwater levels measured in the Shallow Fill Aquifer on June 2, 2009 were used as calibration targets for layer 1 of the groundwater flow model.

Figure B4-1 also shows the groundwater levels measured in the 15 alluvial sand (US) monitoring wells. The US wells represent water levels in layer 2 of the groundwater flow model. Because of the relatively sparse distribution of the US wells, the water levels for the Alluvial Sands were not contoured. However, the measured levels were used as calibration targets for the flow model.

Figure B4-2 shows the groundwater levels measured in the Patapsco Aquifer on June 2, 2009. The potentiometric surface shows a general flow direction from north-northeast to south-southwest, with a band of increased hydraulic gradient in the north-central part of the DMT. Water levels measured in 21 Patapsco Aquifer wells were used as model calibration targets in layer 3.

Estimated Storm Drain Leakage

The original plan for measuring storm drain flow called for several rounds of dry-weather flow monitoring and sampling in the storm drains. However, as discussed elsewhere in the CTS, practical considerations made such measurements difficult and few reliable flow estimates are available. Measurements made in the fall of 2007 by Maryland Environmental Services, Inc. (MES) suggested the following:

10th Street Drain—Measurements made on November 30, 2007 along this drain, after exclusion of tidal influences, indicated a flow of 7 gpm at an upstream manhole (M-2) and no flow at downstream manholes (M-1 and S-1). Because the storm drain inverts upgradient

of manhole M-2 are at or above the groundwater table, the indication of 7 gpm in the drain line was not attributed to groundwater inflows.

11th Street Drain—Dry-weather flows of 5 gpm were measured at manholes M-115 and M-116 on October 12, 2007. These measurements are accepted as plausible estimates.

12th Street Drain—Tidal exclusion was implemented for this drain on October 8, 2007, but no flows were recorded. This suggests little, if any, groundwater leakage into this storm drain.

13th Street Drain—Measurements made with tidal exclusion in the drain line on October 4-5, 2007 indicated 3.2 gpm of dry-weather flow at upgradient manhole M-128 and 6.7 gpm at downgradient manhole M-120.

In addition to the MES measurements, observations made during and after installation of an interim remedial measure near the downgradient end of the 13th Street Drain provided a more reliable estimate of 5.1 gpm made after construction and cleaning of the drain and installation of a tidal exclusion vault.

Groundwater inflow estimates for the 14th Street storm drain have been made using the pumping records from the groundwater treatment plant. Dry-weather flow in the 14th Street storm drain is captured in a sump at the drain outlet structure and is pumped to the treatment plant on an almost daily basis. The inflow records to the groundwater treatment plant are somewhat difficult to interpret because total pumping is recorded daily, but it is often not clear to what extent the flow includes rainfall runoff.

Recorded inflows measured between February 1, 2007, and March 31, 2009, were examined with the objective of estimating the average groundwater inflow rate to the drain. The average total daily flow pumped from the 14th Street Drain over this period was 28.27 gpm. However, adjusting for wet weather events, an estimate of approximately 21 gpm for the dry-weather inflows was obtained. Because this estimate is an average of the total flow with identifiable storm events excluded, it is likely that the groundwater inflow component is less than 21 gpm. Therefore, the target flow for model calibration is estimated to be from 15 to 20 gpm.

Similar analysis of treatment plant inflow records suggested a dry-weather flow rate of 37 gpm for the 15th Street storm drain. However, this drain extends offsite into the community of Dundalk and not all of its dry-weather flow can be attributed to groundwater inflow from the DMT. It has been estimated that DMT groundwater leakage accounts for approximately half of the 15th Street drain dry-weather flow. A weir has been installed near the site boundary to measure these offsite inflows, but no dry-weather measurements are yet available from it. Therefore, a relatively uncertain estimate of 19 gpm was used as the calibration target for the 15th Street Drain.

B.4.2 Calibration Procedures

Calibration of the groundwater flow model was done using a combination of manual trial-and-error adjustments and automated parameter estimation using the PEST optimization package.

PEST (Watermark Numerical Computing, 2004) is a model-independent parameter estimation software package that is frequently used to assist in the calibration of groundwater models. The function of the PEST software is to minimize the numerical value of an objective function quantifying the difference between the groundwater model output and the calibration targets. The objective function used for this calibration was the sum of the squared differences between the measured groundwater elevations of June 2, 2009 and the simulated water levels at the monitoring well locations. The PEST software was set up to adjust model input values for each of the 38 layer-1 hydraulic conductivity zones, the two characteristic soil hydraulic conductivity values for layer 2 (alluvial sand and alluvial silt), the vertical hydraulic conductivity values of the semiconfining units, the infiltration rates in the six recharge zones, and the leakage coefficients of the horizontal flow barriers on the north, south, and southwest sides of the DMT.

With this many input values to adjust, the stability of the numerical optimization process is tenuous. Also, many of the input values being adjusted are correlated, so the uncertainty of the inputs remains high even when an optimized solution is achieved. To overcome these optimization difficulties, a process called regularization was employed. Regularization is based on the concept that additional information to supplement the calibration targets is available in the form of relationships between the model input parameters. For instance, the 38 hydraulic conductivity zones in layer 1 were developed as an outgrowth of observations about the prevalence of different soil types in different area of the site. Parameter zones that have a preponderance of COPR should have similar hydraulic conductivity values. Likewise, parameter zones having a preponderance of non-COPR fill should have similar values. This concept was used to place constraints on the adjustment of hydraulic conductivity parameters. It was implemented by adding equations to the optimization process that increase the objective function (the function to be minimized) when the PEST code selects hydraulic conductivity values that are significantly different for two adjacent parameter zones of the same basic soil type. This means that PEST will attempt to minimize both the model residuals (differences between simulated and observed water levels) and the differences in input parameters for adjacent hydraulic conductivity zones.

Further constraints to the optimization process were added in the form of prior information about hydraulic conductivity at the locations of the DMT-23S and DMT-24S aquifer tests. The results of these tests are considered relatively reliable, and the parameters estimation should not result in substantial deviations from the values measured there.

In addition to the automated parameter estimation procedure, manual adjustments were made to the storm drain leakage coefficients during calibration. The objective of these adjustments was to obtain simulated groundwater inflow rates that agreed with the estimated rates while maintaining simulated groundwater levels that closely matched the measured levels.

B.4.3 Calibration Results

Head Residuals

Figure B4-3 shows the potentiometric surface simulated in the Shallow Fill Aquifer by the calibrated model. Comparison with the contoured synoptic data in Figure B4-1 show close similarity in general trends, but differences in some details. It should be noted that,

although the two maps are intended to represent the same thing, they are based on different information and are contoured by different methods. The map of observed water levels in Figure B4-1 is contoured using geostatistical (kriging) interpolation between data points that are several hundred feet apart. The maps of simulated water levels is contoured from simulated water levels at each model cell in layer 1, where cell centers are 20 to 100 feet apart. Also, the simulated water levels conserve fluid mass and obey Darcy's law, as embodied in the governing equation of groundwater flow. Hence, differences in detail between the two maps are to be expected.

Figure B4-4 shows contours of the simulated groundwater levels in the Patapsco Aquifer. These contours also agree closely with the measured water levels shown for the Patapsco in Figure B4-2.

A more quantitative evaluation of the simulated head residuals is given in Table B4-1, which lists the observed and simulated groundwater levels, and the model residuals at each calibration target well in Layer 1. The average of the residuals was 0.010 feet, indicating a very small negative bias to the solution. The standard deviation and root-mean-square residual values were both less than 0.22 feet. This is a statistical indication that most of the simulated water levels were within three inches of the observed levels.

Tables D4-2 and D4-3 list the residual statistics for the Alluvial sands and the Patapsco Aquifer, respectively. For both of these model layers, the residual means were less than one tenth of a foot and the standard deviations were less than 0.3 ft.

For the model as a whole, all three layers, the residual mean was 0.03 ft and the standard deviation was 0.23 ft. The measured water levels in the calibration data set ranged from 1.7 ft BCD to 14.08 ft BCD. The residual standard deviation is approximately 2 percent of the measured range, which is indicative of a good model calibration.

Drain Flow Residuals

In addition to the June 2, 2009 head calibration targets, a second measure of model calibration was its ability to simulated realistic groundwater leakage rates into the storm drains. As discussed above, the available estimates of dry-weather flows in the drains are rather uncertain, and are not associated with a specific measurement date of groundwater flow condition. However, the estimates do serve as a check on the credibility of the model.

Table B4-4 compares the estimated and simulated dry-weather drain flows. For each of the drains, the simulated inflow rate is close to the estimated rate or within the range of estimates.

B.4.4 Calibrated Model Water Balance

One form of output from the MODFLOW-2000 code is the simulated volumetric flux between all of the model cells and to and from the boundary conditions. Using appropriate post-processing software, this information can be examined to reveal the components of the hydrologic budget for the model domain. The post processing program ZONEBUDGET (Harbaugh, 1990) was used for this purpose. The most informative presentation of this information is done for the DMT model on a layer-by-layer basis.

Simulated Flow to and from Model Layer 1

The water-balance components of the calibrated model for layer 1 were as follows:

Inflows

- Direct Recharge: 102.48 gpm
- Upward Flow from Layer 2: 14.80 gpm
- Net Inflow from Constant Heads: 31.25 gpm
- Total inflows: 148.53 gpm

Outflows:

- Seepage to Drains: 58.61 gpm
- Flow through Bulkheads: 10.95 gpm
- Flow through River Bank: 10.86 gpm
- Downward Flow to Layer 2: 68.11 gpm
- Total outflows: 148.53 gpm

The value listed above for total outflow through the river bank (10.86 gpm) in layer 1 includes a segment of Patapsco River bank that is south of the DMT. The portion of flow to the river that occurs on the DMT, but east of the bulkheads in layer 1 is 7.63 gpm.

Simulated Flow to and from Model Layer 2

The water-balance components of the calibrated model for layer 2 were as follows:

Inflows:

- Downward Flow from Layer 1: 68.11 gpm
- Flow from Upgradient Constant Heads: 3.39 gpm
- Total Inflows: 1.75 gpm

Outflows:

- Flow through Bulkheads: 10.78 gpm
- Flow through River Bank: 3.28 gpm
- Upward Flow to Layer 1: 14.80 gpm
- Downward to Layer 3: 0.63 gpm
- Net outflow to boundaries: 42.01 gpm
- Total Outflows: 71.50 gpm

The figure listed above for total outflow through the river bank (3.28 gpm) in layer 2 also includes a segment that is south of the DMT. The portion of flow to the river that occurs on the DMT, but east of the bulkheads in layer 2 is 2.82 gpm.

Simulated Flow to and from Model Layer 3

Inflows:

- Downward Flow from Layer 2: 0.63 gpm
- Inflow from Upgradient Boundaries: 154.35gpm
- Total Inflow: 154.98 gpm

Outflows:

- Out to Downgradient Boundaries: 154.98 gpm

B.4.5 Model Verification with Aquifer Test

In November 2006, a 53-hour aquifer test was run in the Shallow Fill Aquifer at well DMT-23S, with DMT-02S as the primary observation well. This test was simulated with a transient run of the calibrated model to test the ability of the model to realistically represent flow in the aquifer.

Conversion of the model from the steady-state mode to transient required supplying primary and secondary storage coefficients in the unconfined upper layer, and primary storage coefficients in each of the confined lower layers. Also, a series of stress periods and time steps needed to be established to accurately estimate the changes in pumping rate and potentiometric head that occurred during the test. The storage coefficients used for the transient simulations were a specific yield of 0.027 and a specific storage of 0.001/ft for layer 1, and specific storage values of 0.001/ft and 0.0001/ft for layers 2 and 3, respectively.

The aquifer test at DMT-23S was intended to be a constant-rate pumping test, but in practice the pumping rates varied from 3.5 to 4.3 gpm. Based on the field notes recorded during the test, the model simulation was set up with the following five stress periods, pumping rates, and time steps:

Period 1: 25 hours at 4.3 gpm simulated in 10 steps, time-step expansion ratio = 1.5

Period 2: 5 hour at 3.5 gpm simulated in 2 steps, time-step expansion ratio = 1.5

Period 3: 45 minutes at 3.75 gpm simulated in 1 time step

Period 4: 2.75 hours at 4.0 gpm simulated in 3 steps, time-step expansion ratio = 1.5

Period 5: 23.5 hours at 3.5 gpm simulated in 6 steps, time-step expansion ratio = 1.5

Figure B4-8 shows a comparison of the simulated time-drawdown curve at observation well DMT-02s and the measured drawdown curve. The correspondence is very close, indicating that the model simulation is realistic. Although the model will be used in steady-state mode, this test shows the model is viable in either mode.

B.5 Model Sensitivity and Uncertainty

The groundwater flow model is constructed using a large number of different types of input variables representing the properties of the aquifers and aquitards, the boundary conditions, and the hydrologic stresses. All of these properties are spatially variable, and some of them cannot be directly measured. The input values used in the calibrated model were determined through an adjustment process, with the goal of achieving model simulations that matched observed water levels and groundwater flow rates as closely as possible while keeping the input parameters within reasonable ranges and close to prior estimates, where such estimates were available. After calibration, there are still varying degrees of uncertainty about the exact values of the input parameters. This will never be completely eliminated; however, sensitivity analysis can help to demonstrate what influence varying levels of uncertainty will have on the model output.

The relationships between model sensitivity and parameter uncertainty have been classified by the American Society of Testing and Materials (ASTM) into the following four sensitivity types (ASTM, 1994):

Type I Sensitivity – This is when variation of an input causes insignificant changes in the calibration residuals and in the model’s conclusions. This type is of little concern because input uncertainty does not affect the conclusions.

Type II Sensitivity – This is when variation of an input causes significant changes in calibration residuals but has little effect on the model’s conclusions. This type is also of little concern because input uncertainty does not affect the conclusions.

Type III Sensitivity – This is when variation of an input parameter causes significant change in both the model’s calibration residuals and the model’s conclusions. This is of minor concern as long as the model is well calibrated.

Type IV Sensitivity – This is when variation of an input parameter has little effect on the calibration residuals, but significantly changes the conclusions to be drawn from the model output. This type of sensitivity is a serious matter because use of improper input values could lead to faulty conclusions, which would not be recognized through degraded calibration residuals. A model with this type of sensitivity generally requires additional information to reduce the uncertainty of the associated parameter.

B.5.1 Sensitivity Analysis Procedures

Sensitivity analysis was performed on each of the following input parameters:

- Horizontal hydraulic conductivity of the Shallow Fill Aquifer
- Vertical hydraulic conductivity of the upper semiconfining unit
- Vertical hydraulic conductivity of the lower semiconfining unit
- Recharge rate
- Drain leakage coefficients
- Bulkhead leakage coefficients

For each of these parameter types the model was run 10 times using an input parameter multiplier to give a range of inputs centered on the calibrated input values. The results of each series of model runs was evaluated in terms of changes in the calibration statistics (residual mean and standard deviation) and changes in simulated volumetric flow rates to relevant receptors.

B.5.2 Sensitivity to Layer 1 Hydraulic Conductivity

The hydraulic conductivity distribution in model layer 1 is important because it directly affects the simulated flow into leaking storm drains and simulated groundwater discharges to the river. For this sensitivity analysis, the two-dimensional array defining layer 1 hydraulic conductivity was varied by a multiplier that ranged from 0.2 to 2.0. The results are shown in Figure B5-1.

Panel A of Figure B5-1 shows how the residual means and standard deviations changed when layer-1 hydraulic conductivity values were varied from 20 percent to 200 percent of the calibrated values. The layer-1 residual mean is closest to zero at the calibration point. For

multipliers that are less than 1.0, the mean is quite strongly influenced by changes in hydraulic conductivity, but for multipliers greater than 1.0 the sensitivity diminishes rapidly. The layer-2 residual mean is a minimum at a multiplier between 1.0 and 1.2 times the calibration point. The sensitivity of the layer-2 mean is less than the layer 1 mean, but the minimum is clearly defined.

The layer-1 residual standard deviation is a minimum at the calibration point, but is almost the same with a multiplier of 0.8. At multipliers less than 0.8 and greater than 1.0, the quality of the layer-1 calibration is clearly diminished.

Panel B of the figure shows the sensitivity of the simulated groundwater discharge to the river to changes in hydraulic conductivity. Flux to the river is divided into four categories, flux through the bulkheads in layers 1 and 2, and flux through the river bank in the area east of the bulkhead in both layers. The figure shows that leakage through the bulkheads is not strongly affected by hydraulic conductivity changes in the range that was tested. Flow through the river bank in layer 2 is also not very sensitive to this parameter. River bank flux in layer 1, however, does increase significantly with increasing hydraulic conductivity, rising from approximately 8 gpm to approximately 13 gpm when the hydraulic conductivity is doubled.

Panel C of figure D5-1 shows the sensitivity of simulated groundwater leakage into the storm drains to layer-1 hydraulic conductivity. The relatively low rates of leakage into the 11th and 12th Street drains are insensitive to hydraulic conductivity. Flow into the 13th, 14th, and 15th Street drains increases with greater hydraulic conductivity. Since these drain leakage rates have been estimated by means other than the groundwater model, this sensitivity information serves mainly to confirm the model calibration.

B.5.3 Sensitivity to Upper Semiconfining Unit Hydraulic Conductivity

Figure B5-2 illustrates the results of the sensitivity analysis for the vertical component of hydraulic conductivity in the upper semiconfining unit. Panel A shows that the calibration statistics for layers 1 and 2 are sensitive to this parameter. The layer-1 residual mean decreases with increasing values of semiconfining unit hydraulic conductivity, and crosses the zero line at a multiplier of between 0.8 and 1.0. The layer 2 residual mean increases with increasing hydraulic conductivity.

The layer-1 residual standard deviation is a minimum at the calibration value, but is almost the same with a multiplier of 0.8. The layer 2 residual standard deviation decreases with increasing hydraulic conductivity of the semiconfining unit, suggesting that a better layer-2 calibration might result from increasing the hydraulic conductivity. However, this indication is contradicted by the layer-2 residual mean. Hence, the calibrated value is seen as a good compromise between the conflicting indicators.

Panels B and C of Figure B5-2 show that simulated flux to the river and simulated drain leakage are relatively insensitive to the hydraulic conductivity of the upper semiconfining unit.

B.5.4 Sensitivity to Lower Semiconfining Unit Hydraulic Conductivity

The vertical component of hydraulic conductivity in the lower semiconfining unit can be expected to affect calibration in all three model layers because it controls the degree of hydraulic separation between the alluvial sands and the Patapsco Aquifer. Sensitivity analysis for this parameter consisted of seven model runs with hydraulic conductivity values increasing from 1.0×10^{-7} to 1.0×10^{-1} ft/day in factors of ten. The results are listed in Table B5-1.

The table shows that the calibration statistics for all three model layers, as well as the simulated downward groundwater flux rate to layer 3, are all insensitive to this parameter for values lower than 1.0×10^{-4} ft/d. For hydraulic conductivity values greater than 1.0×10^{-3} ft/d, the calibration statistics in layers 2 and 3 are substantially affected by changes with indications of decreased calibration accuracy. Simulated groundwater flux from layer 2 to layer 3 is also quite low for hydraulic conductivity values less than the calibration value. Above the calibration value, downward flux increases almost in proportion to the increases in hydraulic conductivity. This shows that simulation results would be significantly affected by uncertainty in this parameter. The value used in the calibrated model is supported by both laboratory testing of soil samples and in-situ aquifer testing. Using a reasonable range of uncertainty in hydraulic conductivity from 1.0×10^{-4} ft/d to 1.0×10^{-3} ft/d, the simulated total flux to layer 3 could range from 0.2 to 2.2 gpm.

B.5.5 Sensitivity to Recharge Rates

In this analysis, the spatial distribution of recharge rates was varied by applying multiplier values ranging from 0.2 to 2.0 to the calibrated recharge array. Panel A of Figure B5-3 shows the effects of these variations on calibration statistics in model layers 1 and 2. In general, calibration was sensitive to recharge in both layers. In layer 1 both the residual mean and the standard deviation were best at the calibration point. In layer 2, the residual mean was zero at a multiplier of just below 0.8, and the standard deviation was at a minimum with a multiplier of approximately 1.5.

Panel B shows that simulated groundwater flux through the bulkheads was sensitive to the simulated recharge, particularly in layer 1. Simulated groundwater flux through the river bank east of the bulkhead was less sensitive to recharge.

Panel C shows that simulated leakage to the 13th through 15th Street drains was also strongly influenced by the recharge rate. Since these rates have been independently estimated, this sensitivity helps to reduce the uncertainty in the simulated recharge rates.

B.5.6 Sensitivity to Drain Leakage Coefficients

Calibration adjustment of the drain coefficients was done by drain segment, and in some locations on a cell-by-cell basis to simultaneously match simulated aquifer levels and drain leakage rates to the calibration targets. In the sensitivity analysis, however, all of the drain coefficients were adjusted simultaneously by applying multipliers over the range of 0.2 to 2.0.

Panel A of Figure B5-4 shows the effects of varying the drain coefficients on model calibration statistics. All of the statistics showed sensitivity to this parameter. Layer-1

calibration is obviously optimized at the calibration point (multiplier = 1.0). In Layer 2, the residual mean would be improved by an increase in drain leakage, but the standard deviation would be better with a lower leakage multiplier. The calibration values appear to be a good compromise with respect to all of the statistical indicators.

Panel B shows that simulated flux to the river is moderately sensitive to the drain leakage coefficients. Simulated flow through the bulkheads was reduced from approximately 14 gpm per layer to approximately 10 gpm when the multiplier increased from 0.2 to 2.0. Simulated flux through the river bank was somewhat less sensitive to this parameter.

Panel C shows that simulated flux to the 15th Street Drain was highly sensitive to the drain coefficient multiplier, increasing from approximately 7 gpm to nearly 30 gpm over the range tested. Flow to the other storm drains was much less sensitive, but all were affected by this parameter.

B.5.7 Sensitivity to Bulkhead Leakage Coefficients

Sensitivity analysis for bulkhead leakage was performed separately for the northern construction bulkhead, which separates the COPR Fill Area from the former airport area and for the southern bulkheads, which line the river bank along the south and southwest edges of the DMT. For both bulkheads, the horizontal flow boundary (HFB) leakage coefficient was varied using a multiplier that ranged from 0.01 to 10.

Figure B5-5 shows the results for the northern bulkhead. The calibration residuals were insensitive for multiplier values less than 1. At higher multipliers the residual means and the layer-1 standard deviation showed sensitivity, while the layer-2 standard deviation did not. Considering the increase in layer-1 standard deviation and the departure of the layer 1 residual mean from zero at multiplier values above 1.0, actual bulkhead leakage coefficients that are substantially higher than the calibrated values appear unlikely.

Panels B and C of Figure B5-5 show that the simulated groundwater fluxes to the river and the storm drains are relatively insensitive to the northern bulkhead.

Figure B5-6 shows the sensitivity analysis results for the southern bulkhead. The calibration statistics in Panel A indicate that the model is quite sensitive to this parameter, and that the values used in the calibration are near optimal. Panel B shows that groundwater flux to the river through the southern bulkhead is also quite sensitive to this parameter, as would be expected. Groundwater flux through the river bank east of the bulkhead is insensitive. Panel C of Figure B5-6 shows that simulated groundwater discharge to the storm drains is mildly sensitive to bulkhead leakage. The most sensitive drain was the 13th Street Drain, in which the simulated groundwater inflow was reduced from approximately 16 gpm to approximately 10 gpm when the bulkhead leakage coefficients were increased by three orders of magnitude.

B.6 Summary and Conclusions

B.6.1 Summary

The multi-phase groundwater investigation that has been conducted at the DMT since 2005 has resulted in diverse types of information that illuminate various aspects of the

hydrogeologic nature of the site. Taken together, this information has supported the development of a realistic conceptual model of the groundwater flow system, from the ground surface down to the bottom of the Patapsco Aquifer, and its hydraulic interaction with the Patapsco River. Based on this conceptual model, a numerical groundwater flow model has been developed which is capable of quantitatively simulating potentiometric levels and groundwater fluxes, including leakage to the storm drains, discharge to the river through and around the bulkheads, and downward groundwater migration into the Patapsco Aquifer.

The geometric configuration of the model is based on site stratigraphy developed from installation of over 300 borings and piezometers. Characterization of aquifer parameters is supported by aquifer testing at four shallow aquifer test sites and multiple tests at a central location in the Patapsco Aquifer. Additional information from soil grain size analysis and laboratory permeability testing was used to supplement the in-situ test results. The model was calibrated using synoptic measurements made in over 120 monitoring wells and piezometers, plus estimated flows in six storm drains as calibration targets. Calibration residual standard deviation was approximately 2 percent of the range of potentiometric heads simulated. In addition the model was verified by accurately simulating the hydraulic response observed during a 53-hour aquifer test.

Sensitivity analysis was performed by individually varying the major input parameters and recording the effects on calibration statistics and major modeling results. The results show that the uncertainty of individual input parameters is constrained by the sensitivity of the model calibration. Sensitivity of model outputs to variation of the major input parameters is such that significant errors in specific parameter values would be identified either by degradation of the calibration statistics or by deviation from prior observations. This, in itself, does not mean that the calibration is unique, because correlation between input parameters makes it possible to get similar head residuals for various combinations of hydraulic conductivity, recharge, and boundary condition coefficients if the parameters are varied simultaneously in the proper way. Consequently, it is very important that the DMT model has been calibrated using both measured water levels and estimated drain flows, and that it incorporates prior information on hydraulic conductivity from a variety of sources including aquifer tests.

B.6.2 Conclusions

The model that is documented here is suitable for its intended uses, which were stated in the model development objectives as follows:

- To provide a computational framework that combines the diverse forms of hydrogeologic information collected at the DMT into a predictive tool governed by the equations of groundwater flow,
- To support estimates of the current potential for offsite migration of chromium dissolved in groundwater, both through groundwater discharge to the storm drains or through direct interactions between the aquifers and the Patapsco River, as required in the Chromium Transport Study,
- To provide a quantitative mechanism for future predictive simulations of potential actions that could be taken to mitigate dissolved chromium migration.

Table B2-1
Hydraulic Conductivity Estimates from Grain-Size Analysis

Sample ID	Depth Interval, ft	%Gravel	%Sand	%Fines	Estimated Hydraulic Conductivity (ft/day)	Cross-Section Strata	Material	K GeoMean/ St.Dev.
SBA-I-2	18 - 20	18.75	77.55	3.70	50.55	Type II Fill	?	
SBA-H-5	16 - 17	0.66	89.73	9.61	35.21	Type II Fill	FL1	
CSG-2	14 - 16	0.14	90.50	9.37	30.32	Type II Fill	FL2	
DMT-52US	24 - 26	2.08	92.66	5.26	66.86	Type II Fill	FL2	
DMT-52US	31 - 32	0.00	92.81	7.19	64.91	Type II Fill	FL2	
SBA-A-2	15 - 16	9.28	84.92	5.80	98.88	Type II Fill	FL2	61.50
SBA-B-1	14 - 16	3.31	95.72	0.97	67.63	Type II Fill	FL2	24.28
B-130	8 - 9	10.71	81.16	8.14	162.08	Type II Fill	NCF	
B-130	9 - 11	11.38	83.87	4.75	260.97	Type II Fill	NCF	
DMT-05S	8 - 10	37.00	54.20	8.80	149.17	Type II Fill	NCF	
DMT-41S	10 - 12	20.67	72.34	7.00	67.06	Type II Fill	NCF	
SBA-B-2	3 - 5	58.01	33.46	8.53	363.45	Type II Fill	NCF	
SBA-B-2	7 - 9	10.88	79.61	9.51	50.06	Type II Fill	NCF	
SBA-D-2	6 - 8	3.88	92.14	3.98	56.64	Type II Fill	NCF	
SBA-D-4	18 - 20	4.28	91.92	3.80	47.61	Type II Fill	NCF	
SBA-E-1	6 - 8	0.98	91.91	7.12	51.35	Type II Fill	NCF	
SBA-E-1	16 - 18	6.18	86.71	7.11	53.49	Type II Fill	NCF	
SBA-F-4	11 - 12	6.36	89.64	4.00	31.67	Type II Fill	NCF	
SBA-F-5	25 - 26	2.33	93.57	4.10	62.86	Type II Fill	NCF	77.43
SBA-G-1	9 - 10	0.29	93.30	6.41	31.65	Type II Fill	NCF	101.84
DMT-47S	6 - 8	66.15	28.09	5.75	1079.28	Type II Fill	NCF	
SBA-G-1	27 - 28	0.95	93.72	5.32	47.77	Type II Fill	S1	
DMT-46S	19 - 21	29.77	68.96	1.28	197.59	Type II Fill	SF	
DMT-33S	4.5 - 6	5.30	85.50	9.20	46.89	GB COPR	GB1	
INC-16	3 - 5	28.60	63.60	7.80	76.49	GB COPR	GB1	
INC-16	11 - 12	28.60	63.64	7.77	26.44	GB COPR	GB2	
DMT-06S	20 - 22	9.00	84.20	6.80	38.17	GB COPR	GB3	
DMT-07S	12 - 14	13.00	81.20	5.80	33.66	GB COPR	GB3	
DMT-43S	18 - 19	18.95	75.27	5.78	46.27	GB COPR	GB3	
DMT-43S	19 - 20	5.20	91.86	2.93	49.96	GB COPR	GB3	
INC-08	12 - 14	5.90	85.80	8.20	23.96	GB COPR	GB3	
INC-09	12 - 14	6.40	84.10	9.50	50.26	GB COPR	GB3	
SBA-A-1	10 - 12	22.70	67.74	9.56	46.52	GB COPR	GB3	43.50
SBA-H-2	15 - 17	19.55	72.02	8.43	66.94	GB COPR	GB3	15.76
DMT-44S	16 - 18	35.95	54.22	9.84	202.03	GB COPR	GB3 & HB3	
B-130	21 - 22	1.47	95.40	3.13	56.27	Alluvial Sand	C2	
B-131	16 - 18	8.45	88.76	2.79	191.93	Alluvial Sand	C2	
DMT-46S	24 - 26	0.00	95.48	4.52	25.58	Alluvial Sand	C2	
DMT-54US	15 - 17	4.28	86.07	9.65	79.83	Alluvial Sand	C2	68.53
DMT-54US	23 - 25	2.88	93.53	3.59	86.37	Alluvial Sand	PAT	72.50
B-100	26 - 28	0.15	97.65	2.20	39.25	Alluvial Sand	S1	
CSG-2	24 - 26	19.50	75.06	5.44	70.09	Alluvial Sand	S1	
DMT-33S	27 - 29	0.06	93.95	5.99	16.50	Alluvial Sand	S1	
DMT-45S	25 - 27	1.44	96.79	1.77	38.41	Alluvial Sand	S1	
DMT-57S	25 - 27	0.63	95.25	4.12	41.86	Alluvial Sand	S1	
DMT-57S	30 - 32	2.46	95.18	2.35	62.60	Alluvial Sand	S1	41.11
INC-12	34 - 36	1.30	95.70	3.00	43.42	Alluvial Sand	S1	17.51
DMT-51US	40 - 42	0.00	95.22	4.78	20.52	Alluvial Sand	S1A	
DMT-36M	102 - 103.5	24.41	68.43	7.17	127.58	Patapsco Sand		
B-124	87 - 89	4.63	87.26	8.11	36.01	Patapsco Sand		
IC-A-1	31 - 32.5	49.71	49.14	1.15	808.54	Patapsco Sand		
IC-A-1	35 - 37	16.59	80.99	2.42	138.05	Patapsco Sand		
IC-A-1	39 - 41	44.30	54.67	1.03	717.50	Patapsco Sand		182.02
IC-B-1	36 - 38	12.22	83.33	4.45	98.84	Patapsco Sand		345.36

Table B4-1
Simulation Residuals for the Calibrated Model
Model Layer 1, Shallow Fill Aquifer

Calibration Target Well	Measured Water Level (ft BCD)	Simulated Water Level (ft BCD)	Model Residual, (Simulated - Measured) (ft)
DMT-01S	3.43	3.54	0.11
DMT-02S	3.72	3.72	0.00
DMT-03S	3.88	3.75	-0.13
DMT-04S	3.76	3.86	0.10
DMT-05S	3.51	3.76	0.25
DMT-06S	3.47	3.65	0.18
DMT-07S	3.41	3.42	0.01
DMT-08S	3.41	3.12	-0.29
DMT-09S	3.53	3.54	0.01
DMT-10S	5.32	5.26	-0.06
DMT-11S	2.56	2.71	0.15
DMT-12S	3.59	3.78	0.19
DMT-14S	3.66	3.11	-0.55
DMT-15S	3.91	3.59	-0.33
DMT-17S	3.27	3.31	0.04
DMT-18S	3.39	3.19	-0.20
DMT-22S	3.26	3.42	0.16
DMT-23S	3.76	3.72	-0.04
DMT-24S	3.23	3.13	-0.10
DMT-25S	5.27	5.22	-0.05
DMT-29S	4.53	4.59	0.06
DMT-30S	4.87	4.96	0.09
DMT-31S	3.51	3.55	0.04
DMT-32S	3.53	3.65	0.12
DMT-33S	3.91	3.57	-0.34
DMT-39S	4.60	4.80	0.20
DMT-42S	2.99	3.15	0.16
DMT-43S	3.72	3.86	0.14
DMT-44S	3.41	3.60	0.19
DMT-45S	2.25	2.08	-0.17
DMT-47S	14.08	13.97	-0.11
DMT-57S	2.12	1.90	-0.22
DMT-58S	1.46	1.75	0.29
DMT-61S	9.13	9.26	0.13
DMT-62S	11.48	11.28	-0.20
DMT-63S	3.37	3.29	-0.08
EA-02S	6.08	6.28	0.20
EA-03S	9.97	10.04	0.07
EA-06S	3.68	3.58	-0.10
EA-08S	8.41	8.17	-0.24
EA-10S	3.29	3.67	0.38
EA-11S	3.22	3.20	-0.02
EA-12S	4.31	3.89	-0.42
EA-14S	3.60	3.71	0.11
EA-15S	4.23	4.27	0.04
EA-16S	3.54	3.69	0.15
EA-17S	3.98	4.03	0.05
EAC-01S	9.78	9.52	-0.26
EAC-03S	2.53	2.93	0.40
EAS-01A	3.37	3.31	-0.06

Table B4-1
Simulation Residuals for the Calibrated Model
Model Layer 1, Shallow Fill Aquifer

Calibration Target Well	Measured Water Level (ft BCD)	Simulated Water Level (ft BCD)	Model Residual, (Simulated - Measured) (ft)
EAS-01B	3.36	3.27	-0.09
EAS-02B	3.68	3.40	-0.28
P-04	3.75	4.08	0.33
P-05	5.16	4.84	-0.32
P-06	3.72	3.94	0.22
P-07	4.20	4.39	0.20
P-08	3.06	3.43	0.37
P-09	3.30	3.22	-0.09
P-10	3.62	3.50	-0.12
P-11	5.82	5.73	-0.09
TPZ-04	3.51	3.52	0.01
TPZ-05	3.54	3.55	0.01
TPZ-06	3.63	3.60	-0.03
TPZ-07	3.65	3.72	0.07
TPZ-08	2.16	2.37	0.21
TPZ-09	2.28	2.51	0.23
TPZ-10	2.39	2.70	0.31
TPZ-11	2.78	3.16	0.38
TPZ-12	2.70	2.72	0.02
TPZ-14	3.28	2.93	-0.35
TPZ-15	3.83	3.28	-0.55
TPZ-16	3.69	3.52	-0.17
TPZ-17	3.64	3.53	-0.11
TPZ-19	3.67	3.57	-0.10
TPZ-20	3.38	3.68	0.30
TPZ-21	3.39	3.68	0.29
TPZ-22	3.34	3.67	0.33
TPZ-27A	7.42	7.35	-0.07
TPZ-30A	8.36	8.75	0.39
TPZ-34	4.98	4.99	0.01
TPZ-35	3.83	3.86	0.03
TPZ-37	3.78	3.56	-0.22
TPZ-44	4.21	4.53	0.32
TPZ-45	5.44	5.59	0.15
TPZ-46	5.49	5.44	-0.05
TPZ-47	4.61	4.33	-0.28
TPZ-A	3.54	3.23	-0.31
TPZ-B	5.47	5.33	-0.14

Layer-1 Calibration Statistics

Residual Mean: 0.010 ft
Residual Standard Deviation: 0.218 ft
Root Mean Square Residual: 0.217 ft

Table B4-2
Simulation Residuals for the Calibrated Model
Model Layer 2, Alluvial Sands

Calibration Target Well	Measured Water Level (ft BCD)	Simulated Water Level (ft BCD)	Model Residual, (Simulated - Measured) (ft)
DMT-49US	2.83	3.13	0.30
DMT-50US	3.00	2.92	-0.08
DMT-51US	3.52	3.91	0.39
DMT-52US	3.51	4.14	0.63
DMT-53US	5.82	5.60	-0.22
DMT-54US	6.29	6.43	0.15
DMT-64US	2.44	2.52	0.08
DMT-65US	2.50	2.75	0.25
DMT-67US	3.34	3.19	-0.15
DMT-70US	2.55	2.83	0.28
DMT-71US	3.31	3.01	-0.30
DMT-72US	3.25	3.57	0.32
DMT-73US	4.74	4.45	-0.29
DMT-74US	3.64	3.96	0.32
DMT-75US	4.31	4.63	0.32
DMT-10S	5.32	4.96	-0.36
DMT-45S	2.25	2.26	0.02

Layer-2 Calibration Statistics

Residual Mean: 0.096 ft.
Residual Standard Deviation: 0.289 ft.
Root Mean Square Residual: 0.296 ft.

**Table B4-3
Simulation Residuals for the Calibrated Model
Model Layer 3, Patapsco Aquifer**

Calibration Target Well	Measured Water Level (ft BCD)	Simulated Water Level (ft BCD)	Model Residual, (Simulated - Measured) (ft)
DMT-01M	2.24	2.80	0.56
DMT-34M	2.09	2.09	0.00
DMT-35M	5.20	4.95	-0.25
DMT-36M	2.68	2.94	0.26
DMT-37M	2.06	1.96	-0.10
DMT-38M	3.66	3.76	0.10
DMT-77M	3.00	2.87	-0.13
DMT-78M	2.29	2.56	0.27
DMT-80M	3.29	3.33	0.05
EA-02M	4.19	4.08	-0.11
EA-06M	2.66	2.48	-0.18
EA-07M	2.39	2.34	-0.05
EA-08M	4.53	4.46	-0.07
EA-11M	1.70	1.70	0.00
EA-13M	1.85	2.09	0.24
EA-14M	1.64	1.67	0.03
EA-15M	1.63	1.86	0.23
EAC-02M	4.39	4.21	-0.18
EAC-03M	1.84	1.99	0.15

Layer-3 Calibration Statistics

Residual Mean: 0.044 ft
Residual Standard Deviation: 0.203 ft.
Root Mean Square Residual: 0.202 ft.

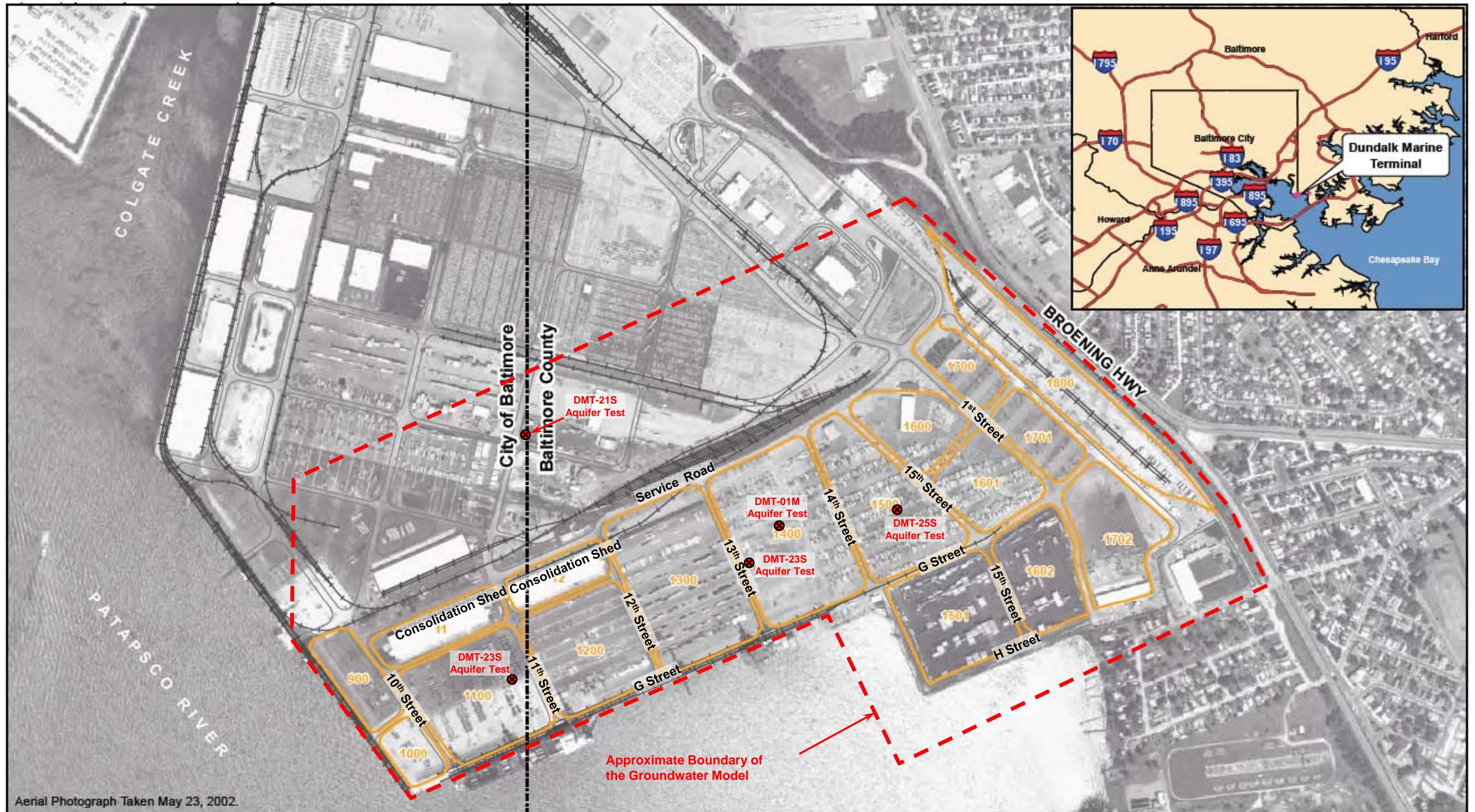
Table B4-4

Estimated vs. Simulated Groundwater Inflows to Storm Drains

Drain	Estimated Dry-Weather Drain Flow (gpm)	Simulated Groundwater Inflow (gpm)
10th Street	0	0.43
11th Street	5	3.87
12th Street	0	0.70
13th Street	5 - 14	12.71
14th Street	15 - 20	18.01
15th Street	19	21.63

Table B5-1

Model Sensitivity to Vertical Hydraulic Conductivity of the Lower Semi-Confining Unit									
Vertical Component of Hydraulic Conductivity (Kz)		Layer 1 Calibration Statistics		Layer 2 Calibration Statistics		Layer 3 Calibration Statistics		Flux from Layer 2 to Layer 3	
(ft/day)	(cm/s)	Mean Residual (ft)	Standard Deviation (ft)	Mean Residual (ft)	Standard Deviation (ft)	Mean Residual (ft)	Standard Deviation (ft)	(cfd)	(gpm)
1.00E-07	3.53E-11	-0.004	0.246	0.101	0.287	0.043	0.203	0.044	0.000
1.00E-06	3.53E-10	-0.004	0.246	0.101	0.287	0.043	0.203	0.441	0.002
1.00E-05	3.53E-09	-0.004	0.246	0.101	0.287	0.043	0.203	4.405	0.023
1.00E-04	3.53E-08	-0.005	0.246	0.099	0.288	0.044	0.203	43.946	0.228
1.00E-03	3.53E-07	-0.013	0.246	0.079	0.293	0.050	0.204	429.740	2.232
1.00E-02	3.53E-06	-0.079	0.247	-0.076	0.344	0.097	0.213	3534.600	18.362
1.00E-01	3.53E-05	-0.271	0.269	-0.507	0.529	0.230	0.271	13875.000	72.078



Aerial Photograph Taken May 23, 2002.

- Legend**
- Areas
 - Railroad Centerline
 - Curb
 - County/City Boundary

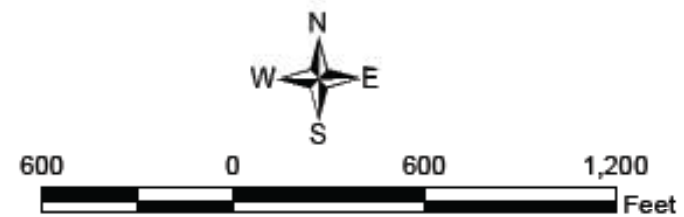
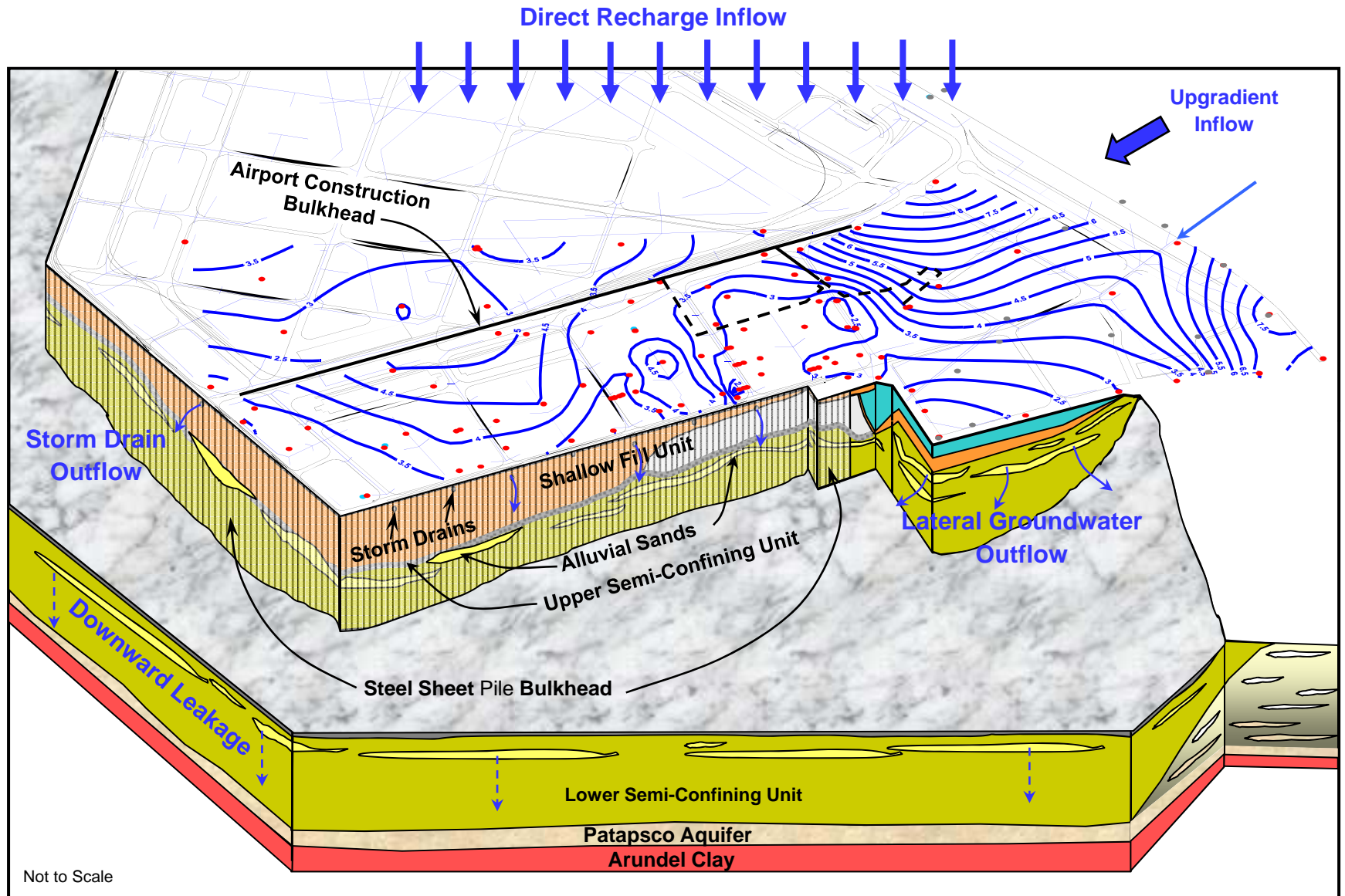
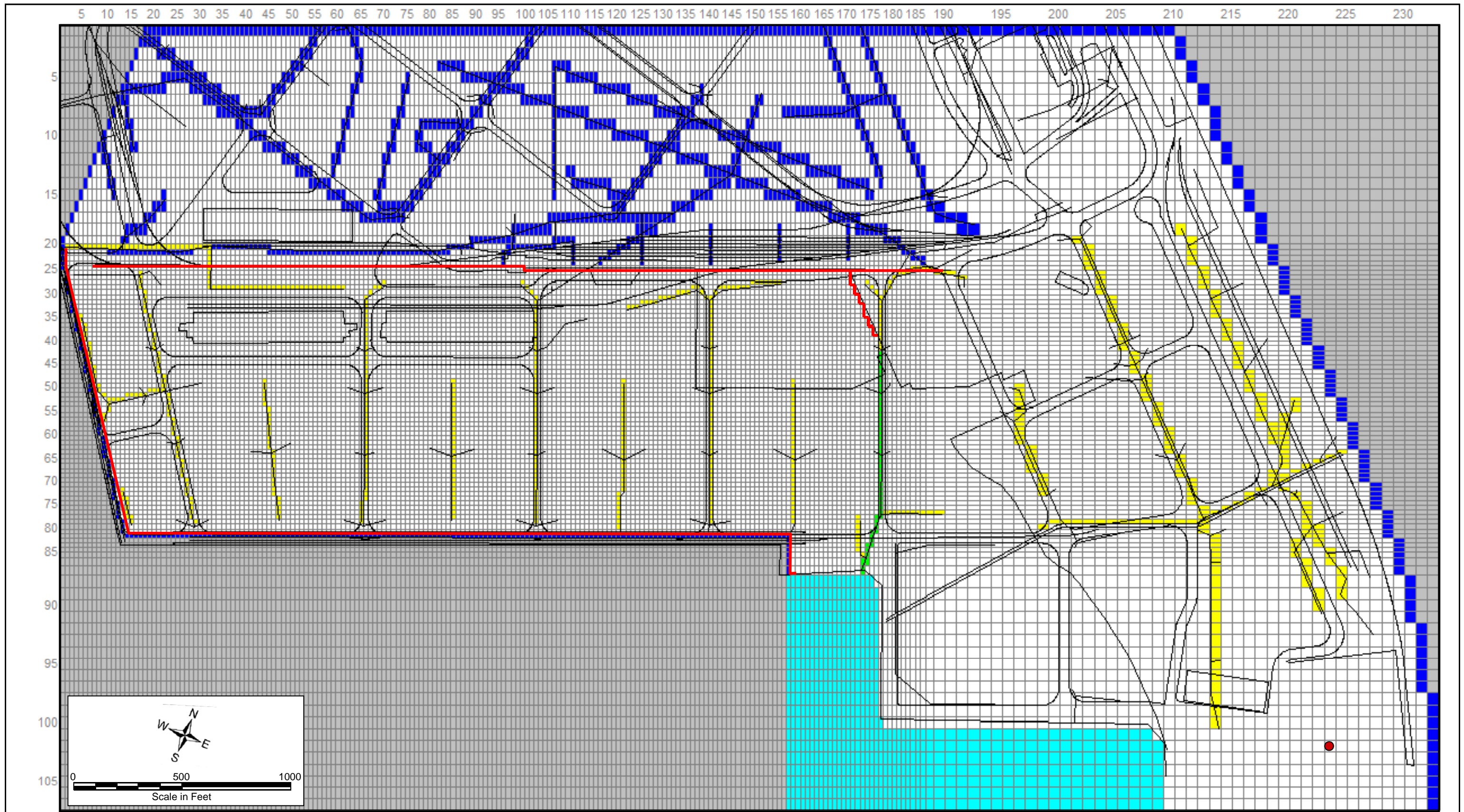


Figure B1-1
Vicinity Map of Dundalk Marine Terminal
Showing the Area of the Groundwater Model



Not to Scale

Figure B2-1
 Schematic Representation of the
 DMT Hydrogeologic Conceptual Model
 Dundalk Marine Terminal
 Baltimore, Maryland



- Boundary Condition Legend**
- Constant-Head Boundary Cell
 - Head-Dependent Flux Cell (GHB)
 - Head-Dependent Outflow Cell (DRN)
 - Head-Dependent Flux Cell (RIV)
 - No-Flow (Inactive) Cell
 - Specified Flux Injection Well
 - Horizontal Flow Barrier

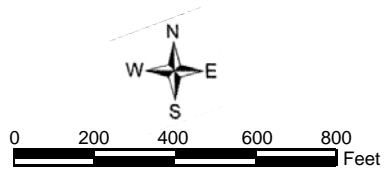
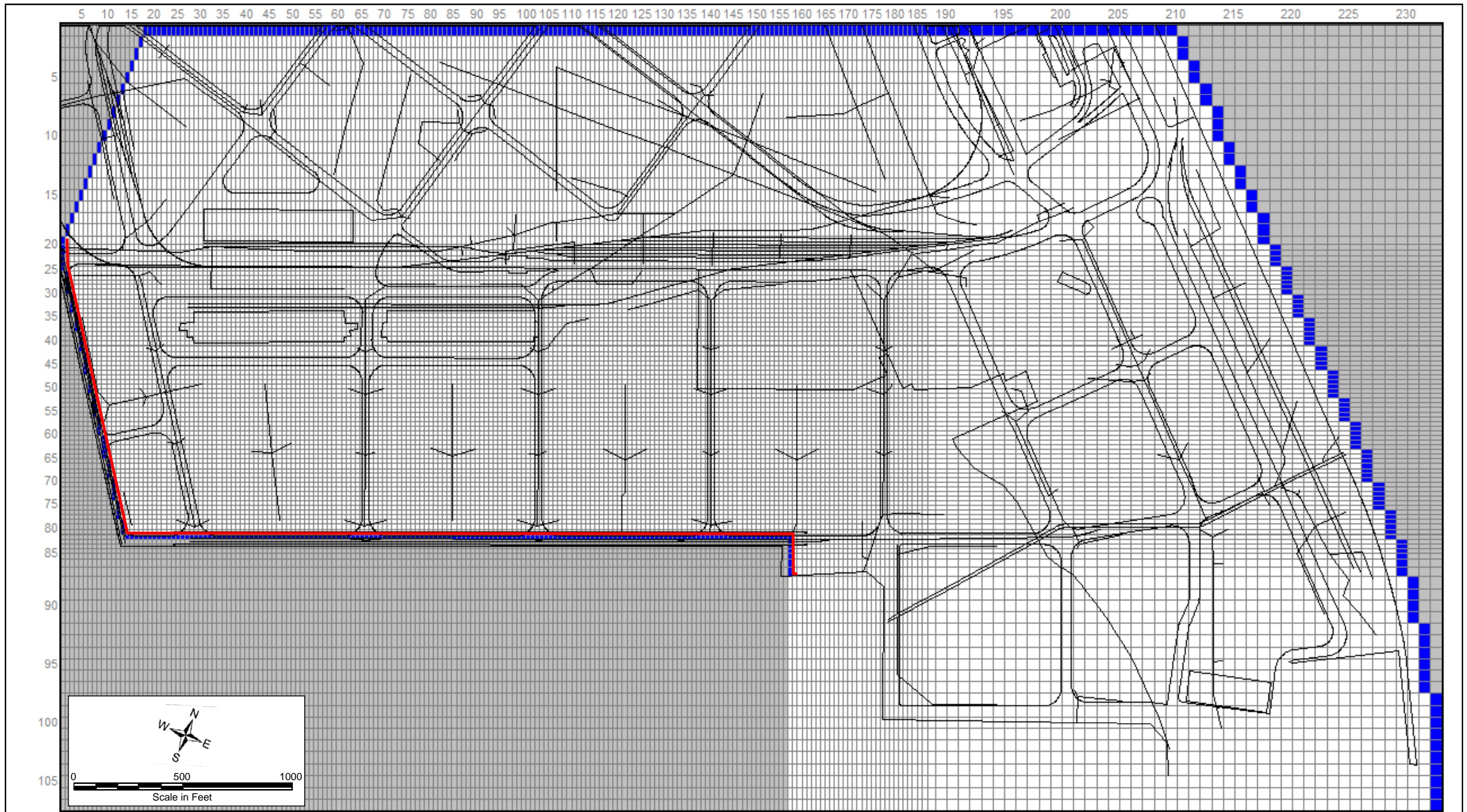
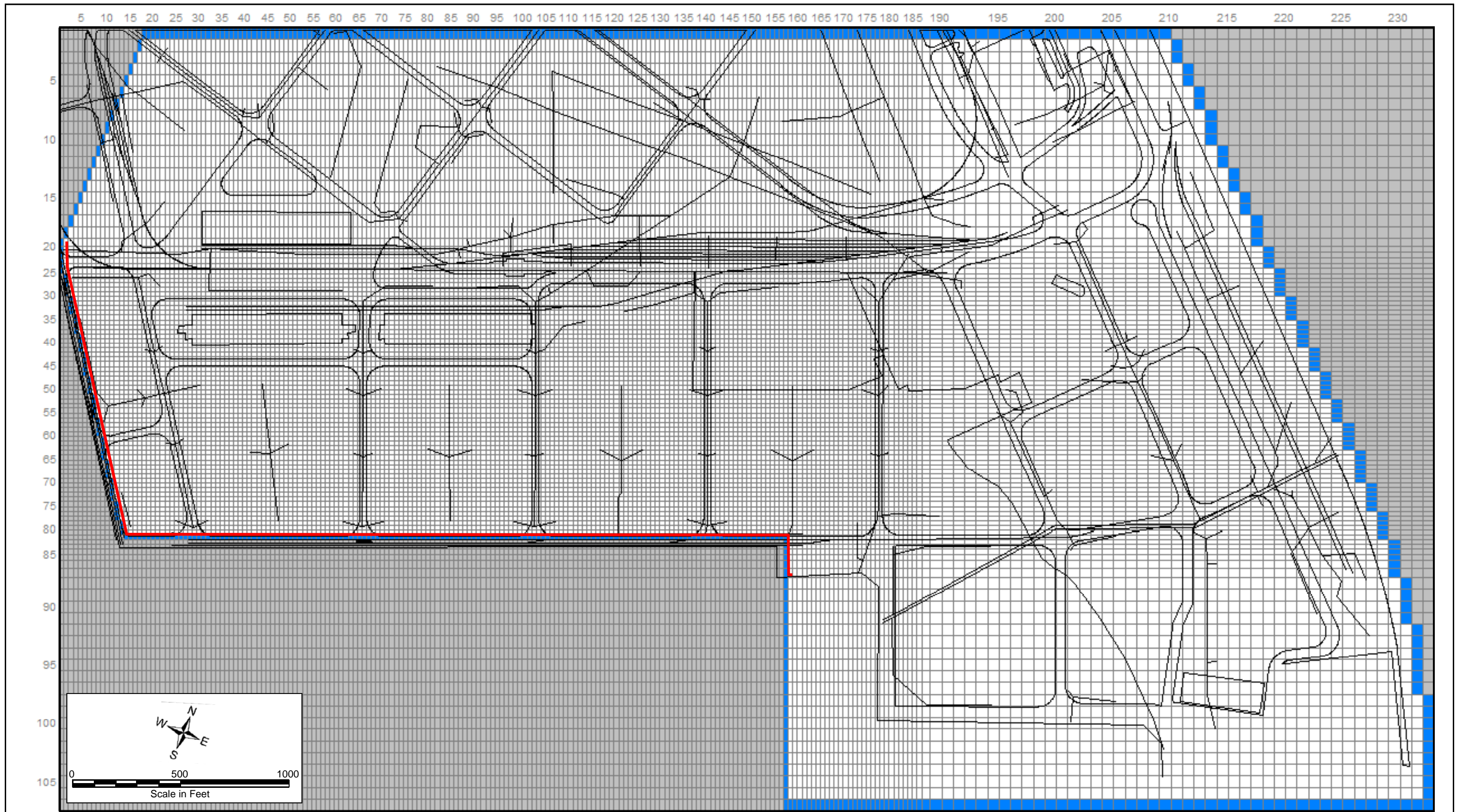


Figure B3-1
 Horizontal Grid Layout and Boundary Conditions in Layer 1
 Dundalk Marine Terminal
 Baltimore, Maryland



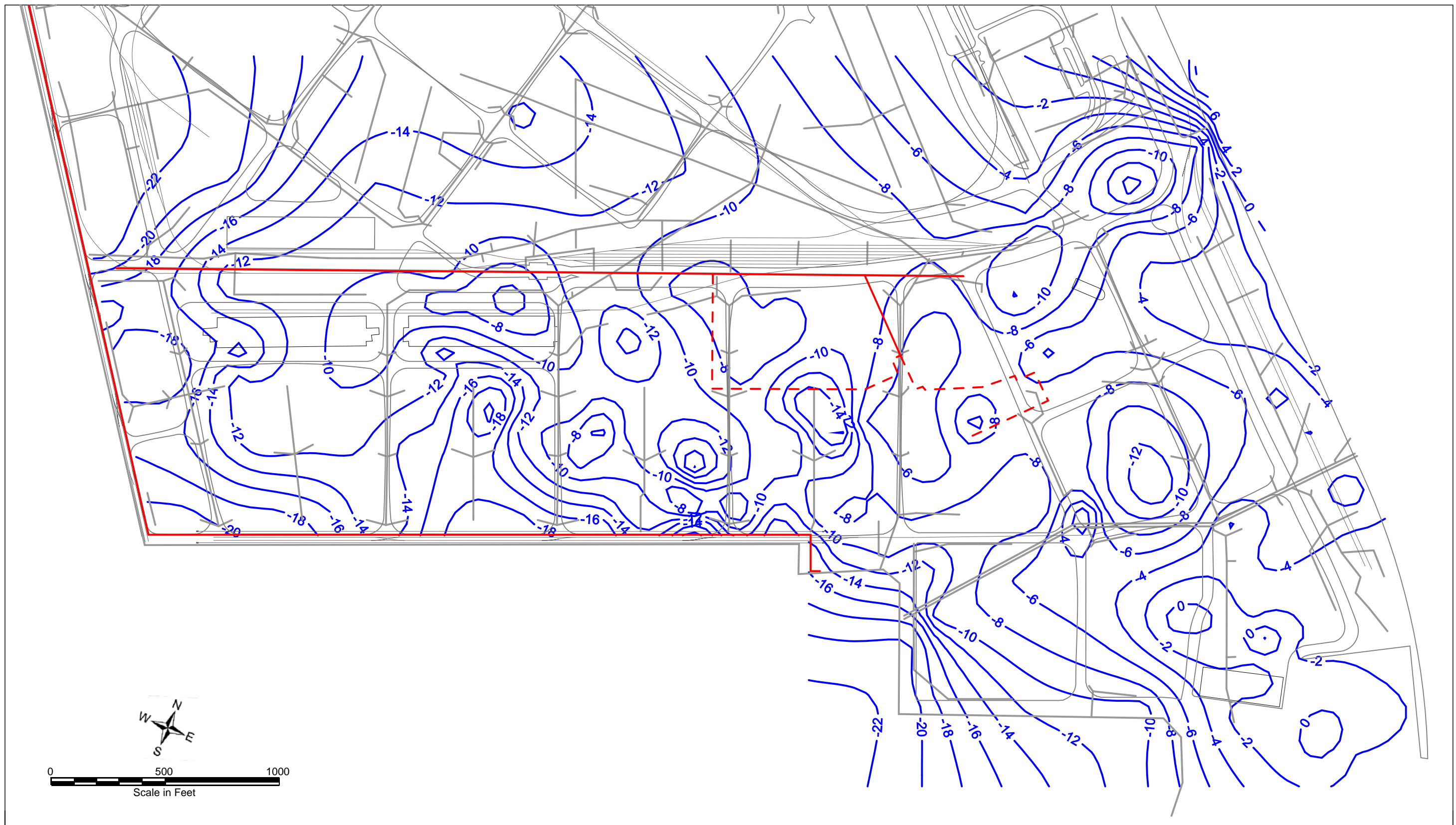
- Boundary Condition Legend**
- Constant-Head Boundary Cell
 - No-Flow (Inactive) Cell
 - Horizontal Flow Barrier

Figure B3-2
 Horizontal Grid Layout and Boundary Conditions in Layer 2
 Dundalk Marine Terminal
 Baltimore, Maryland



- Boundary Condition Legend**
- Constant-Head Boundary Cell
 - No-Flow (Inactive) Cell

Figure B3-3
 Horizontal Grid Layout and Boundary Conditions in Layer 3
 Dundalk Marine Terminal
 Baltimore, Maryland







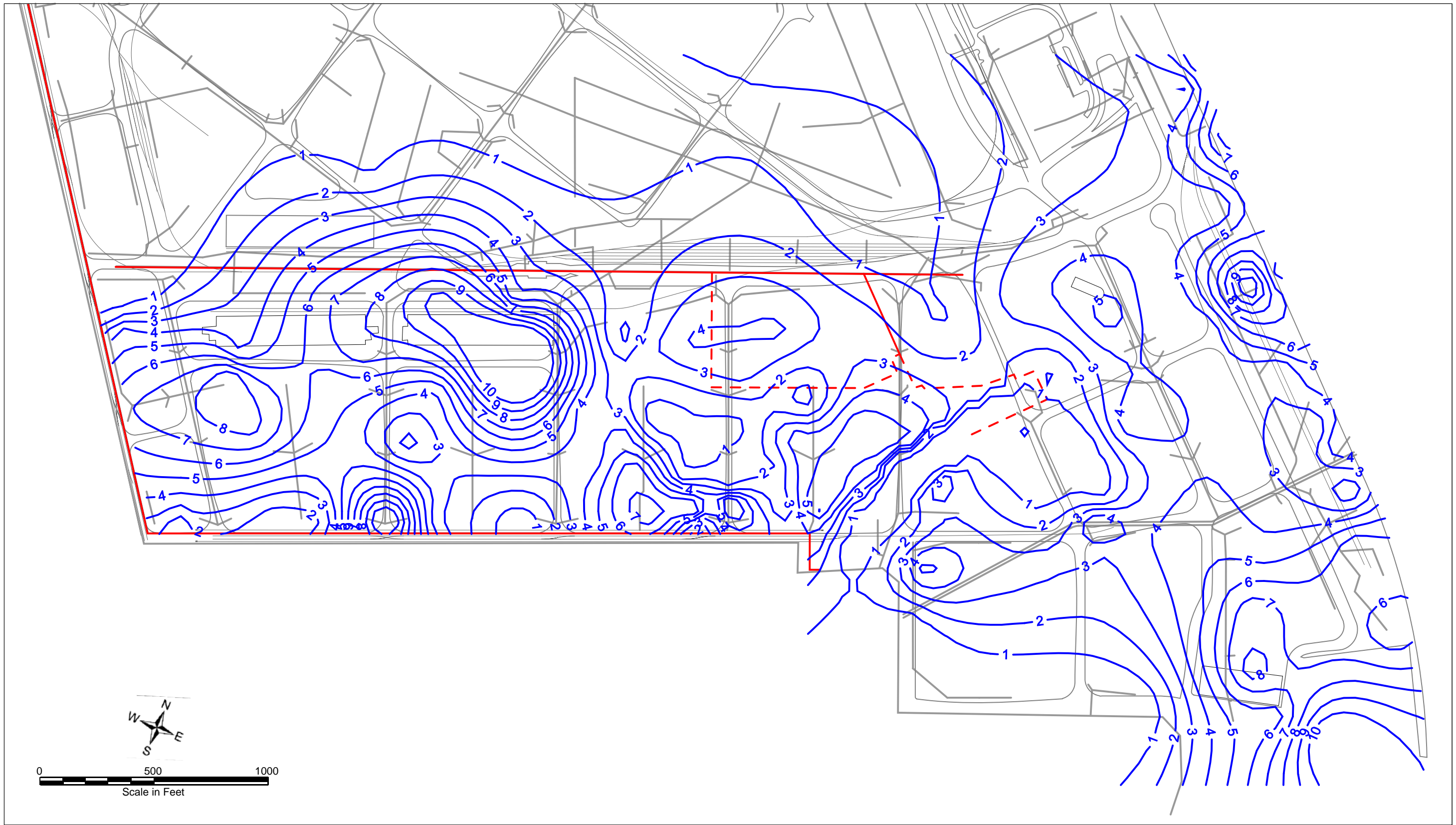
Legend	
	Storm Drain
	Existing Bulkhead
	Historic Bulkhead
	Elevation Contour (ft BCD)

Figure B3-4
 Bottom Elevation of Model Layer 1 (Shallow Fill Aquifer)
 Dundalk Marine Terminal
 Baltimore, Maryland







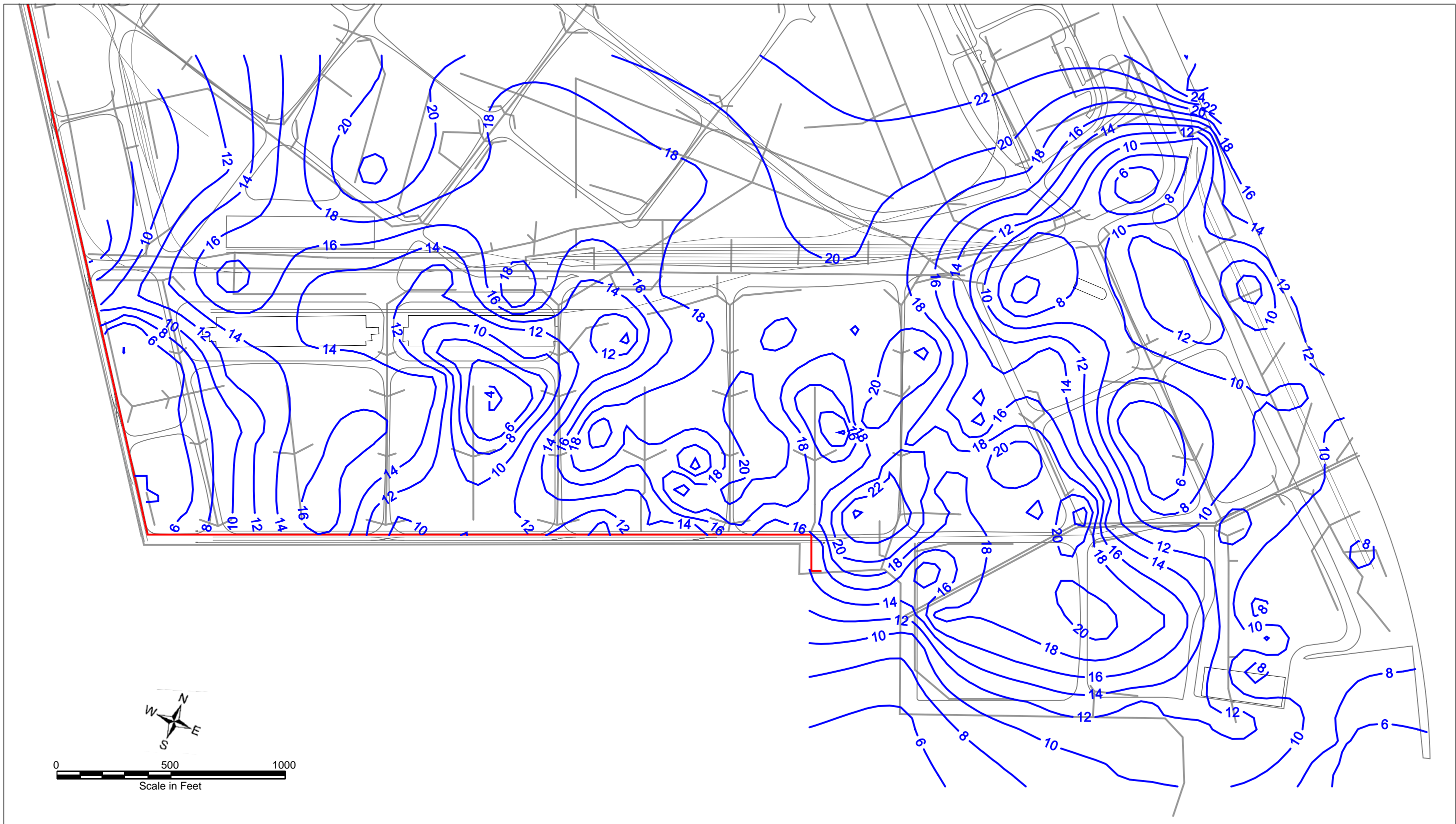
Legend	
	Storm Drain
	Existing Bulkhead
	Historic Bulkhead
	Thickness Contour (ft)

Figure B3-5
 Thickness of the Upper Semi-Confining Unit
 Between Layers 1 and 2
 Dundalk Marine Terminal
 Baltimore, Maryland






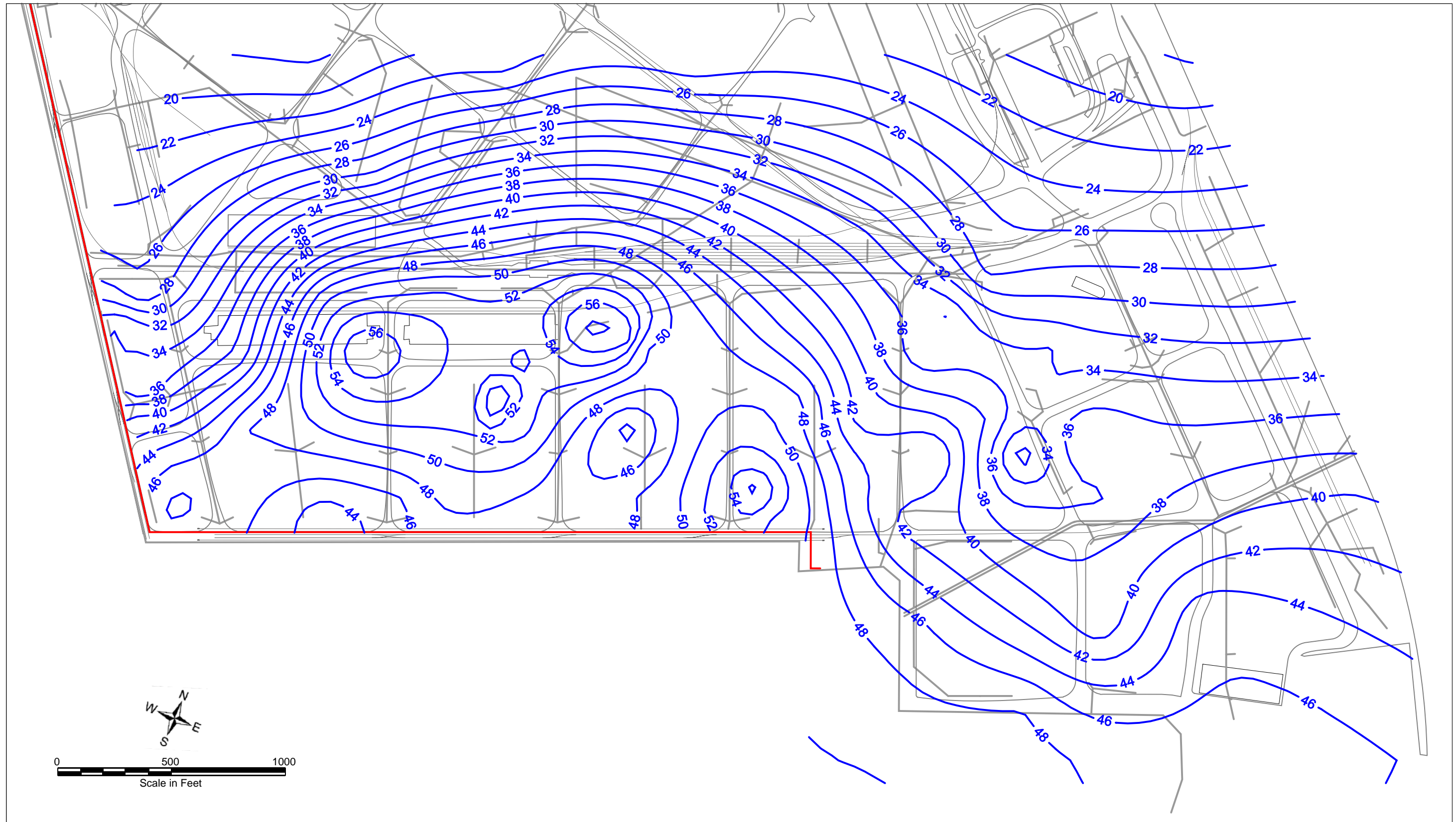
Legend	
	Storm Drain
	Existing Bulkhead
	Thickness Contour (ft)

Figure B3-6
 Thickness of Model Layer 2 (Alluvial Sands)
 Dundalk Marine Terminal
 Baltimore, Maryland






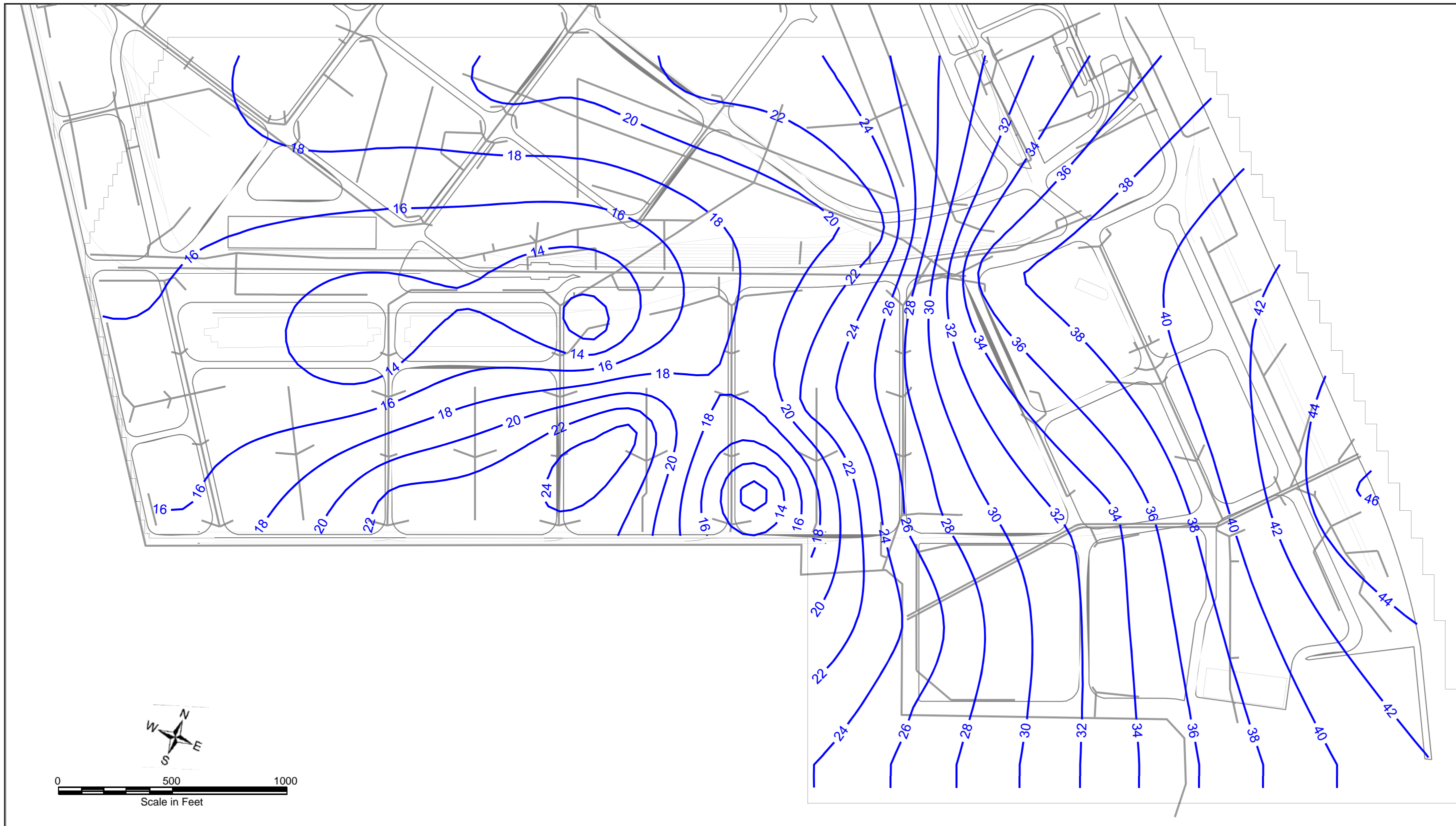
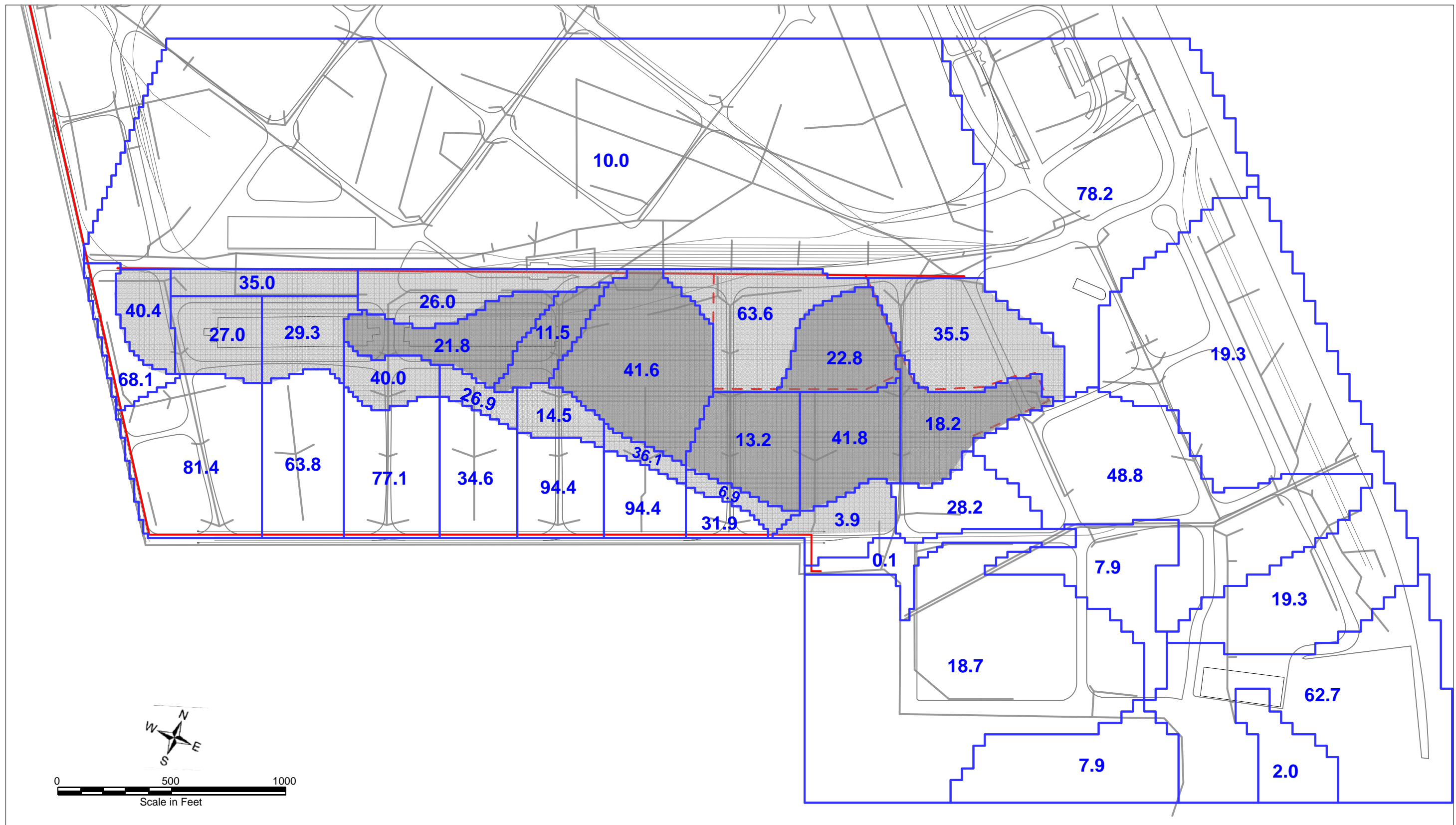
Legend	
	Storm Drain
	Existing Bulkhead
	Thickness Contour (ft)

Figure B3-7
 Thickness of the Lower Semi-Confining Unit
 Between Layers 2 and 3
 Dundalk Marine Terminal
 Baltimore, Maryland



Legend
 — Storm Drain
 — Thickness Contour (ft)

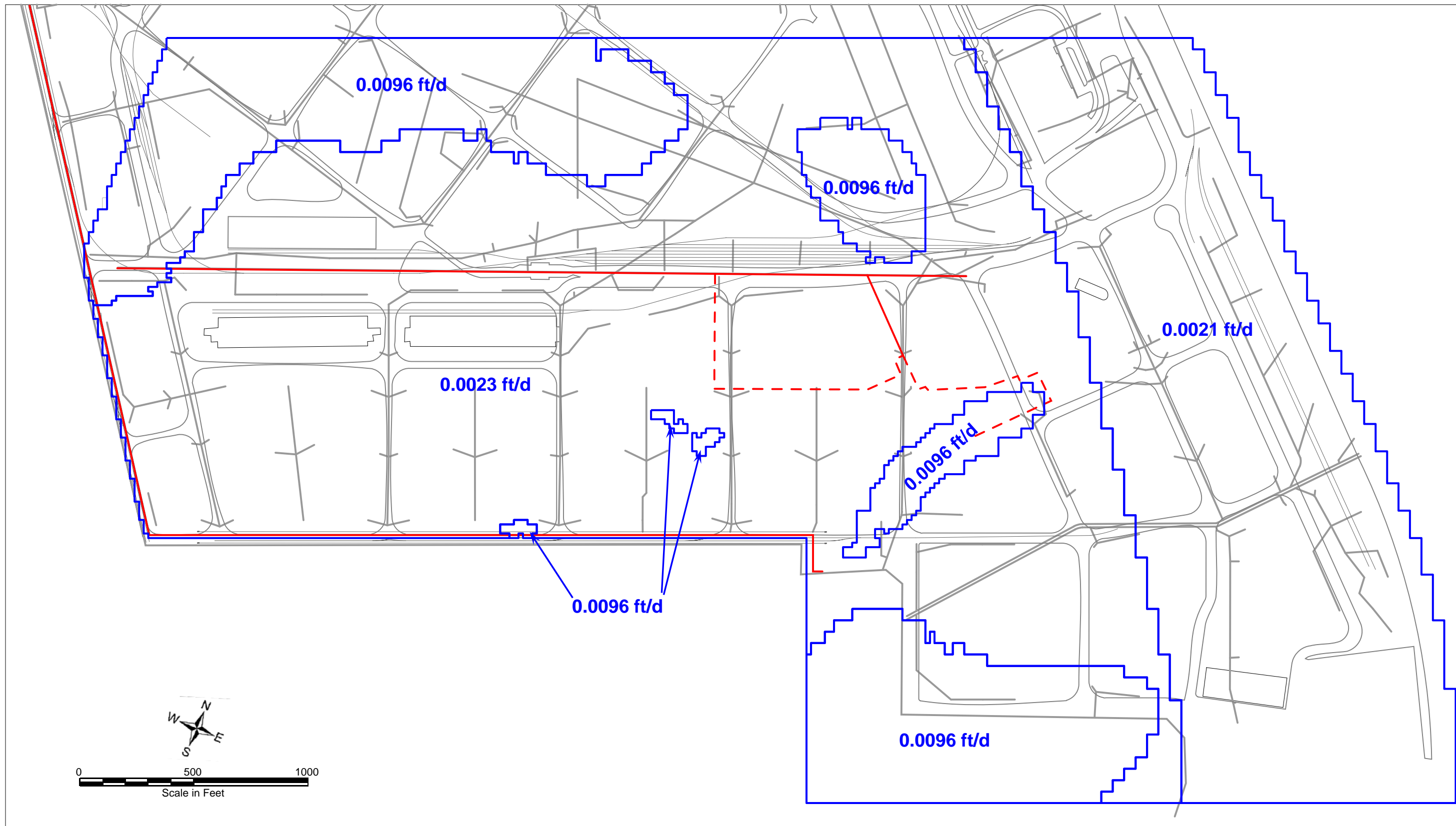
Figure B3-8
 Thickness of Model Layer 3 (Patapsco Aquifer)
 Dundalk Marine Terminal
 Baltimore, Maryland



Legend

- Storm Drain
- Existing Bulkhead
- - - Historic Bulkhead
- Predominantly COPR Fill
- 40% - 60% COPR Fill
- 31.9 Simulated Hydraulic Conductivity (ft/day)

Figure B3-9
 Calibrated Distribution of Hydraulic Conductivity
 In Model Layer 1 (Shallow Fill Aquifer)
 Dundalk Marine Terminal
 Baltimore, Maryland






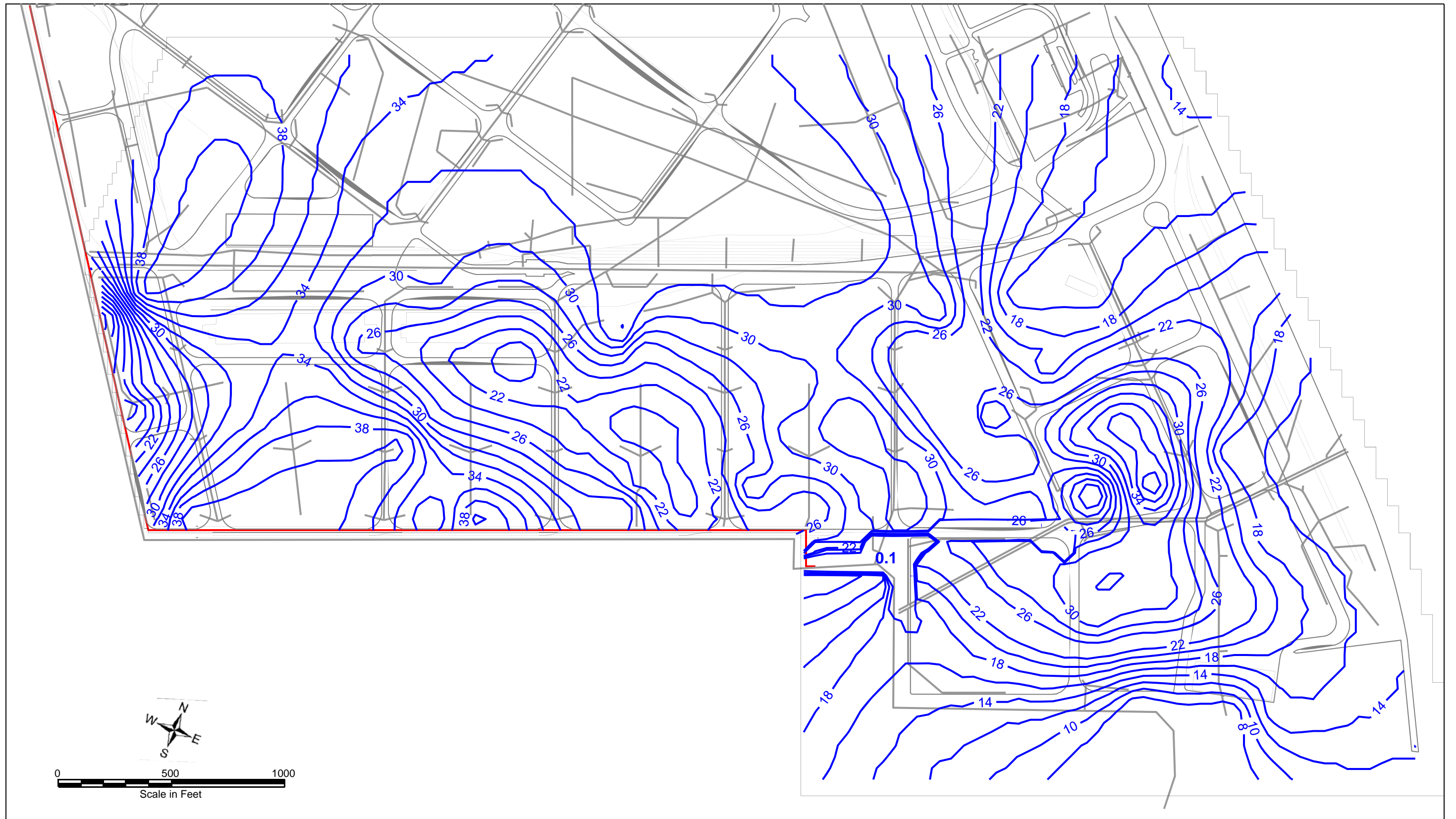
Legend	
	Storm Drain
	Existing Bulkhead
	Historic Bulkhead
0.0023	Simulated Hydraulic Conductivity (ft/day)

Figure B3-10
 Calibrated Distribution of Hydraulic Conductivity
 of the Upper Semi-Confining Unit
 Dundalk Marine Terminal
 Baltimore, Maryland






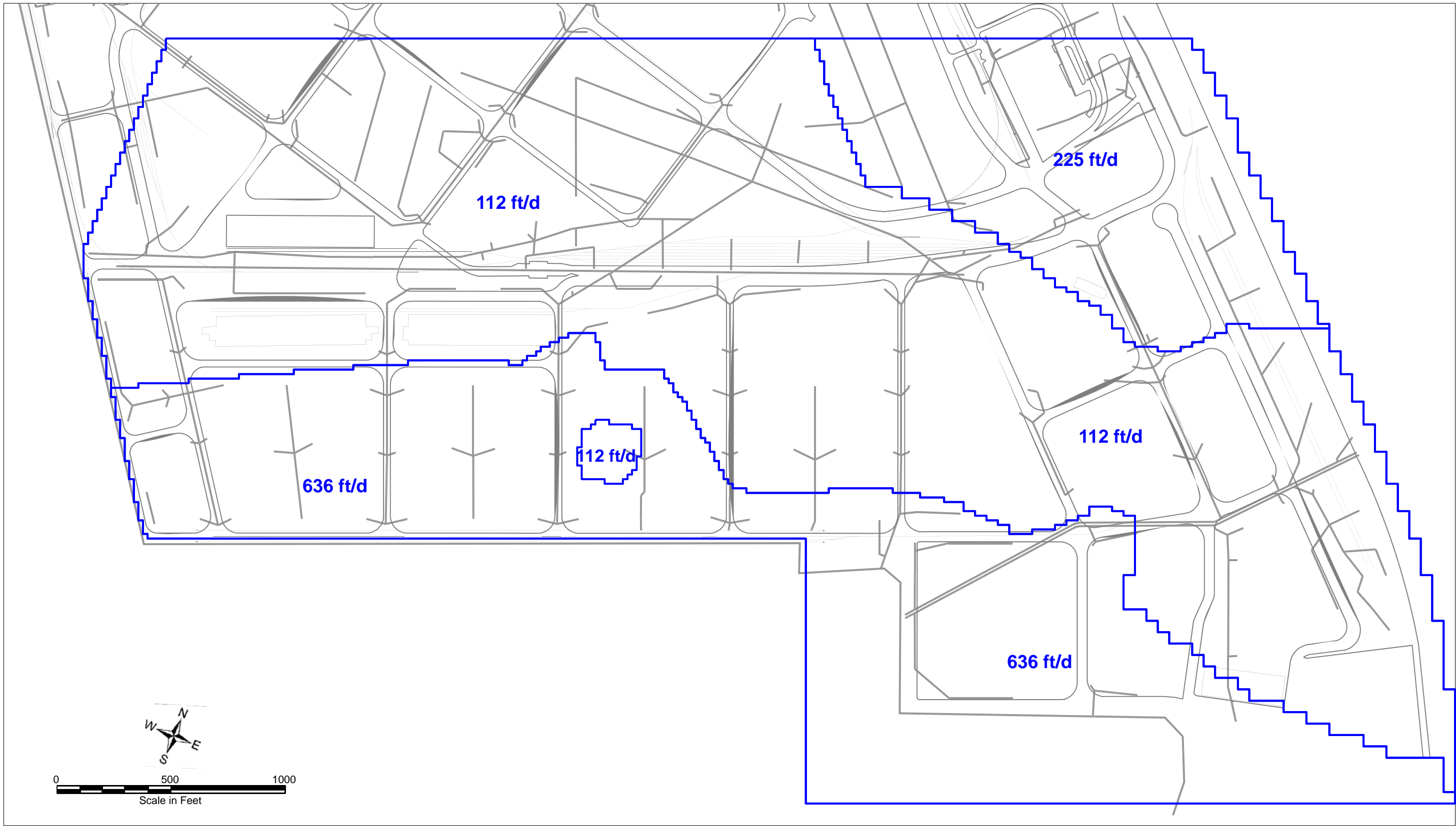
- Legend**
-  Storm Drain
 -  Existing Bulkhead
 -  Hydraulic Conductivity (ft/day)

Figure B3-11
 Calibrated Distribution of Hydraulic Conductivity
 in Model Layer 2 (Alluvial Sands)
 Dundalk Marine Terminal
 Baltimore, Maryland




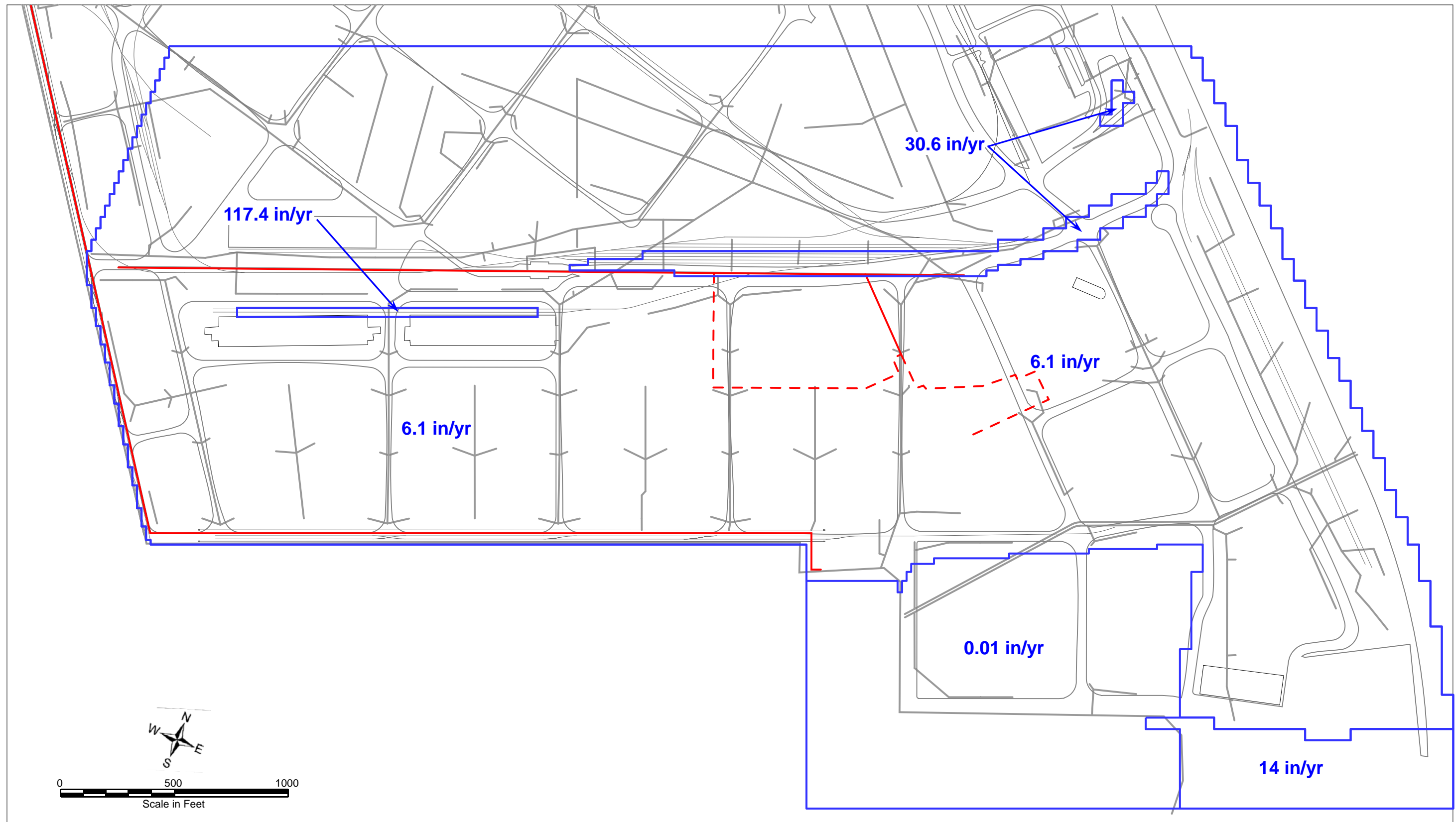
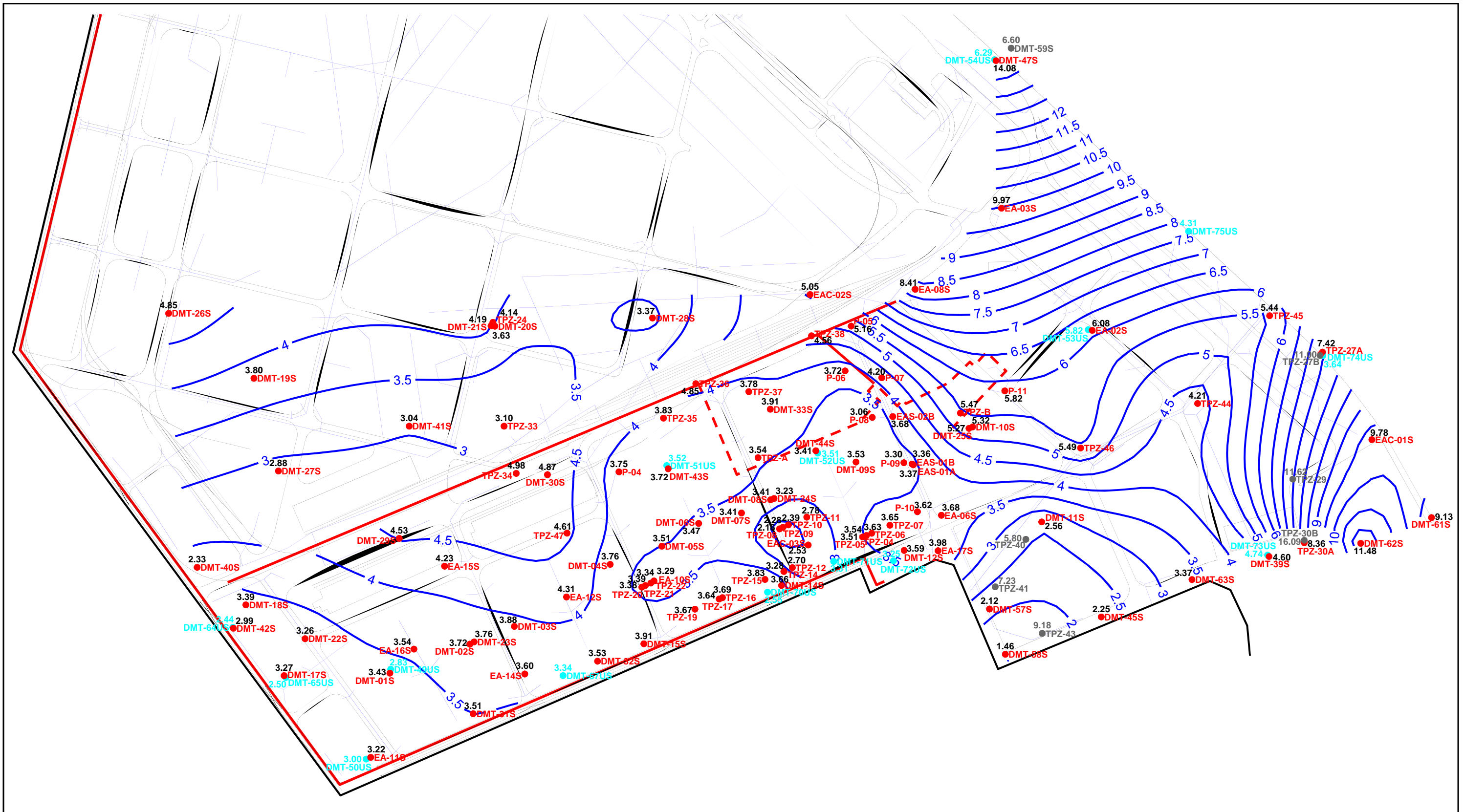
Legend	
	Storm Drain
112	Hydraulic Conductivity (ft/day)

Figure B3-12
 Calibrated Distribution of Hydraulic Conductivity
 in Model Layer 3 (Potomac Aquifer)
 (Hydraulic Conductivity in ft/d)
 Dundalk Marine Terminal
 Baltimore, Maryland



Legend	
	Storm Drain
	Existing Bulkhead
	Historic Bulkhead
6.1	Simulated Recharge Rate (in/yr)

Figure B3-13
 Calibrated Distribution of Recharge
 to Model Layer 1
 Dundalk Marine Terminal
 Baltimore, Maryland



Legend

- 3.36 ● EA-17S Shallow Well and Water Level
- 6.58 ● TPZ-41 Non-Aquifer Well and Water Level
- 3.49 ● DMT-51US Alluvial Sand Well and Water Level
- 4 — Shallow Aquifer Potentiometric Contour
(All Levels in Feet, Baltimore City Datum)
- Bulkhead

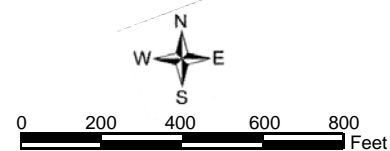


Figure B4-1
 Water Levels Measured in Shallow Fill Aquifer
 and the Alluvial Sand (US) wells on June 2, 2009
 Dundalk Marine Terminal
 Baltimore, Maryland



Legend

- 3.36 ● EA-17S Patapsco Well and Water Level
- 4 — Patapsco Aquifer Potentiometric Contour
- 1.46* Water Level Not Used for Contouring
- 2.09* Measurement Taken on 6/4/09
- (All Levels in Feet, Baltimore City Datum)

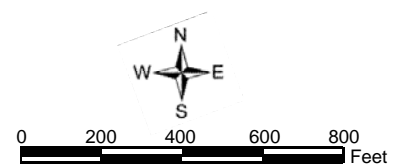
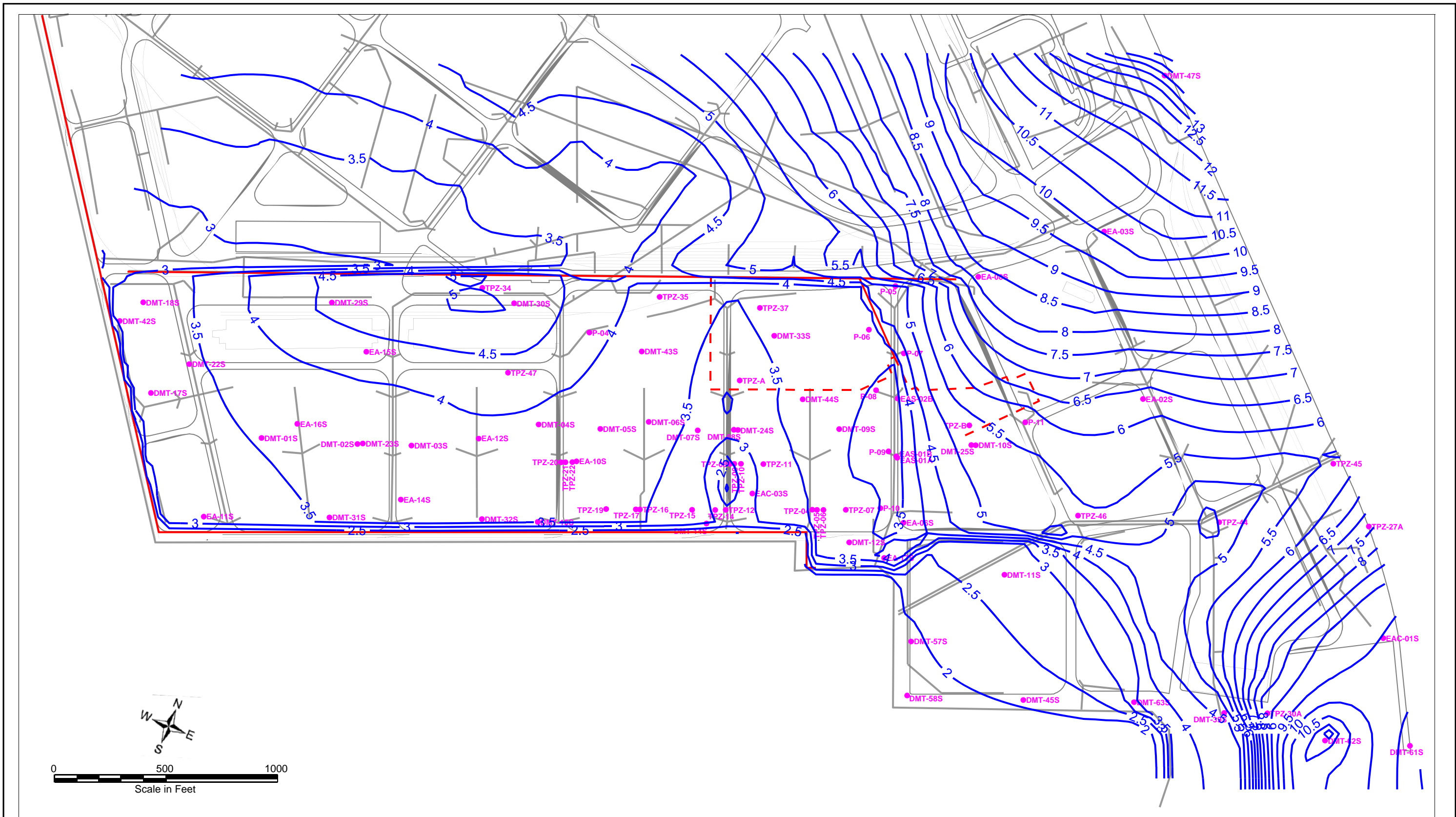
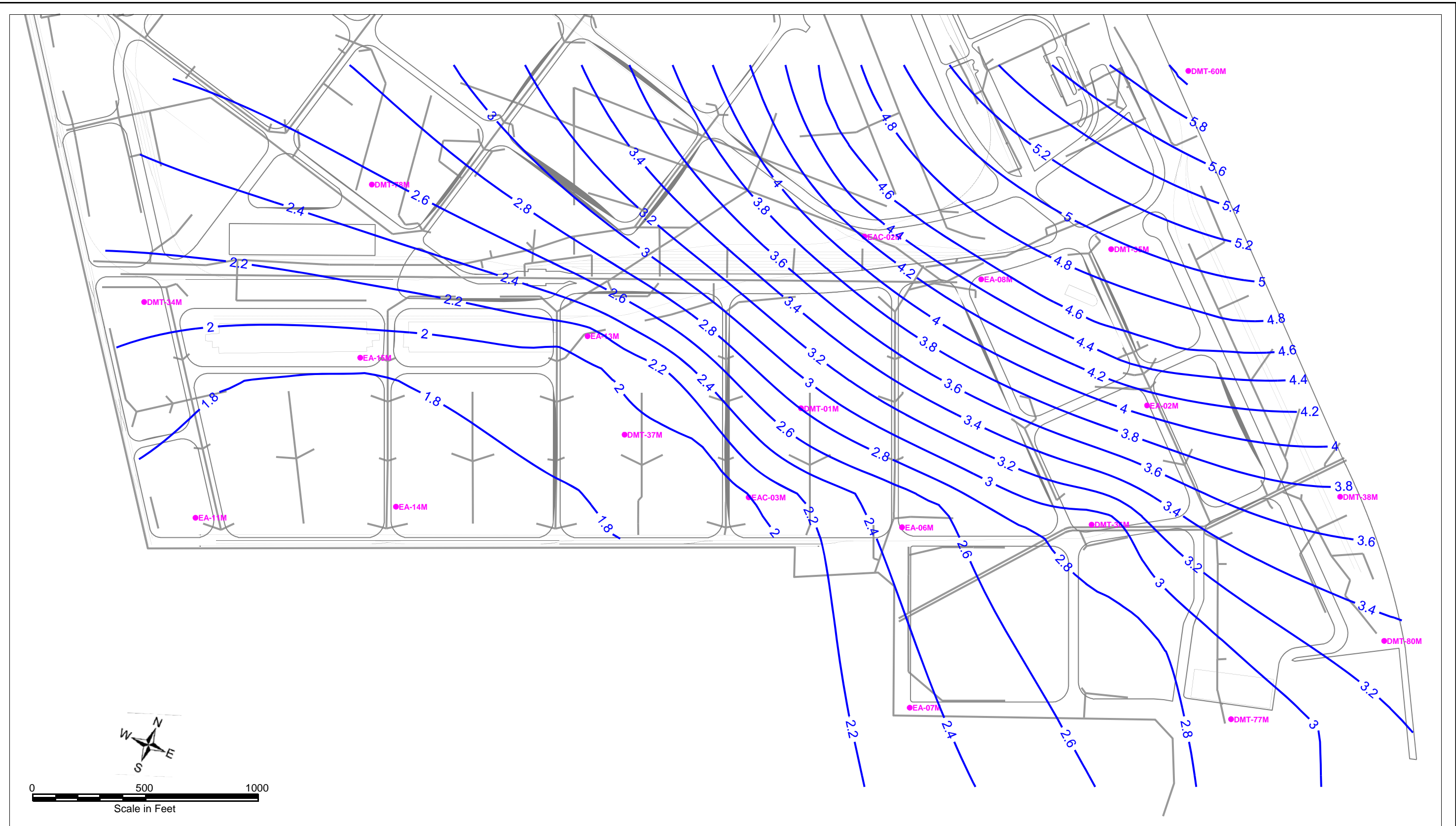


Figure B4-2
 Water Levels Measured in the Patapsco Aquifer
 June 2, 2009
 Dundalk Marine Terminal
 Baltimore, Maryland



- Legend**
- EA-17S Shallow Well
 - 4 — Simulated Shallow Aquifer Potentiometric Contour
(All Levels in Feet, Baltimore City Datum)
 - Bulkhead

Figure B4-3
 Groundwater Levels Simulated in Shallow Fill Aquifer
 for June 2, 2009 by the Calibrated Model
 Dundalk Marine Terminal
 Baltimore, Maryland



Legend

- EA-17S Patapsco Aquifer Well
- 4 — Simulated Patapsco Aquifer Potentiometric Contour
(All Levels in Feet, Baltimore City Datum)

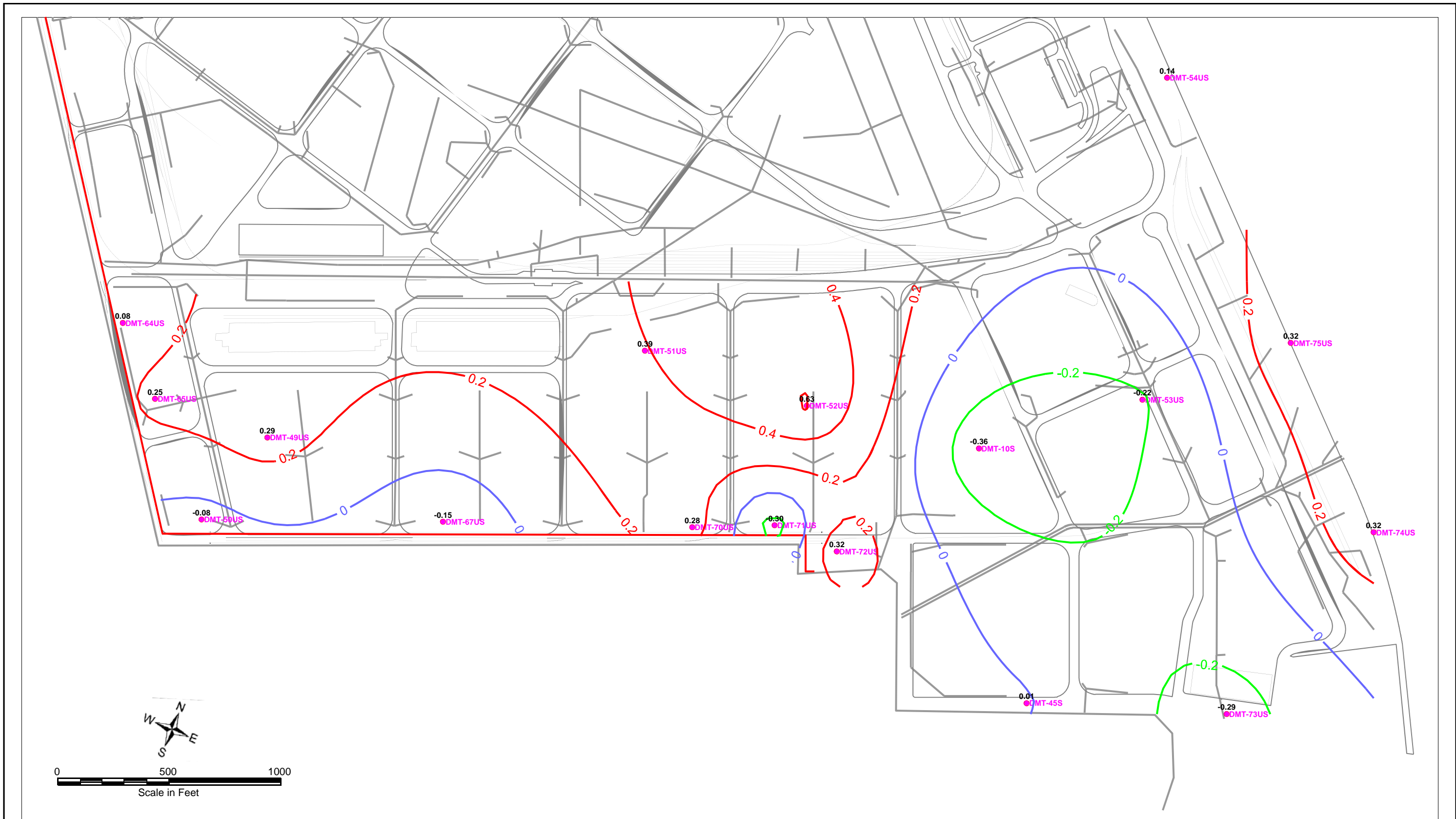
Figure B4-4
 Groundwater Levels Simulated in the Patapsco
 Aquifer for June 2, 2009 by the Calibrated Model
 Dundalk Marine Terminal
 Baltimore, Maryland



Legend

- 0.02 EA-17S Shallow Aquifer Well and Calibration Residual (ft)
- 0.2 Contour of Negative Residual (model lower than measurements)
- 0.2 Contour of Positive Residual (model higher than measurements)
- 0 Contour of Zero Residual (model equals measurements)

Figure B4-5
 Distribution of Residuals in the Shallow Fill Aquifer,
 Simulated Levels Minus Observed Levels, June 2, 2009
 Dundalk Marine Terminal
 Baltimore, Maryland

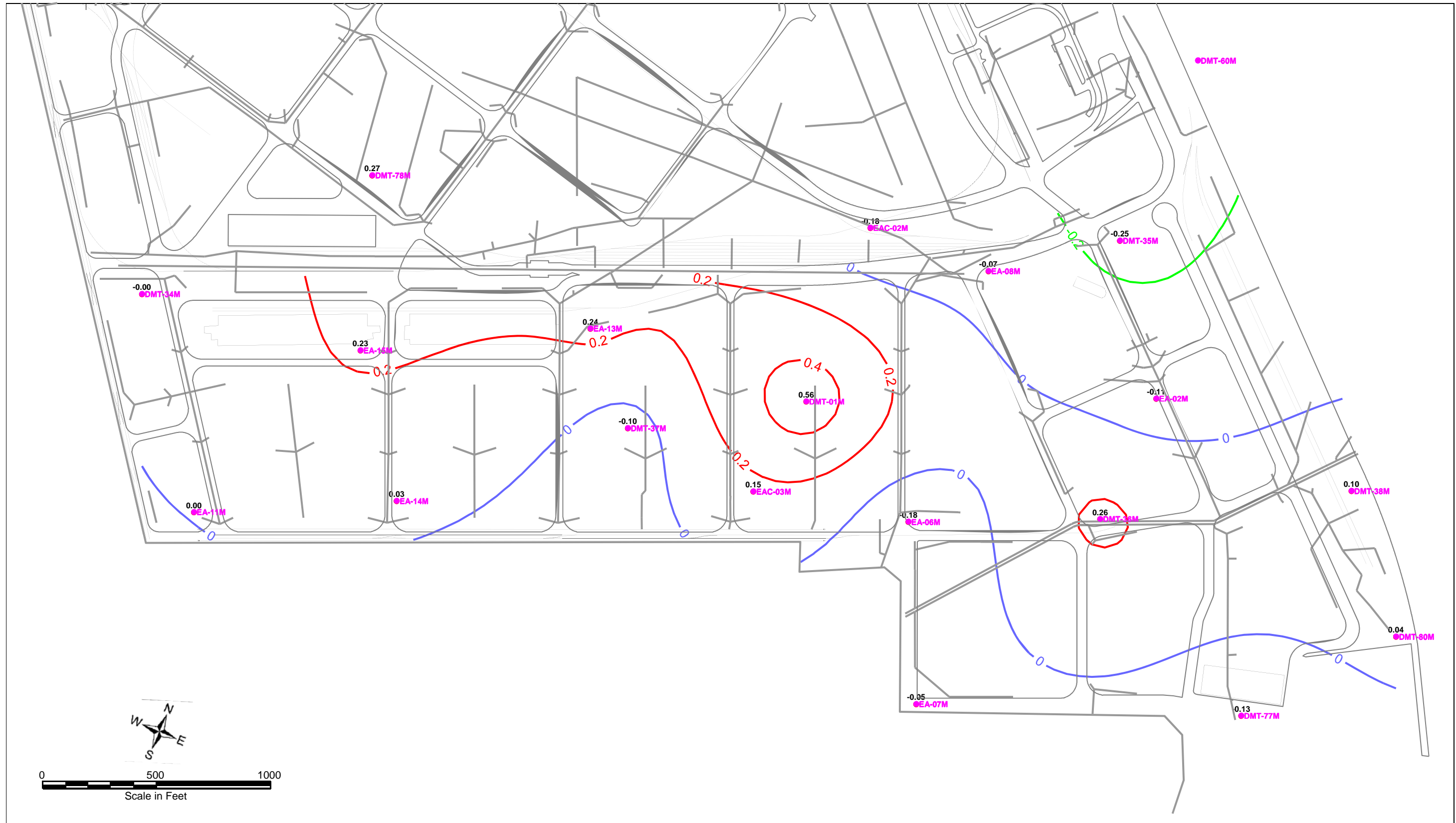


Legend

- 0.02 DMT-50US Alluvial Sand Well and Calibration Residual (ft)
- 0.2 Contour of Negative Residual (model lower than measurements)
- 0.2 Contour of Positive Residual (model higher than measurements)
- 0 Contour of Zero Residual (model equals measurements)

Figure B4-6

Distribution of Residuals in the Alluvial Sands,
 Simulated Levels Minus Observed Levels, June 2, 2009
 Dundalk Marine Terminal
 Baltimore, Maryland



Legend

- -0.2 Contour of Negative Residual (model lower than measurements)
- 0.2 Contour of Positive Residual (model higher than measurements)
- 0 Contour of Zero Residual (model equals measurements)

Figure B4-7
 Distribution of Residuals in the Patapsco Aquifer,
 Simulated Levels Minus Observed Levels, June 2, 2009
 (Residuals in Feet)

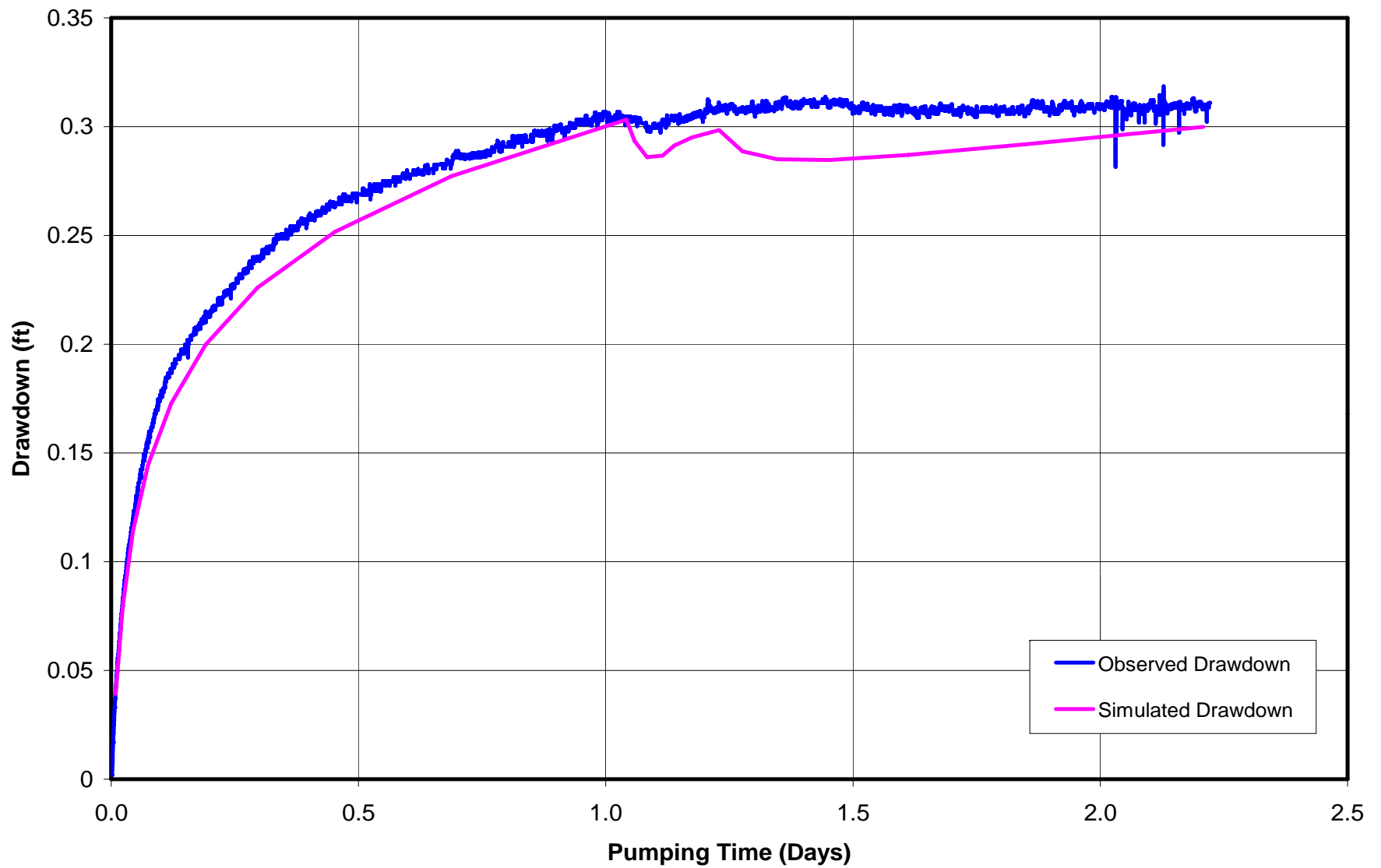


Figure B4-8

Comparison of Simulated vs. Observed Time-Drawdown Response at Observation Well DMT-02S for the Aquifer Test at DMT-23S, November 4 – 6, 2006

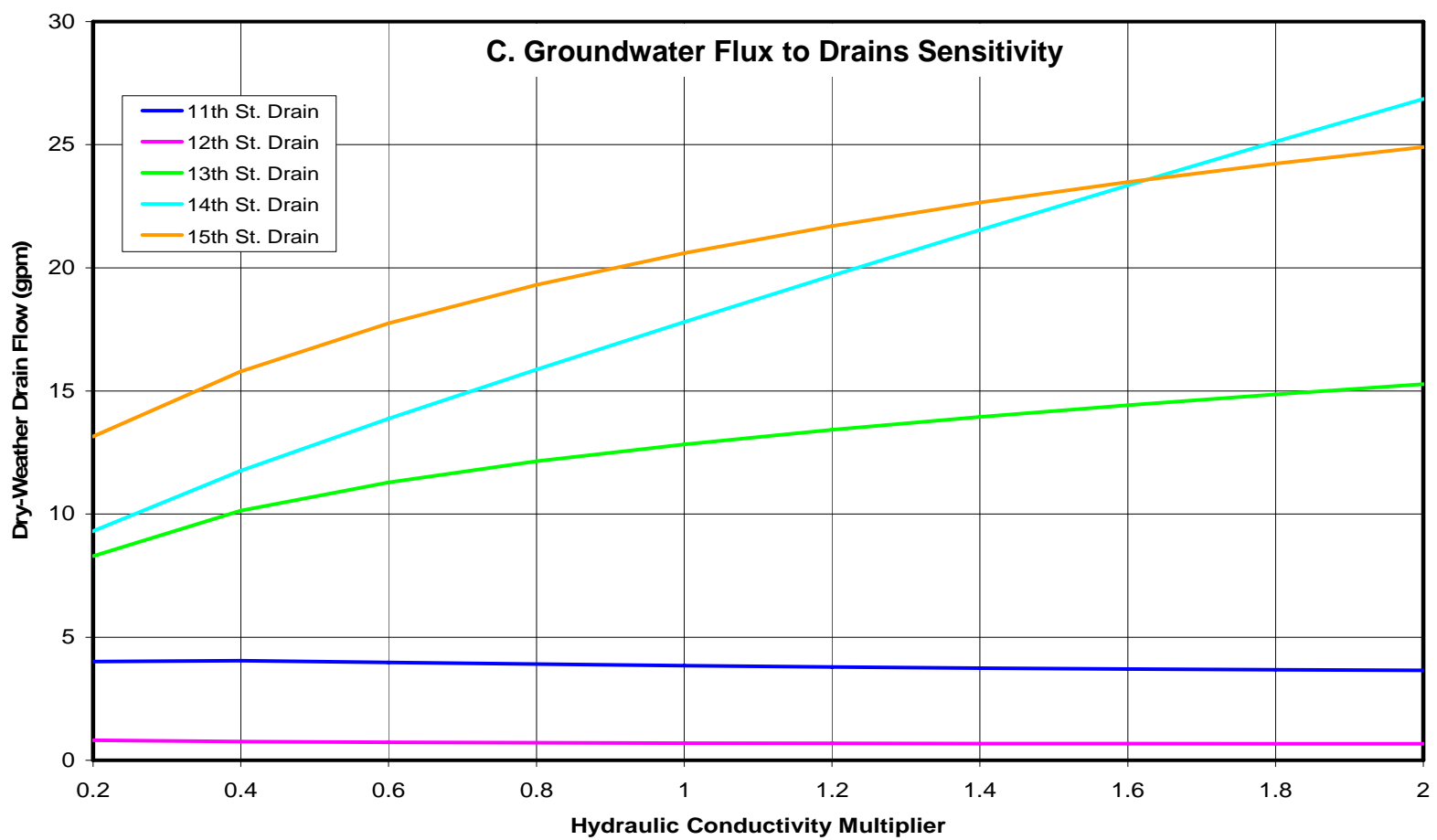
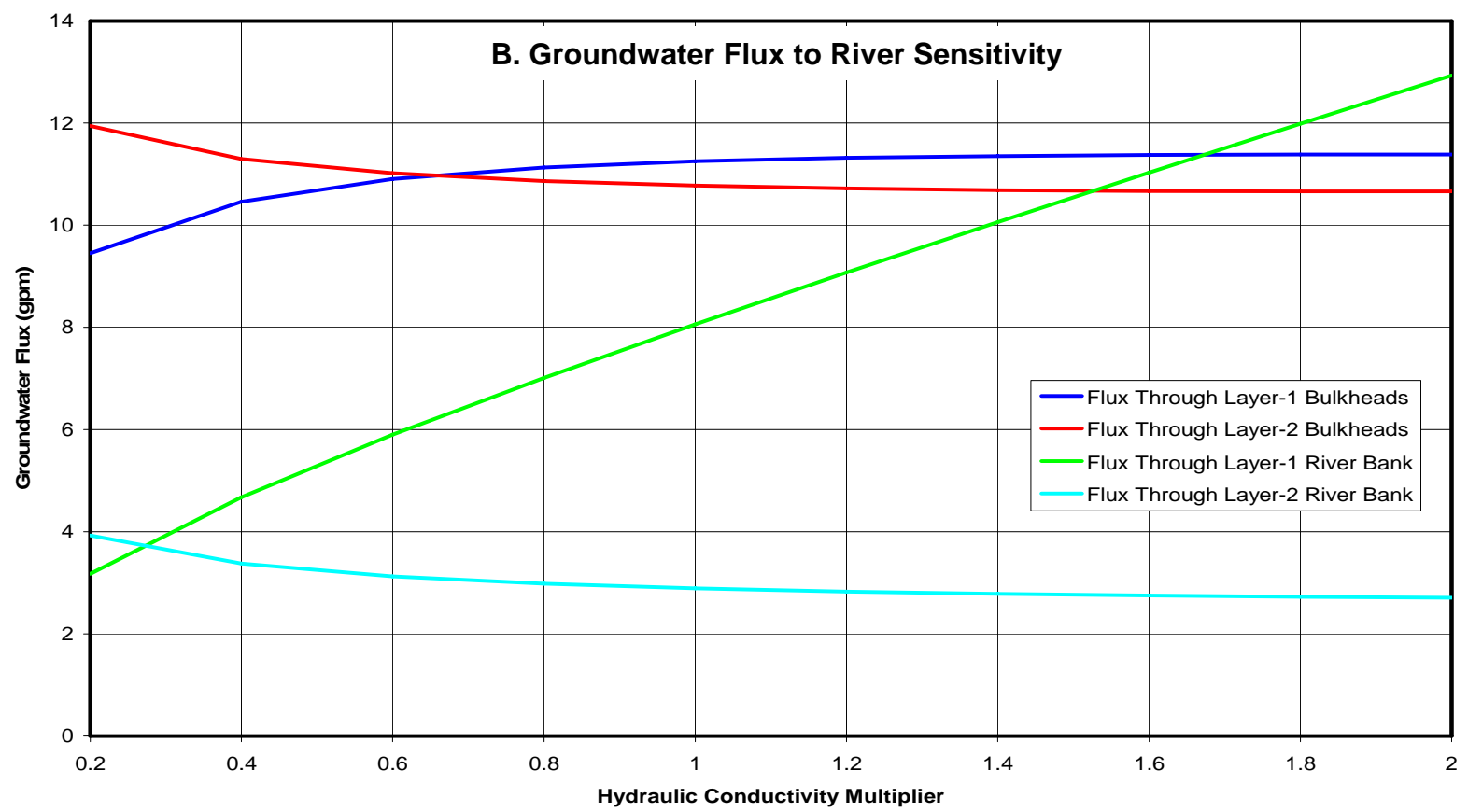
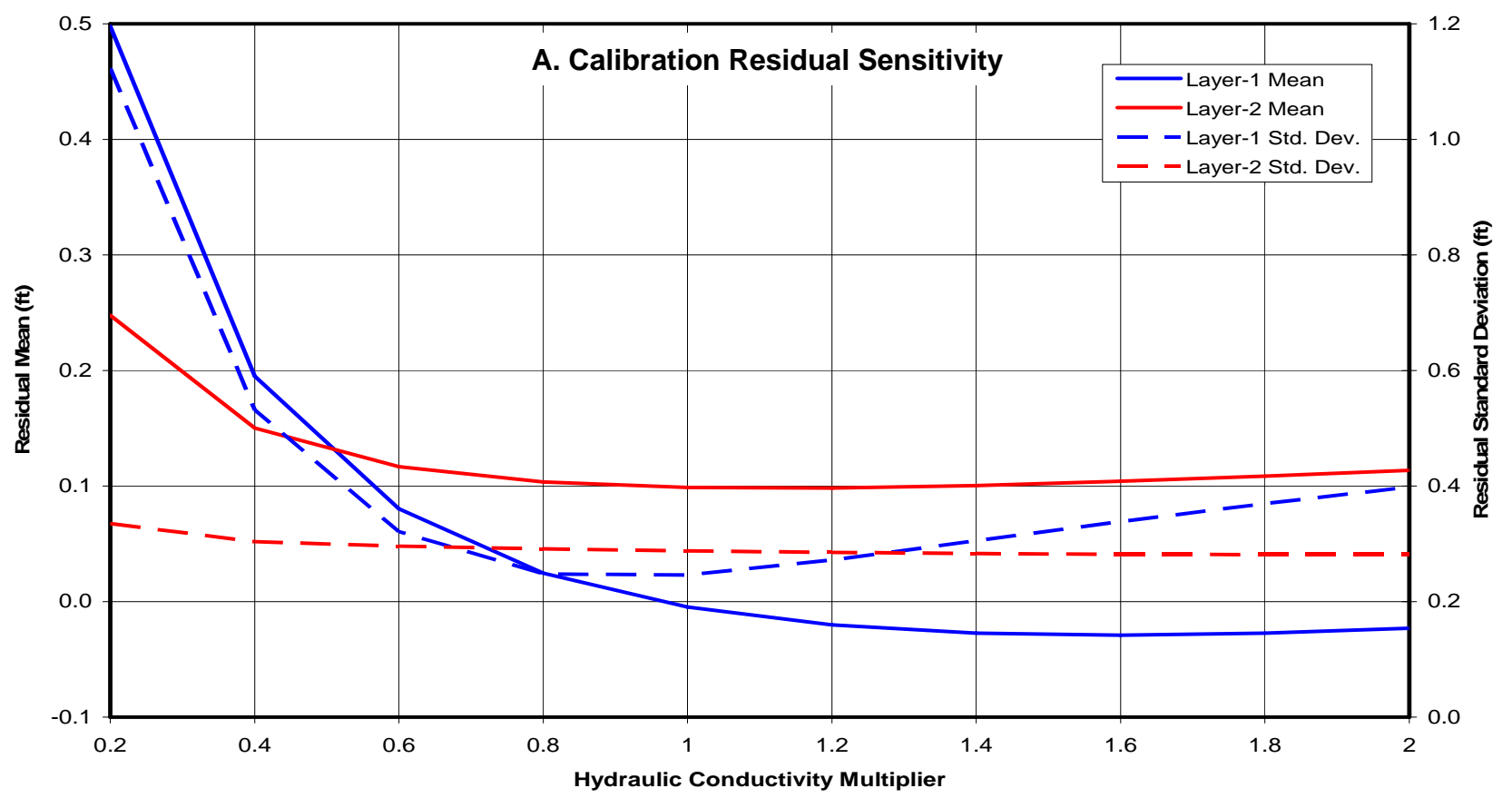


Figure B5-1
Sensitivity Analysis Results for Layer-1 Hydraulic Conductivity

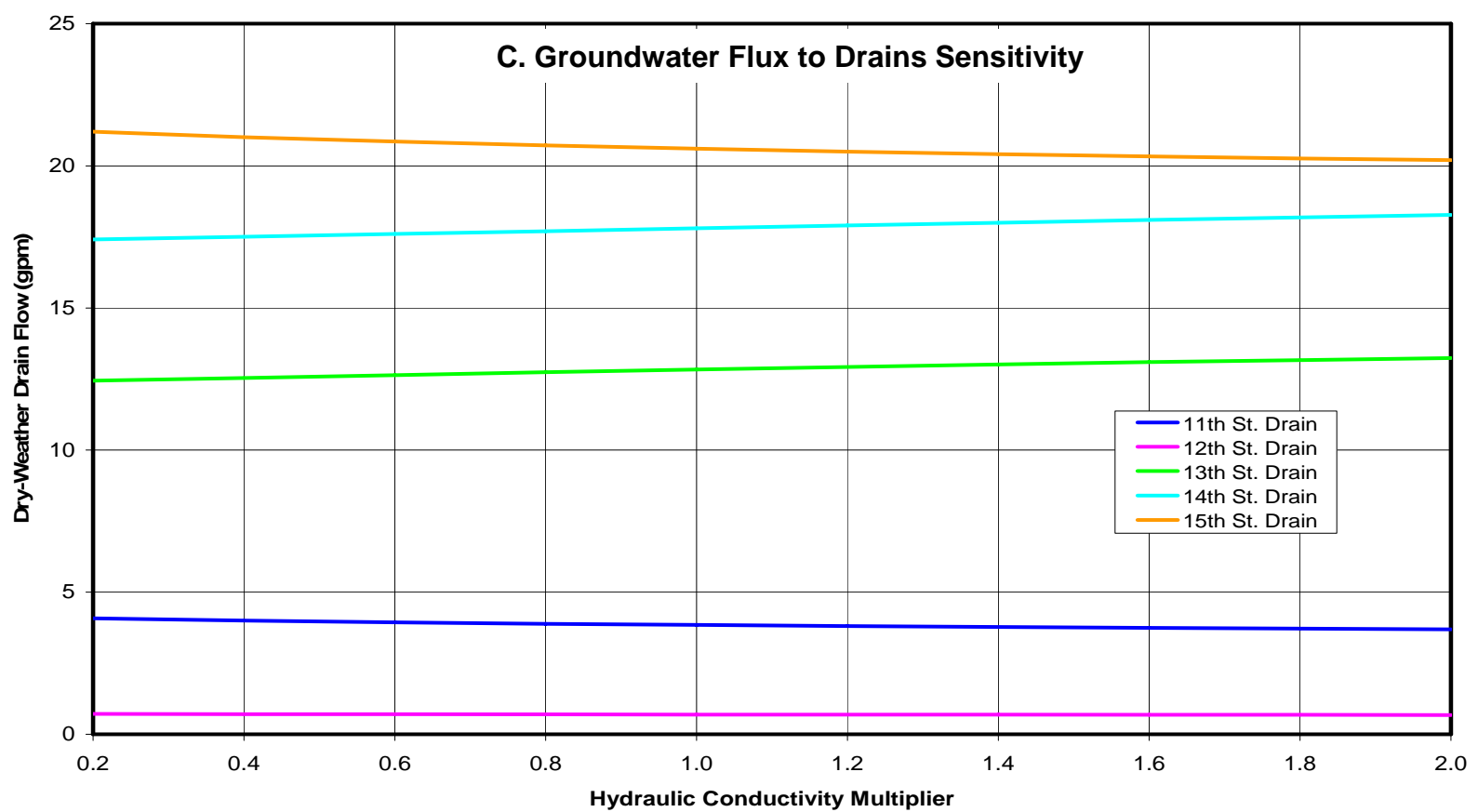
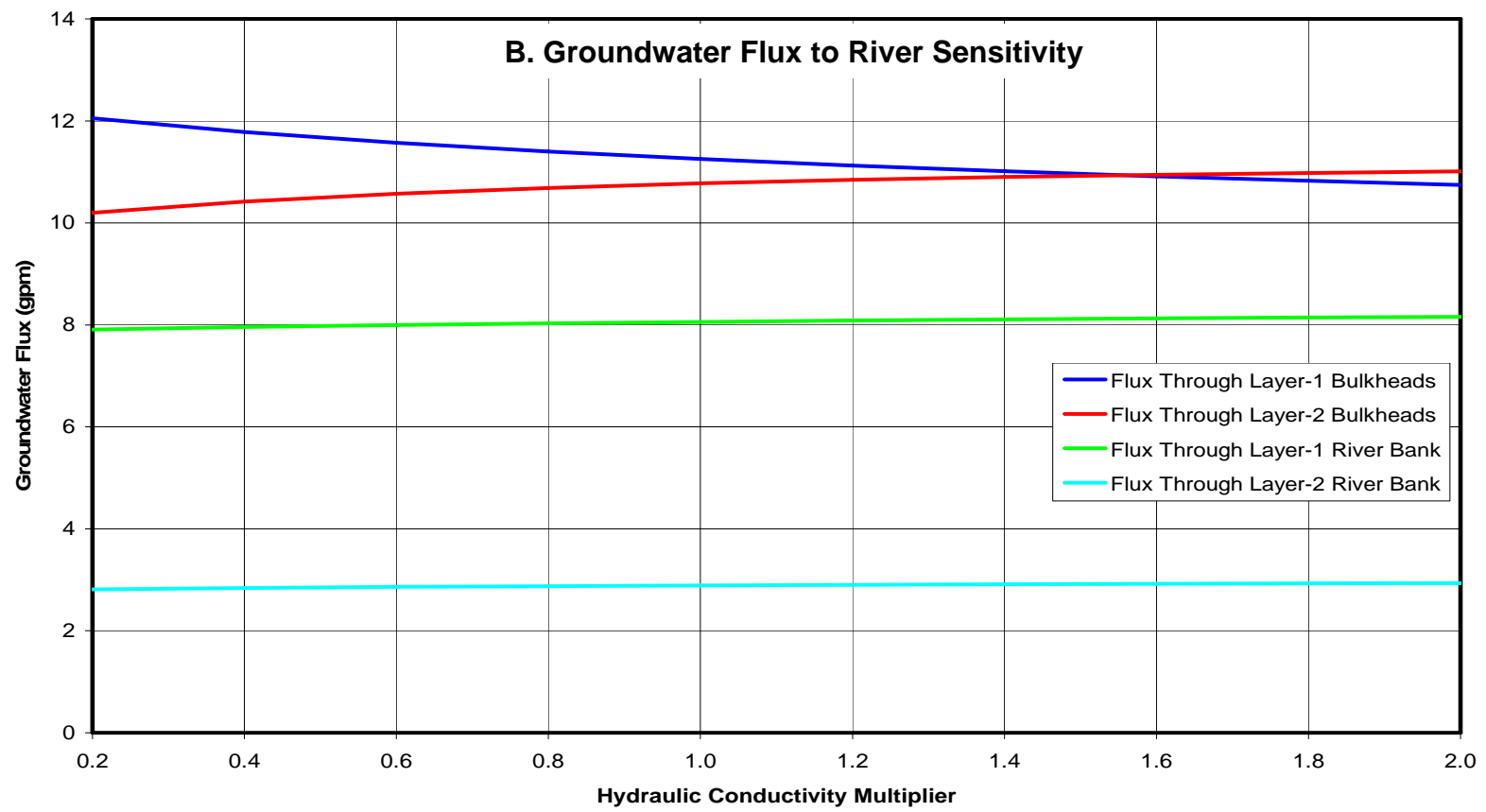
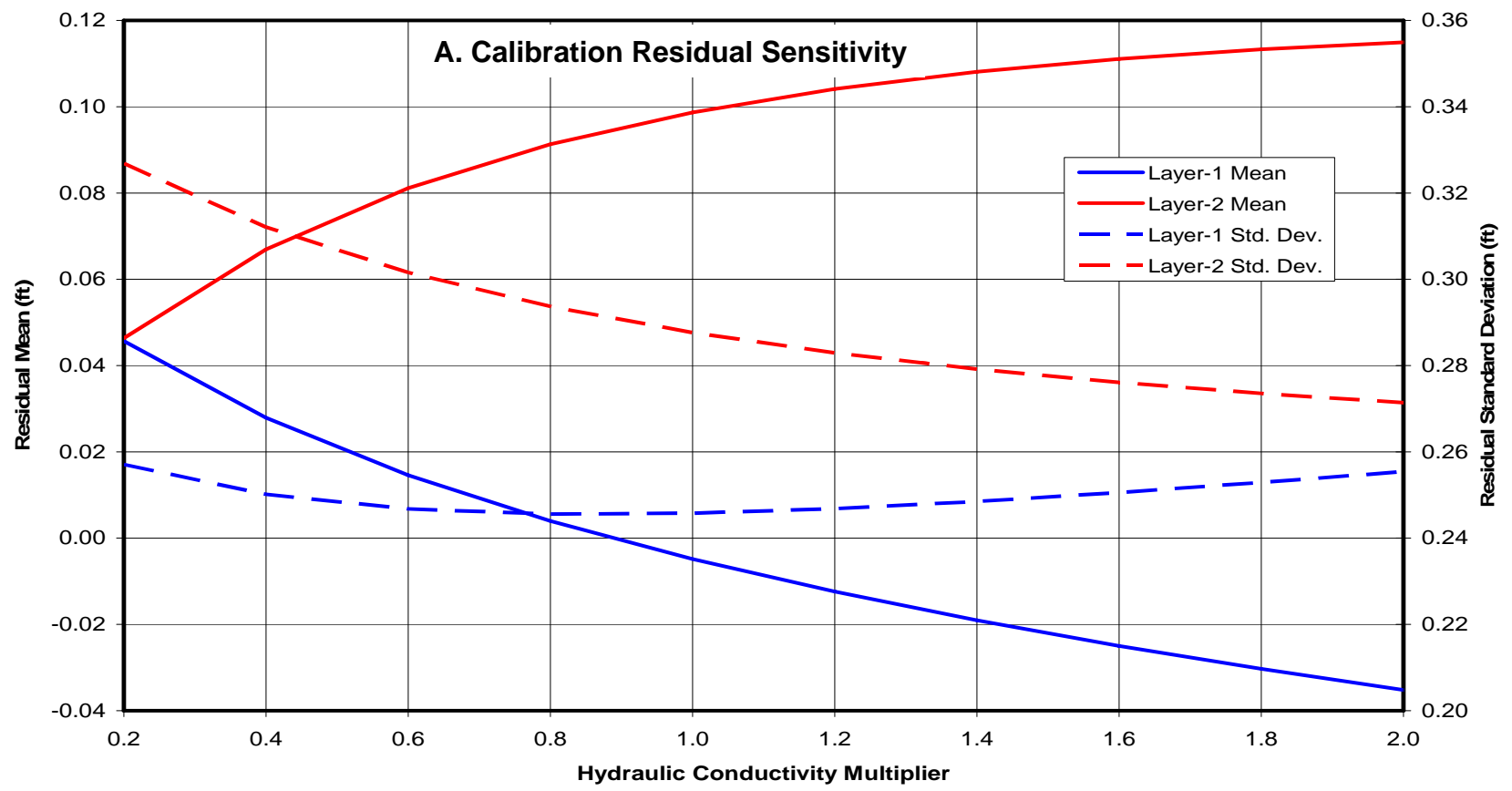


Figure B5-2
Sensitivity Analysis Results for Upper Semi-Confining Unit Hydraulic Conductivity

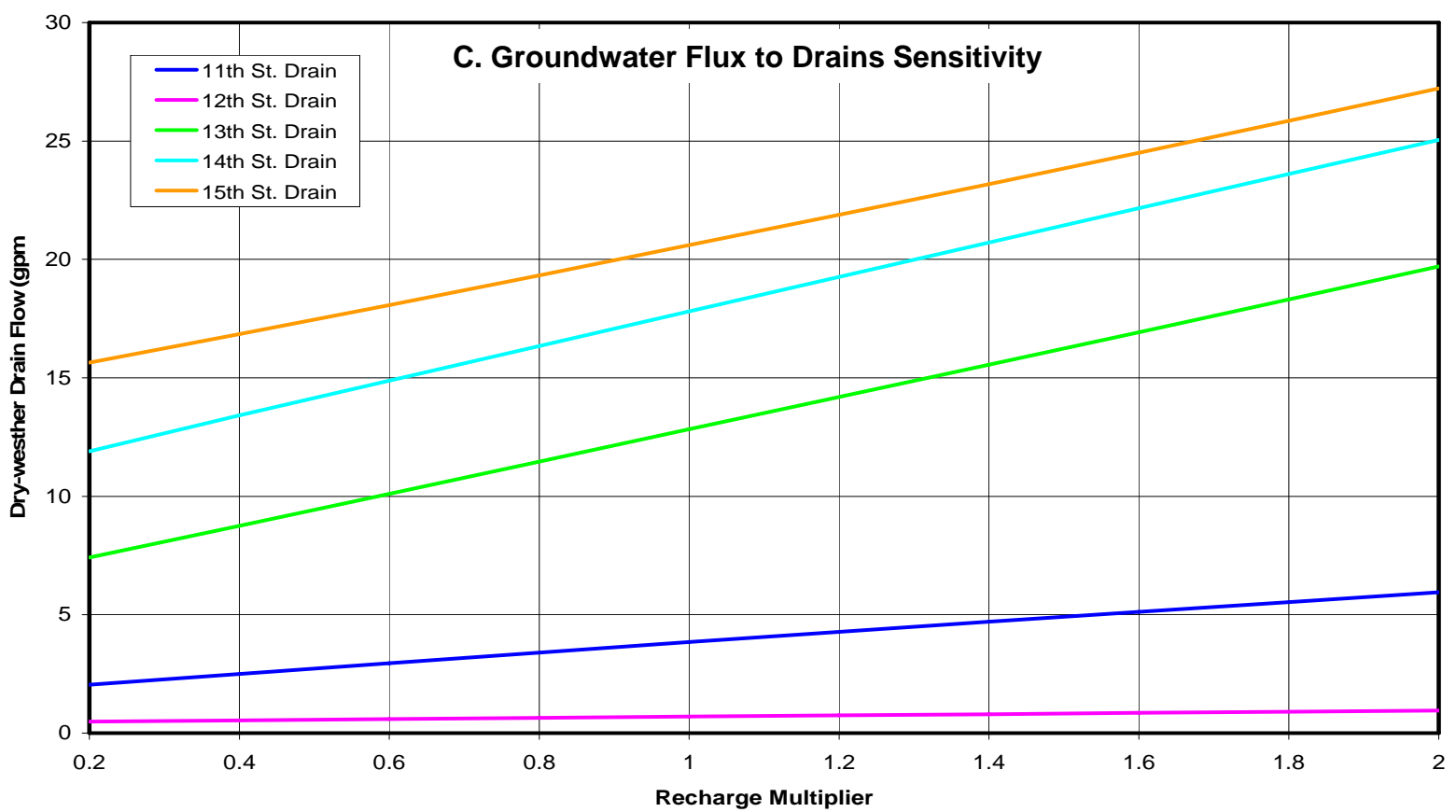
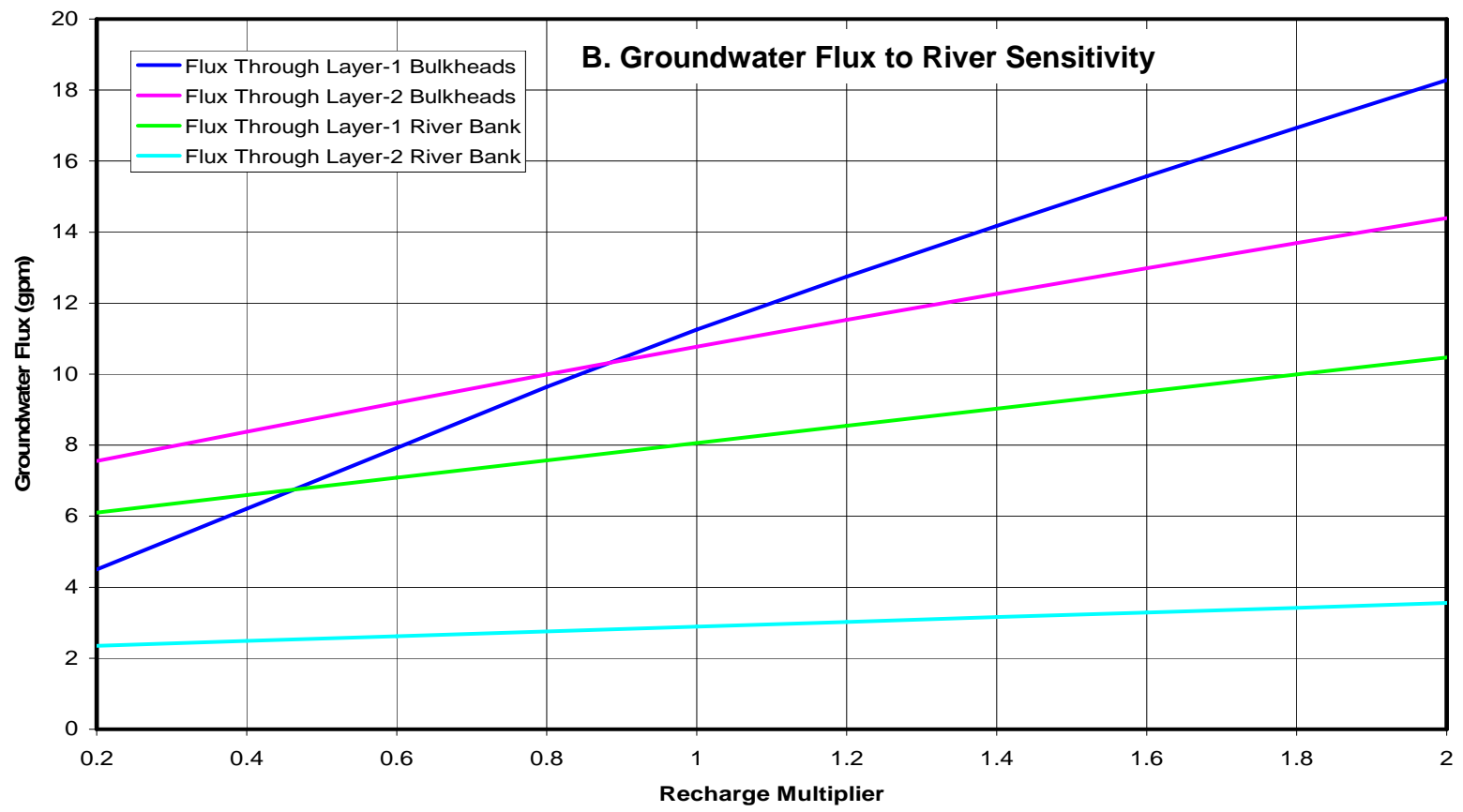
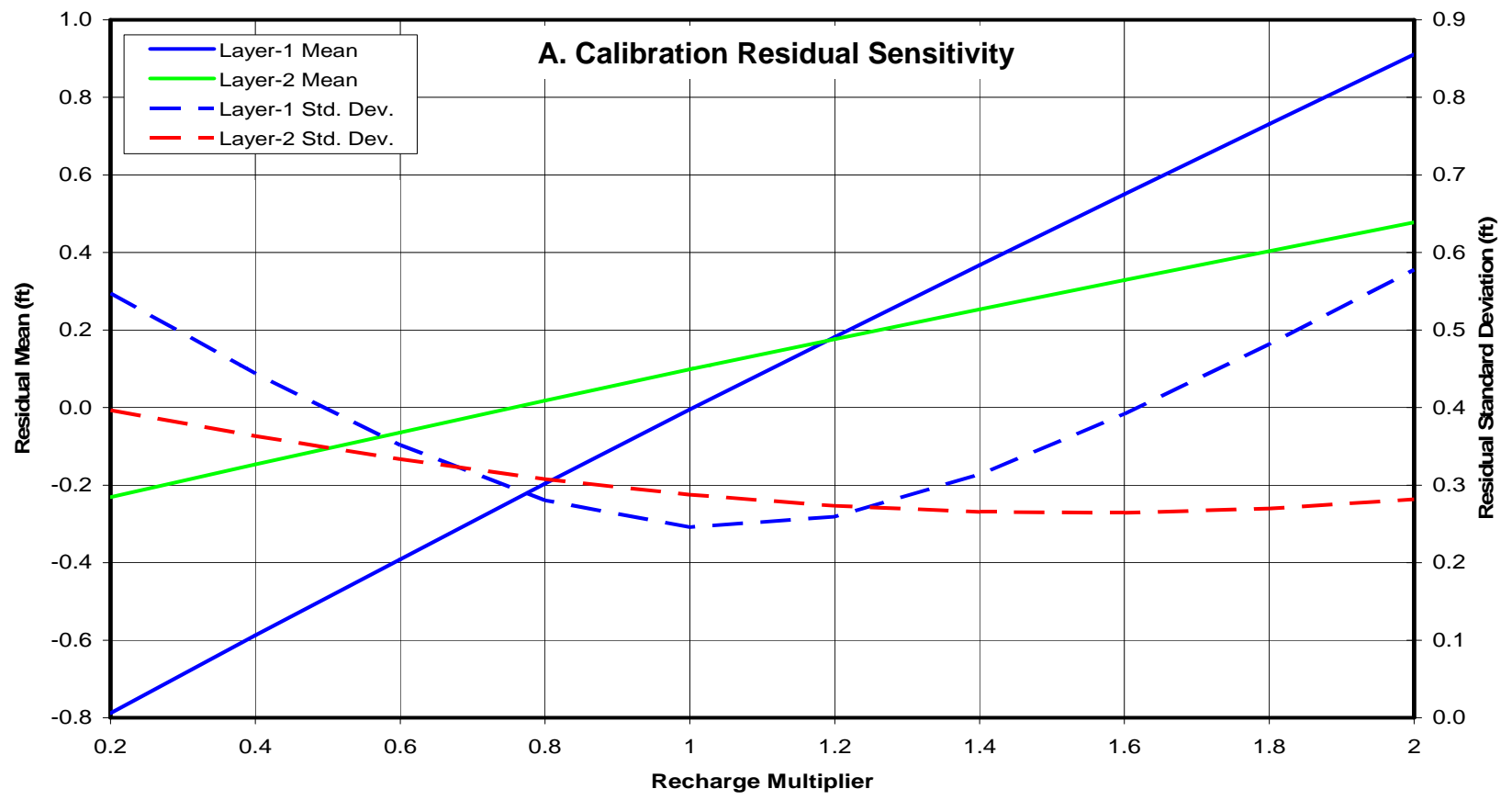


Figure B5-3
Sensitivity Analysis Results for Recharge Rate

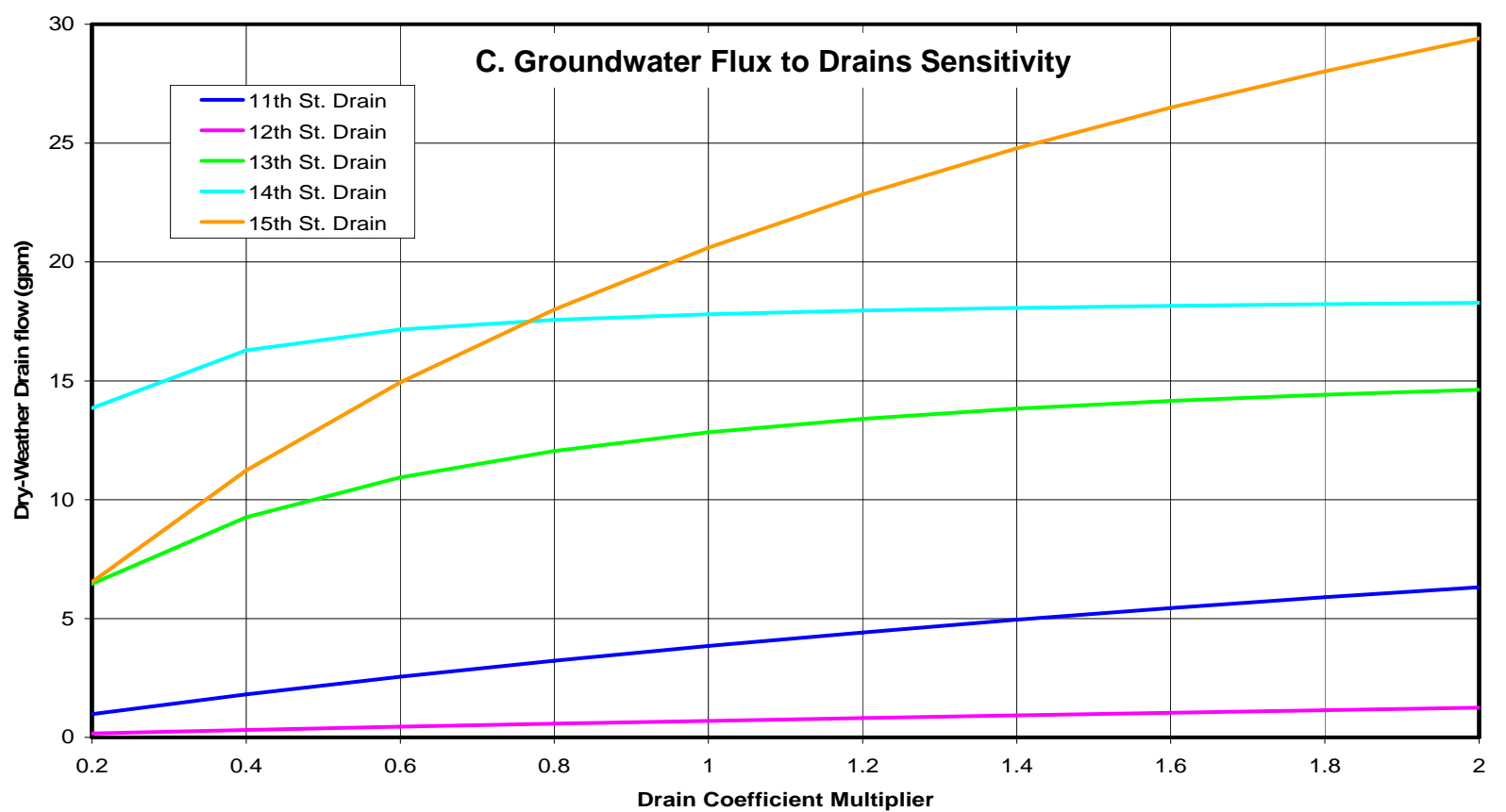
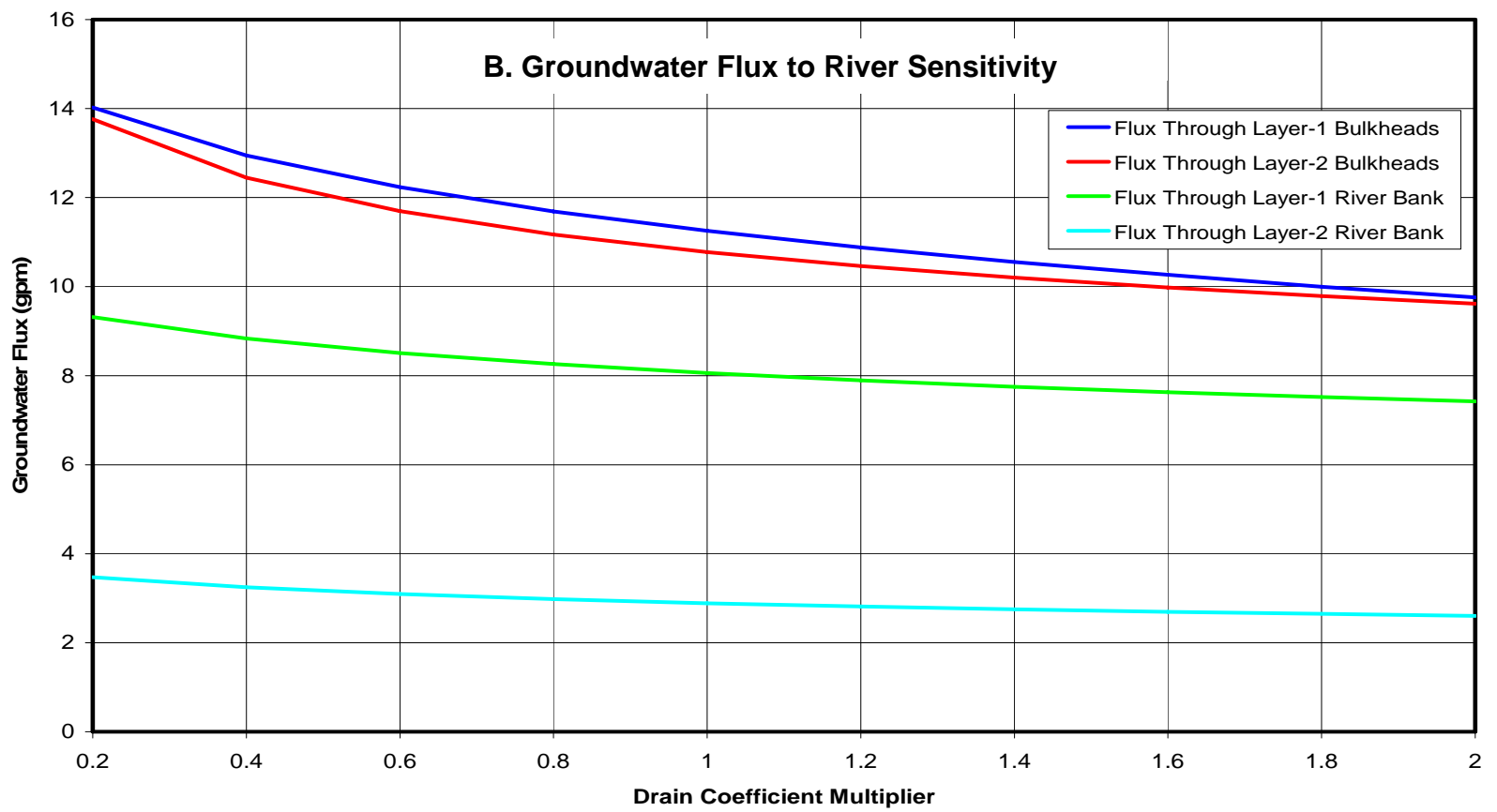
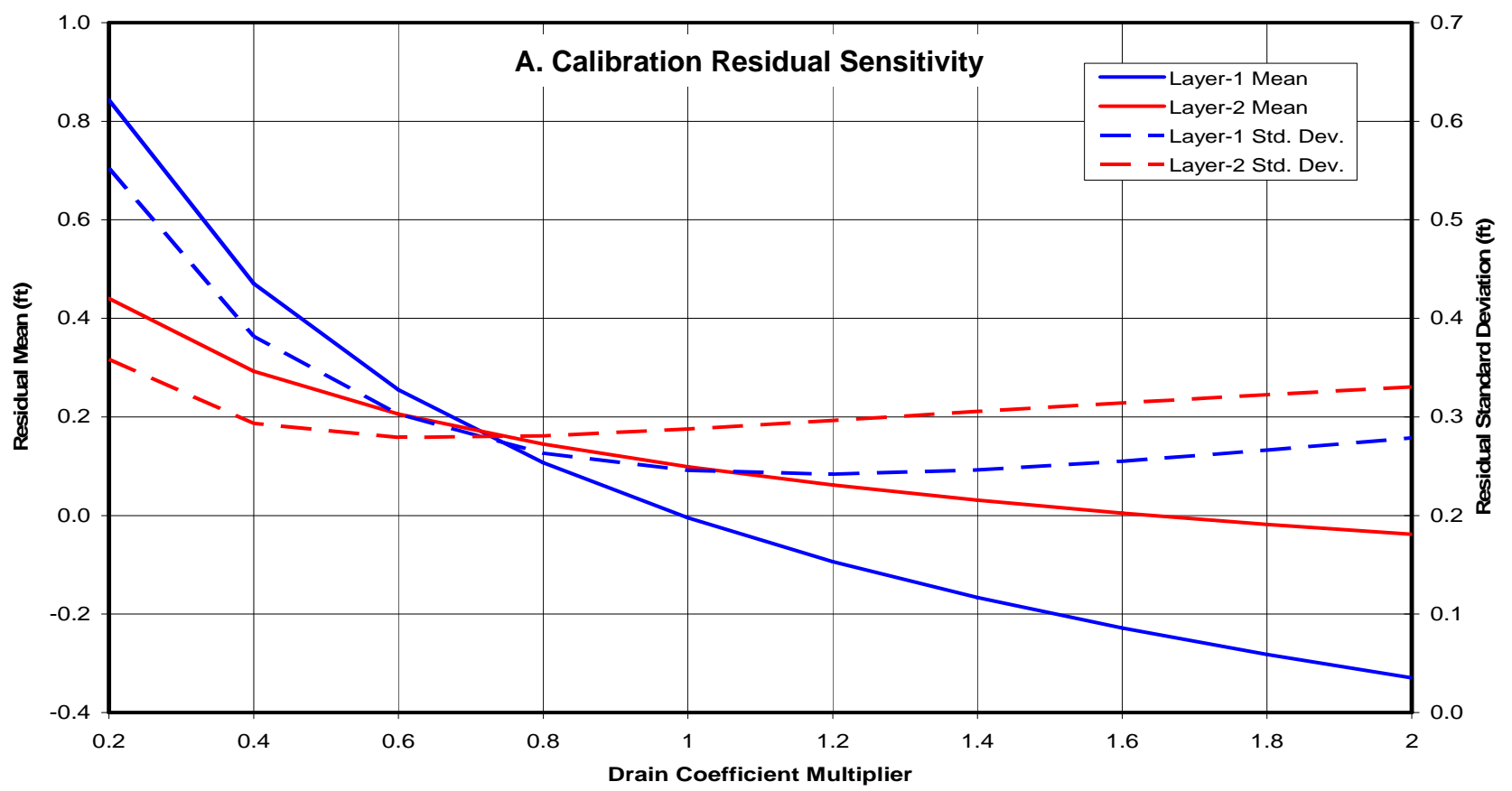


Figure B5-4
Sensitivity Analysis Results for Drain Leakage Coefficients

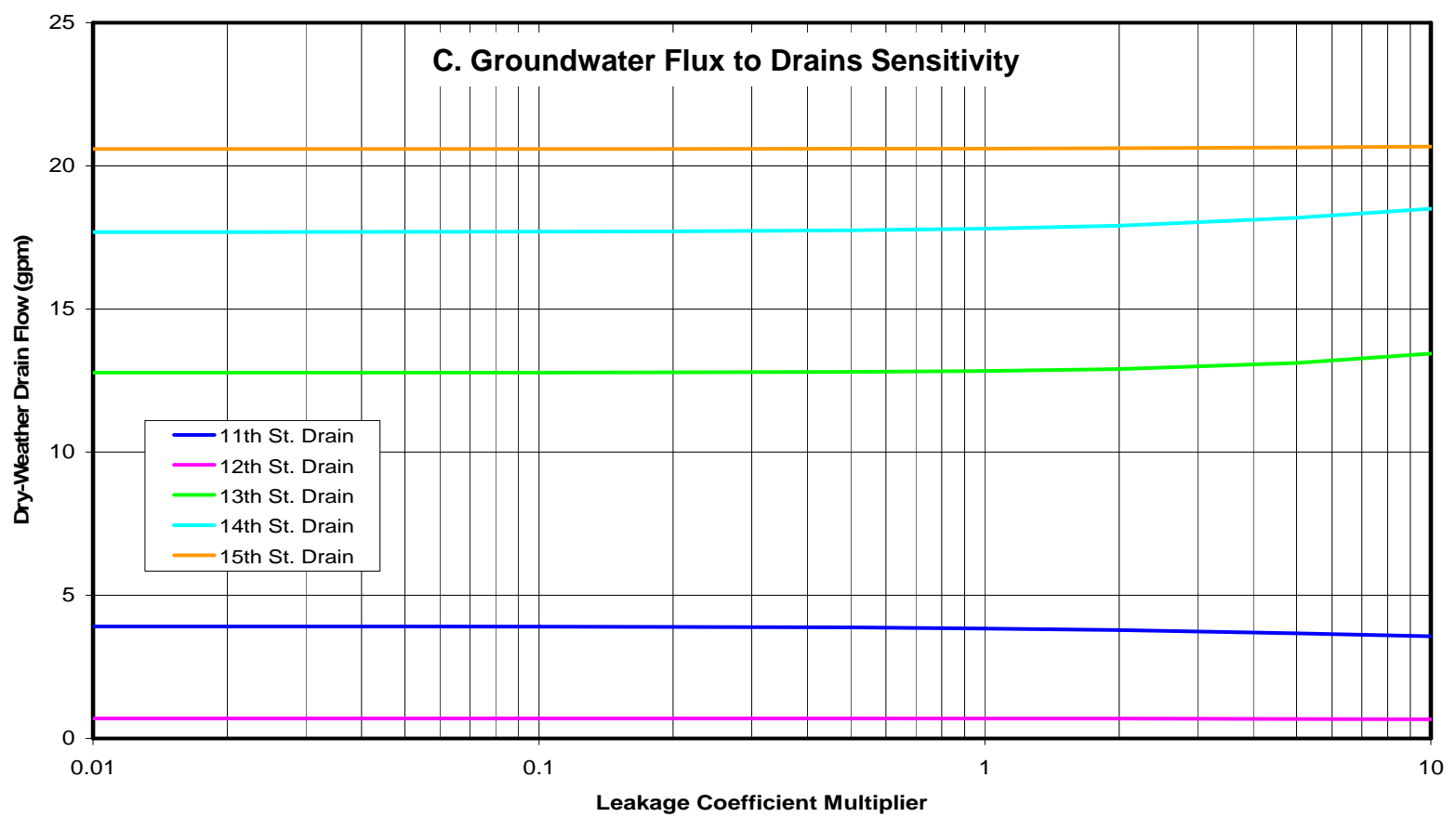
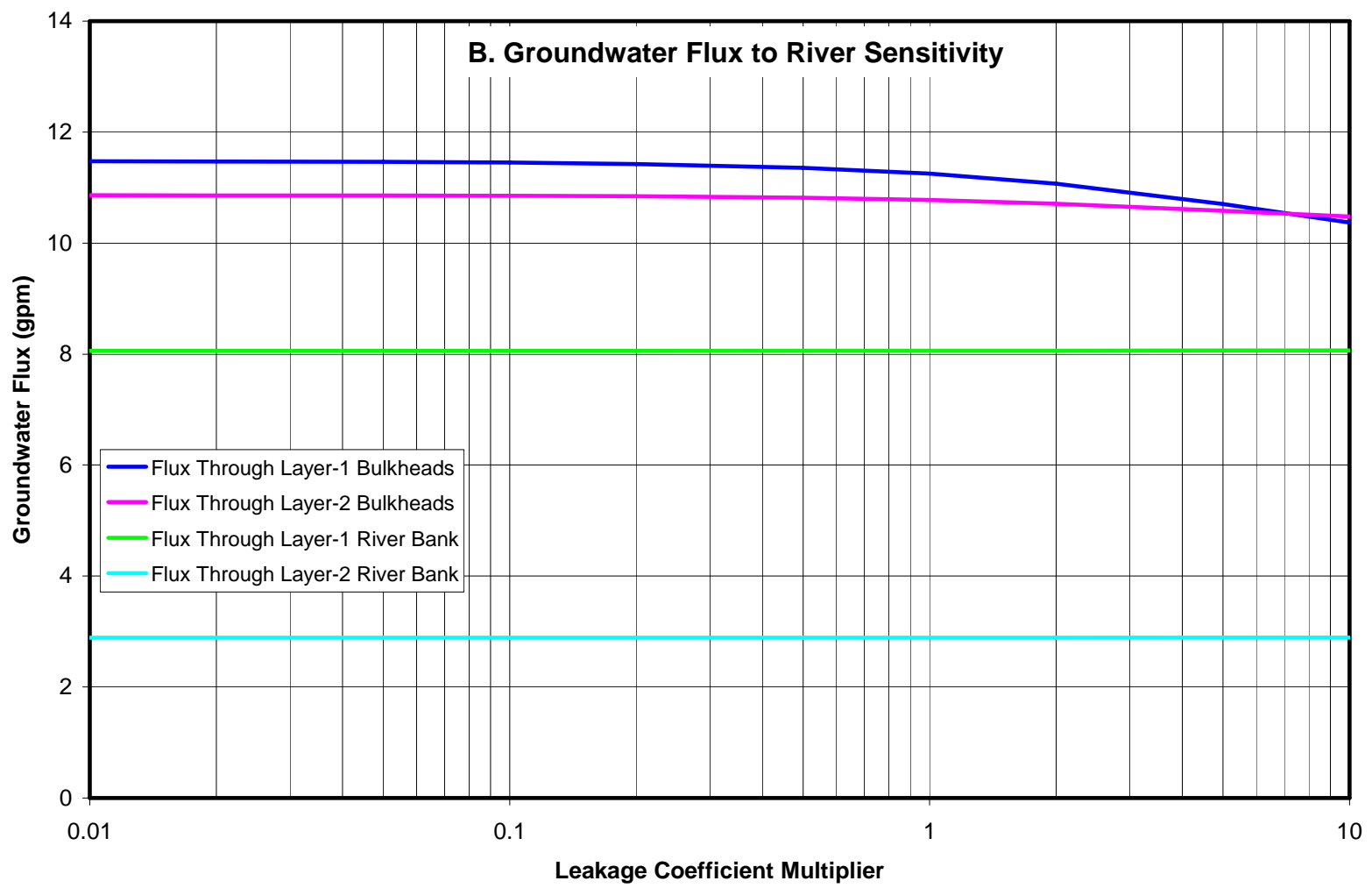
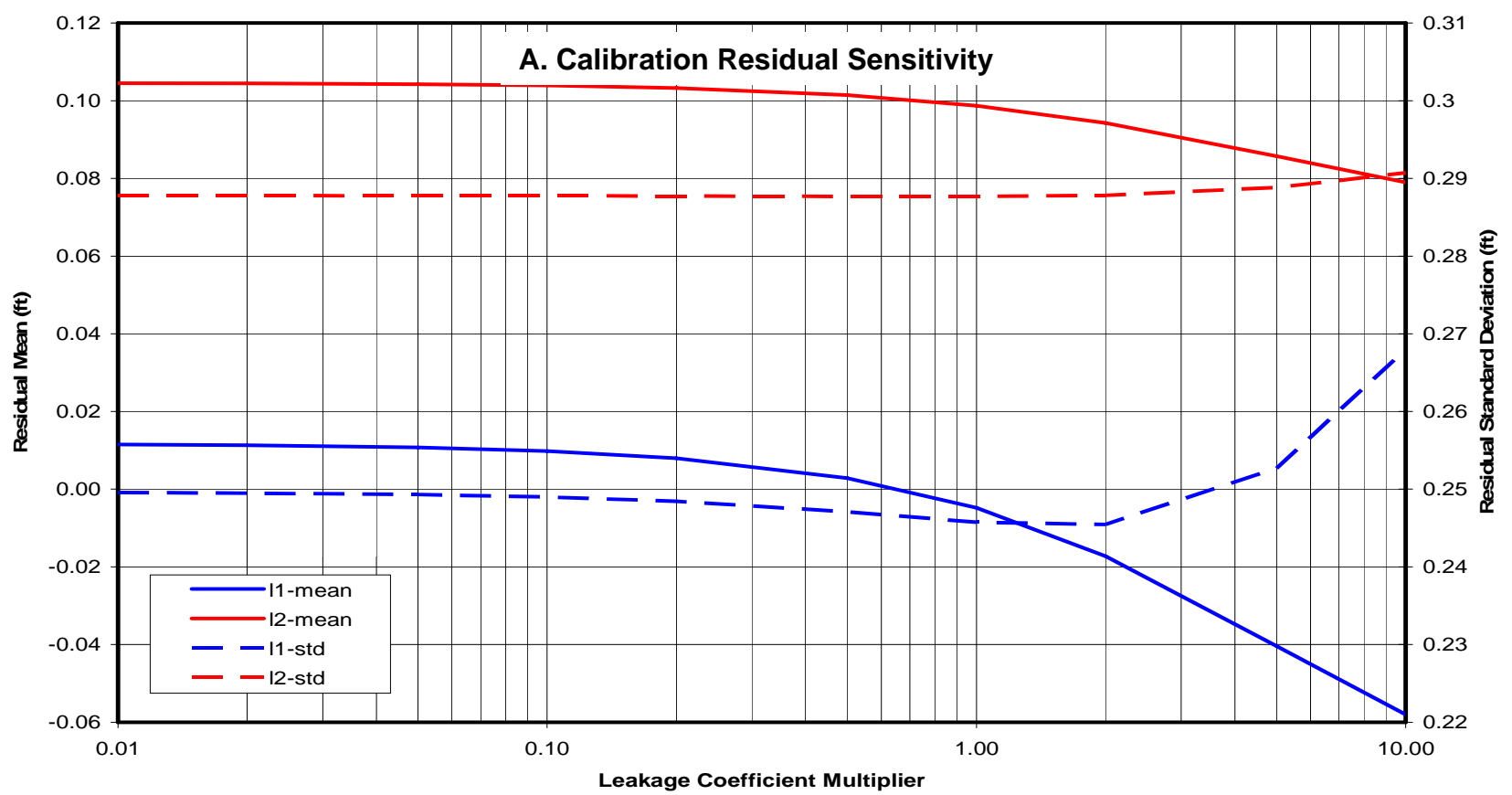


Figure B5-5
Sensitivity Analysis Results for Northern Bulkhead Leakage Coefficients

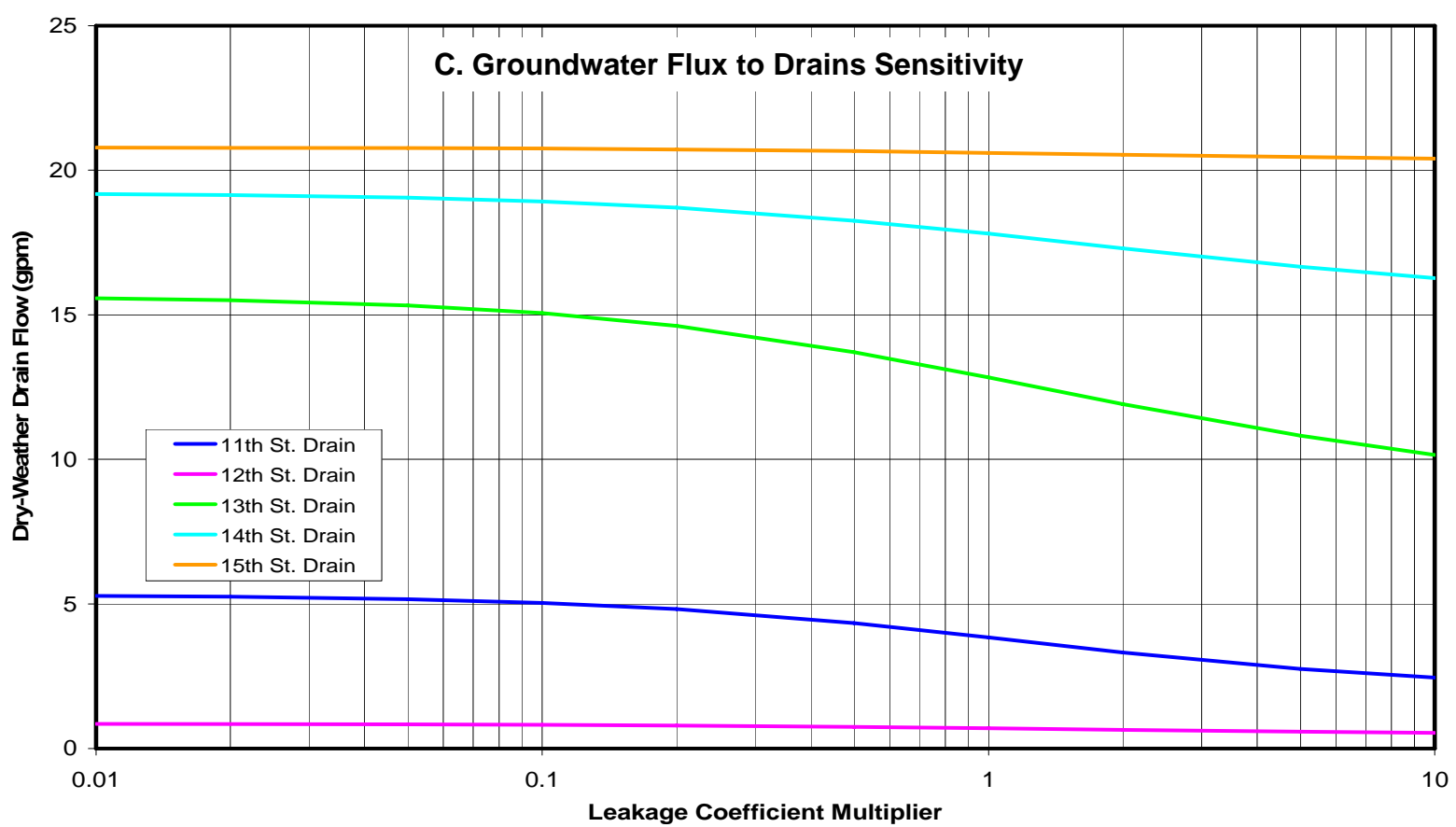
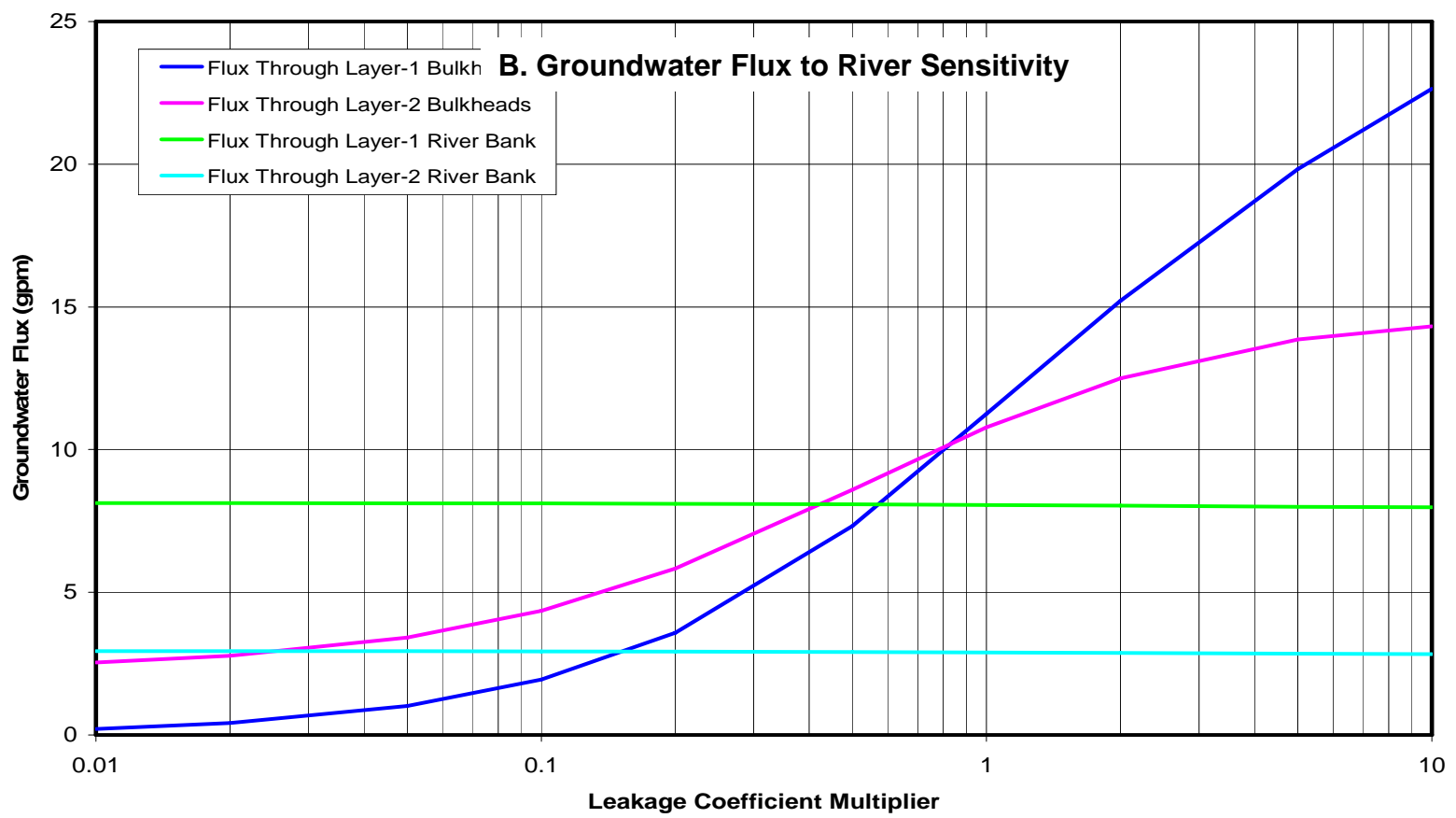
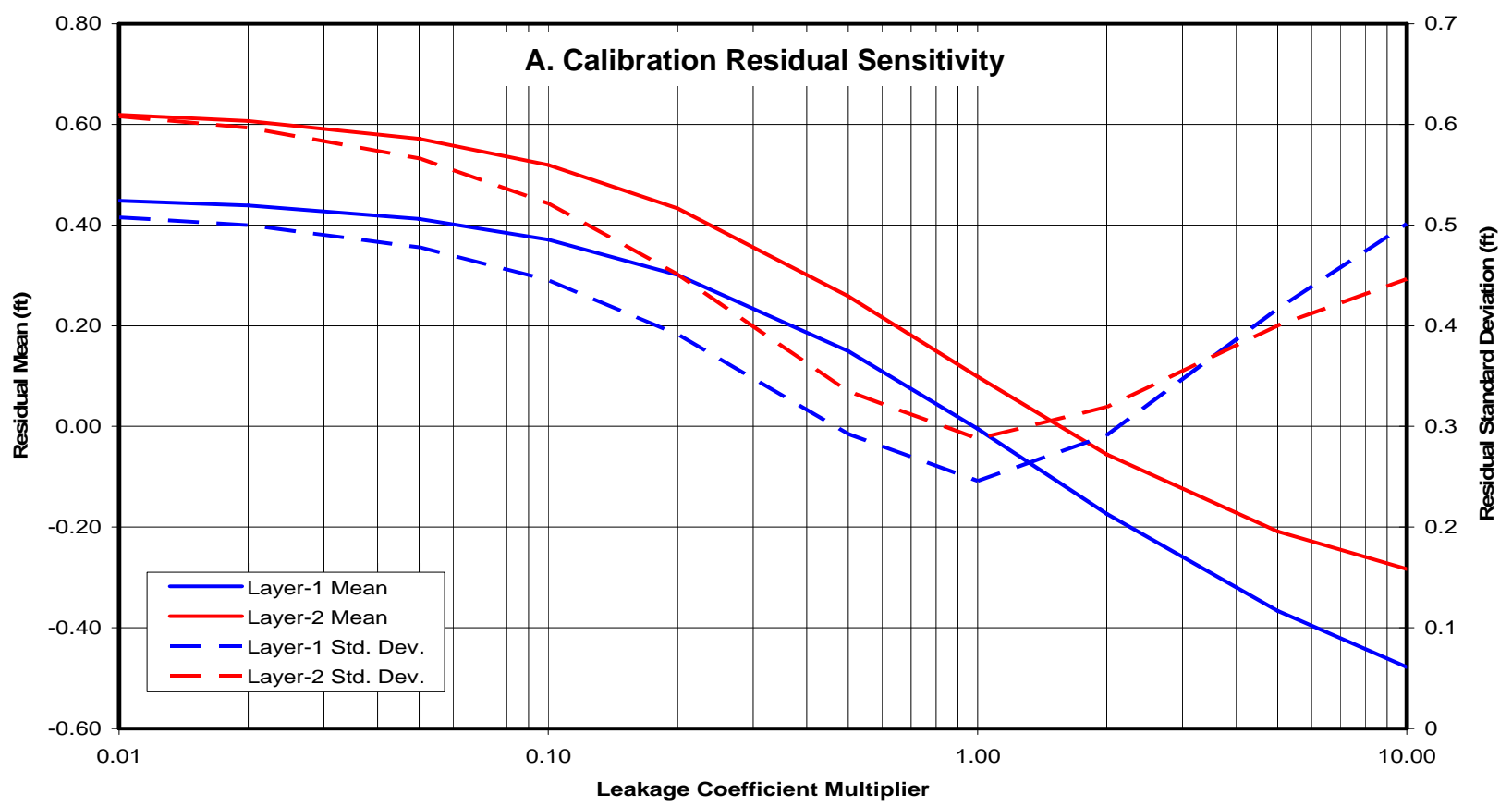


Figure B5-6
Sensitivity Analysis Results for Southern Bulkhead Leakage Coefficients